

https://dspace.org/

Bacterial leaching of nickel literites using chemolithotrophic microorganisms

Simate, Geoffrey Simate

2009-07-17T12:48:51Z
http://hdl.handle.net/10539/7098

Downloaded from a DSpace repository. https://dspace.org/

BACTERIAL LEACHING OF NICKEL LITERITES USING CHEMOLITHOTROPHIC MICROORGANISMS

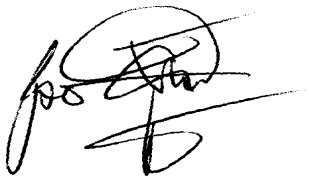
Geoffrey Simate Simate

A dissertation submitted to the Faculty of Engineering and the Built Environment, University of the Witwatersrand, Johannesburg, in fulfillment of the requirements for the degree of Master of Science in Engineering.

Johannesburg, 2009

DECLARATION

I declare that this dissertation is my own unaided work. It is being submitted to the degree of Master of Science in Engineering to the University of the Witwatersrand, Johannesburg. It has not been submitted before for any other degree or examination in any other University.



_____

Geoffrey Simate Simate

19th day of March 2009

ABSTRACT

Biohydrometallurgy, an interdisciplinary field involving geomicrobiology, microbial ecology, microbial biochemistry, and hydrometallurgy, is a promising novel technology for recovering valuable minerals from traditionally difficult-to-process ores. In this study, the possibility to treat nickel laterites biohydrometallurgically using chemolithotrophic microorganisms was investigated. Nickel laterite contains metal values but is not capable of participating in the primary chemolithotrophic bacterial oxidation because it contains neither ferrous iron nor substantial amount of reduced sulphur. Its metal value can, however, be recovered by allowing the primary oxidation of pyrite, or similar iron/sulphur minerals to provide sulphuric acid solutions, which solubilise the metal content.

In order to have an insight on the use of chemolithotrophic bacteria in this process, it was important to first understand the role and effects of sulphuric acid. Its effect was compared to citric acid and ferric sulphate. Results showed that sulphuric acid performed better, in terms of nickel recovery, than citric acid or ferric sulphate of the same initial concentration. However, citric acid performed better at the same initial pH. A synergic effect was observed in a mixture of sulphuric and citric acids.

In the bacterial leaching test works, sulphur substrate exhibited better effects in terms of acidification and nickel recovery than pyrite substrate. Using a statistically-based optimization strategy called response surface methodology, the theoretical optimum conditions for maximum nickel recovery (79.8%) within the range of conditions studied was found to be initial pH of 2.0, 63μm particle size and 2.6% pulp density.

This work has shown that by the addition of a sulphur containing material, nickel laterites can be leached by chemolithotrophic microorganisms via the sulphuric acid produced.

PUBLICATIONS AND PRESENTATIONS

Journal Publications

1. **Simate, G. S**., Ndlovu, S., 2008. Bacterial leaching of nickel laterites using chemolithotrophic microorganisms: Identifying influential factors using statistical design of experiments. *International Journal of Mineral Processing* 88, pp31-36.
2. **Simate, G. S**., Ndlovu, S., 2007. Characterisation of factors in the bacterial leaching of nickel laterites using statistical design of experiments. *Advanced Materials Research* 20-21, pp 66-69.
3. **Simate, G. S**., Ndlovu, S., Gericke, M., 2008. Bacterial leaching of nickel laterites using chemolithotrophic microorganisms: Process optimisation using response surface methodology and central composite rotatable design. *Hydrometallurgy*, Submitted for publication.

Conference Proceedings

1 Ndlovu, S., **Simate G. S.,** Gericke, M., 2009. The microbial assisted leaching of nickel laterites using a mixed culture of chemolithotrophic microorganisms. Accepted for publication and presentation at the 18th International Biohydrometallurgy Symposium, Bariloche, Argentina, September 13-17, 2009.

2 **Simate, G. S.,** .Ndlovu, S., Gericke, M., 2009. The effect of elemental sulphur and pyrite on the leaching of nickel laterites using chemolithotrophic

microorganisms. In: Hydrometallurgy Conference 2009, SAIMM Southern Africa , Muldersdrift, South Africa, February 24 – 27.

3 Ndlovu, S., **Simate, G. S**., 2007. The leaching of nickel laterites using acidic media and ferric ions. In: VII Meeting of the Southern Hemisphere on Mineral Technology, Ouro Preto, Brazil, November 20 – 24.

4 **Simate, G. S**., Ndlovu, S., 2007. Characterisation of factors in the bacterial leaching of nickel laterites using statistical design of experiments. In: 17th International Bio-hydrometallurgy Symposium, Frankfurt am Main, Germany, September 2 – 5.

DEDICATION

Dedicated to my mother Bo ma-Mwiya Mukatimui Mashela, and my family for their everlasting love.

Ni itumezi shaa.

ACKNOWLEDGEMENTS

"...No man is an island, entirely of himself...'' (John Donne, 1572-1631). In executing this work, I passed through and came across a lot of obstacles, but triumphed in one way or the other; mostly through the assistance of others. This is the reality; life is never easy or as straight forward as we would wish it to be.

I am very grateful to my supervisor, Dr. Sehliselo Ndlovu, for her careful questioning and insightful supervision of the research work contained in this dissertation. Her guidance, mentorship, patience and support were invaluable to this study and are highly appreciated.

This research work would not have been completed without the financial support of the Council of Mineral Technology of South Africa, the University of Witwatersrand University Postgraduate Merit Award, and the National Research Foundation of South Africa through THRIP and the African Scholarship flagship programmes. Their financial support, that made this study a success, is dully acknowledged and greatly appreciated.

Special thanks are also due to Dr. Lubinda F. Walubita (of TTI, Texas A&M University System, USA), my old time child friend, though a Civil Engineer by profession, for his valuable critical analysis and review of my dissertation. Keep it up David Kaunda Secondary Technical School 'boys of 1989'.

Lastly but not the least, I wish to thank and acknowledge the love of my family – Namakau (my wife) and my babies – for their moral understanding and unparalleled support during this period of my absence from home. Thanks guys; I love you!!

TABLE OF CONTENTS

Declaration ii

Abstract iii

Publications and Presentations iv

Dedication vi

Acknowledgements vii

Table of contents viii

List of figures xiv

List of Tables xvii

CHAPTERS

1. INTRODUCTION 1

1.1 Introduction 2

1.2 Research Problem 4

1.3 Objective 4

1.4 Research Methodology 5

1.5 Dissertation Layout 5

1.6 Summary 7

2. LITERATURE REVIEW 8

2.1 General Introduction 9

2.1.1 Nickel 9

2.1.2 Nickel Laterites Mineralogy and Occurrence 10
2.1.3 Currently Existing Nickel Laterites Processing Methods 12
2.2 Bacterial Leaching 15
2.2.1 Introduction 15
2.2.2 Microorganisms Used in Leaching 15
2.2.3 Bioleaching of Metal Sulphide Ores 18
2.2.4 The Mechanisms of Bacterial Leaching of Metal Sulphide Ores 19
2.2.5 Bacterial Leaching of Nickel Laterite Ores 23
2.2.6 The Kinetics of Leaching Reactions 26
2.3 Summary 29

3. MATERIALS AND METHODS 31
3.1 Introduction 32
3.2 Materials 32
3.2.1 Nickel Laterite Ore 32
3.2.2 Reagents 33
3.2.3 Pyrite 33
3.3 Bacterial Growth and Maintenance 33
3.3.1 Standard 9K Medium 33
3.3.2 Bacterial Growth 33
3.3.3 Bacterial Cell Harvesting 34
3.3.4 Determination of Bacterial Population using Spectrophotometer 35
3.4 Experimental Methods 36

3.4.1 Design of Experiments 36
3.4.2 Apparatus and Experimentation 38
3.4.3 Experimental Design 38
3.5 Analytical Techniques 39
3.5.1 Nickel Concentration 39
3.5.2 pH and Reduction Oxidation Potential 40
3.6 Data Analysis 41
3.7 Summary 41

4. ACIDIC AND FERRIC LEACHING 43
4.1 Introduction 44
4.2 Materials and Methods 45
4.2.1 Ore Samples and Preparation 45
4.2.2 Chemical Leach Tests at Different Concentrations 45
4.2.3 Chemical Leach Tests at Same Initial pH 46
4.2.4 Chemical Leach Tests at Different Temperatures 46
4.3 Results and Discussion 47
4.3.1 Effect of Initial Lixiviant Concentration 47
4.3.2 Effect of Initial Lixiviant pH 50
4.3.3 Effect of Temperature 51
4.3.4 Kinetic Analysis 52
4.4 Summary and Conclusions 58

5. IDENTIFICATION OF INFLUENTIAL FACTORS 60

5.1 Introduction 61

5.2 Materials and Methods 61

5.2.1 Ore Samples and Preparation 61

5.2.2 Microbes 62

5.2.3 Experimental Plan for Statistical Design of Experiments 62

5.2.4 Methodology for Data Analysis 66

5.2.5 Experimentation 69

5.3 Results and Discussion 70

5.3.1 Significant Factors 70

5.3.2 Influence of Factors on Recovery 74

5.3.3 Leaching Profile 81

5.4 Summary and Conclusions 83

6. EFFECT OF INITIAL pH ON SUBSTRATE TYPE 85

6.1 Introduction 86

6.2 Materials and Methods 86

6.2.1 Ore Samples and Preparation 86

6.2.2 Microbes 86

6.2.3 Experimentation 87

6.3 Results and Discussion 88

6.3.1 Effect of pH and Reduction Oxidation Potential on the Bioleaching of Nickel Laterites 88

6.3.2 Effect of Media Composition on the Changes of pH and Reduction Oxidation Potential 97

6.4 Summary and Conclusions 99

7. OPTIMISATION OF INFLUENTIAL FACTORS 101

7.1 Introduction 102

7.2 Materials and Methods 103

7.2.1 Ore Samples and Preparation 103

7.2.2 Microbes 104

7.2.3 Experimental Design for the Response Surface Methodology and Central Composite Design 104

7.2.4 Experimentation 106

7.3 Results and Discussion 107

7.3.1 Derivation of the Fitted Model 107

7.3.2 Checking the Adequacy of the Developed Model 110

7.3.3 Response Surfaces 115

7.3.4 Determination of Optimum Conditions 119

7.3.5 Confirmatory Experiments 122

7.4 Summary and Conclusions 123

8. CONCLUSIONS AND RECOMMENDATIONS 126

8.1 Conclusion 127

8.1.1 Introduction 127

8.1.2 Acidic and Ferric Leach Tests 128

8.1.3 Bacterial Leach Tests 128
8.1.4 Optimisation Tests 130
8.1.5 Kinetic Studies 131
8.1.6 Potential Application in Industry 132
8.2 Recommendations 132

REFERENCES 135
BIBLIOGRAPHY 153

APPENDICES 158
Appendix A Sample Calculations 159
Appendix B Nickel Laterite Ore Composition and Particle Size Analysis 165
Appendix C Results for the Acidic and Ferric Leaching 168
Appendix D Results for the Identification of Influential Factors 178
Appendix E Results for the Effects of Initial pH on Substrate Type 188
Appendix F Results for the Optimisation of Influential Factors 193
Appendix G Statistical Analysis 197
Appendix H Statistical and Mathematical Methods 200
Appendix I Matlab Programs 219

LIST OF FIGURES

Figure 1.1 Dissertation layout 6

Figure 3.1 The UV-Visible spectrophotometer 34

Figure 3.2 Agitation leaching test equipment 38

Figure 3.3 The Varian SpectrAA-55B atomic absorption spectrophotometer 40

Figure 4.1 Nickel laterite recoveries at same initial pH for different lixiviants 50

Figure 4.2 Nickel laterite recoveries at different temperatures for different lixiviants 52

Figure 4.3 Plot of $1-3(1-X)^{2/3}+2(1-X)$ versus time for sulphuric acid 53

Figure 4.4 Plot of $1-3(1-X)^{2/3}+2(1-X)$ versus time for citric acid 53

Figure 4.5 Plot of $1-3(1-X)^{2/3}+2(1-X)$ versus time for acidified ferric sulphate 54

Figure 4.6 Plot of $1-1(1-X)^{1/3}$ versus time for acidified ferric sulphate at 45°C 54

Figure 4.7 Arrhenius plot for nickel laterite dissolution with various lixiviants 56

Figure 5.1 Normal plot of effects of main and two factor interactions (combined) ... 70

Figure 5.2 Normal plot of effects of main and two factor interactions (basic) 71

Figure 5.3 Normal plot of residuals 73

Figure 5.4 Plot of residuals versus predicted recoveries 74

Figure 5.5 Effect of pH on nickel recovery (combined) 75

Figure 5.6 Effect of particle on nickel recovery (combined) 76

Figure 5.7 Effect of pulp density on nickel recovery (combined) 77

Figure 5.8 Effect of type of substrate on nickel recovery (combined) 78

Figure 5.9 Optical density at 400nm as a function of time 78

Figure 5.10 pH variance profiles (basic) 79

Figure 5.11 pH variance profiles (fold-over) 80

LIST OF FIGURES (CONTINUED)

Figure 5.12 Plot of nickel recovery versus leaching time (basic) 82

Figure 5.13 Plot of nickel recovery versus leaching time (fold-over) 82

Figure 6.1 Effect of pH on the leachability of nickel laterite with sulphur substrate . 88

Figure 6.2 Effect of pH on the leachability of nickel laterite with pyrite substrate 89

Figure 6.3 Dissolution rates of nickel laterite as a function of substrate type at initial pH of 1.0 90

Figure 6.4 Dissolution rates of nickel laterite as a function of substrate type at initial pH of 1.5 90

Figure 6.5 Dissolution rates of nickel laterite as a function of substrate type at initial pH of 2.0 91

Figure 6.6 Dissolution rates of nickel laterite as a function of substrate type at initial pH of 2.5 92

Figure 6.7 Evolution of pH with time for sulphur substrate 93

Figure 6.8 Evolution of pH with time for pyrite substrate 93

Figure 6.9 pH drop for sulphur and pyrite substrates in a week 94

Figure 6.10 pH drop for sulphur and pyrite substrates in a month 95

Figure 6.11 Evolution of ORP with time for sulphur substrate 96

Figure 6.12 Evolution of ORP with time for pyrite substrate 96

Figure 6.13 Evolution of pH with time at initial pH of 1.5 for different media compositions 97

Figure 6.14 Evolution of ORP with time at initial pH of 1.5 for different media compositions 98

LIST OF FIGURES (CONTINUED)

Figure 7.1 Relationship between experimental and predicted nickel recovery 114

Figure 7.2 Response surface and contour plots at constant pH..... 116

Figure 7.3 Response surface and contour plots at constant pulp density..... 117

Figure 7.4 Response surface and contour plots at constant particle size 119

LIST OF TABLES

Table 2.1 Global resource for nickel laterites 12

Table 2.2 Shrinking core models 28

Table 3.1 Experimental design..... 39

Table 3.2 Operating conditions for nickel analysis by AAS..... 40

Table 4.1 Leaching conditions and solubilisation of nickel by H_2SO_4, $C_6H_8O_7$, $Fe_2(SO_4)_3$ and acidified $Fe_2(SO_4)_3$ at 30°C 47

Table 5.1 Experimental factors and levels for controlled factors 63

Table 5.2 Nickel recovery results for the 2^{5-2}_{III} fractional factorial design (basic) 64

Ta2ble 5.3 Nickel recovery results for the 2^{5-2}_{III} fractional factorial design (fold-over)65

Table 5.4 Nickel recovery results for the 2^{5-2}_{III} fractional factorial design (centre points replicates) 68

Table 7.1 Relationship between coded and actual values of the variable..... 104

Table 7.2 Experimental layout and runs for the central composite rotatable design 105

Table 7.3 Observed values for the nickel recovery..... 109

Table 7.4 ANOVA for the fitted model 110

Table 7.5 Regression coefficients for fitted model 111

Table 7.6 ANOVA for the refitted model 113

Table 7.7 Regression coefficients for refitted model..... 113

Table 7.8 Observed and predicted values for the nickel recovery 115

Table 7.9 Nickel recoveries at optimum conditions..... 123

CHAPTER ONE

INTRODUCTION

"…to regard old problems from a new angle requires creative imagination and marks real advances in science...".

- Albert Einstein

1.1 Introduction

Nickel is an important metal that significantly contributes to the vibrancy of the modern-day economy. It is primarily used in the manufacture of alloys because of its unique and special characteristic properties that are essential in the long-term strength and durability of alloys. The resultant characteristic properties of nickel-alloys include superior toughness, strength, corrosion resistance, special magnetic and electronic properties, and the ability to withstand extreme temperatures. These properties are critical for applications such as in the chemical, petrochemical, energy and aerospace industries.

Presently, most of the nickel comes from sulphide deposits. Worldwide reserves of high grade nickel sulphide ores are diminishing due to the rapid demand for metal. The increasing cost of mining sulphide resources underground and increasing environmental compliance costs are also having a strong impact on the economics of mining these deposits. On the other hand, nickel laterites which are formed as a result of prolonged processes of mechanical and chemical weathering, are in abundance contributing over 70% of land based nickel reserves, but accounting for only approximately 40% of the world annual nickel production (Elias, 2002; Gleeson et al., 2003; Dalvi et al., 2004).

Laterites are easily mined by cheap open pit techniques because the ores occur close to the surface (Moskalyk and Alfantazi, 2002). Recovery of nickel laterites currently is through traditional methods – pyrometallurgically and hydrometallurgically. Some of the difficulties involved in the processing of nickel laterites using these traditional methods include poor nickel grades in the feed and high energy requirements (Gleason et al., 2003). The poor nickel grades are a result of lack of definite nickel bearing minerals to result in upgraded ores by conventional upgrading systems (Valix et al., 2001a).

Where low nickel grades exist and other techniques cannot be applied efficiently, bacterial leaching has shown to be of great potential. In general, bacterial leaching implies the solubilisation of metals due to the action of microorganisms. This process is normally applied for two purposes; (1) bioleaching which results in the solubilisation of target metals such as the solubilisation of copper in chalcopyrite, and (2) bioxidation which acts as a pretreatment process to open up the structure of minerals, thereby permitting other chemicals to penetrate the mineral better and solubilise the desired metal such as in the pretreatment of gold-bearing arsenopyrite (Rawlings, 2005). However, the commercial beneficiation of nickel laterites using microorganisms has not yet been fully developed.

The recent previous research in an attempt to use microorganisms in the extraction of nickel from nickel laterites has focused mainly on the use of heterotrophic microorganisms. These microorganisms secrete organic acids such as citric, lactic, oxalic, acetic, formic, malic, succinic and glutaric acids (Bosecker, 1986; Alibhali et al., 1993; Valix et al., 2001a,b; Tang and Valix, 2006). However, the use of heterotrophic organisms poses a danger of possible contamination by undesirable organisms under commercial scale conditions. In addition, commercial mineral biooxidation processes using heterotrophic microorganisms are unlikely to be viable because of the vast amount of carbon sources; for example molasses, required (Rawlings, 2005). As a result, this method has not been commercialized.

The other types of microorganisms used in the mineral industries are classified as chemolithotrophs. The use of these chemolithotrophic microorganisms in the leaching of sulphide minerals is a well established phenomenon commercially used in the recovery of copper, cobalt, uranium, and refractory gold ores (Olson et al., 2003). These microorganisms obtain energy required for metabolism by oxidizing ferrous iron and reduced sulphur.

During the oxidation process of the sulphide ores, metal ions are released from the mineral ore matrix and sulphuric acid is produced. Sulphuric acid is the constituent component that can be utilized in the leaching process of nickel laterites.

1.2 Research Problem

Although the leaching of sulphidic minerals using chemolithotrophic bacteria is the most studied and commercially exploitable aspect of mineral biotechnology today, there is, however, very little information on the dissolution of nonsulphidic minerals such as nickel laterites using these bacteria. However, it is theorized that the metal value in the nickel laterites may be recovered by allowing the primary oxidation of pyrite, or similar iron/sulphur minerals to provide sulphuric acid solutions which solubilises the metal content. This is the conceptual (fundamental) theory upon which this research is based.

1.3 Objectives

The central hypothesis of this study is the development of a process using chemolithotrophic microorganisms to leach nickel laterites.

The overall goal is to investigate the possibility of using chemolithotrophic microorganisms with an external supply of sulphur containing material as an energy source in the bacterial leaching of nickel laterites.

The specific objectives are:-

(i) To investigate the influence of sulphuric acid, citric acid, and ferric sulphate so as to provide useful insights into the process of leaching nickel laterites.

(ii) To determine the specific parameters and conditions which are suitable for the favourable bacterial leaching of nickel laterites.

(iii) To study the effect of pH and hence, the effect of substrate type (sulphur or pyrite) on pH in the bacterial leaching of nickel laterites.

(iv) To optimise the favourable parameters and conditions that will ultimately maximise the leaching process in terms of the output (nickel recovery).

1.4 Research Methodology

The research methodology for this study involved the following major tasks: literature review, experimental design, laboratory testing, laboratory test data analysis, conclusions, recommendations and documentation.

1.5 Dissertation Layout

This dissertation consists of eight chapters including this chapter (Chapter One) that provides the motivation for the research, the problem statement, and the overall objectives of this study. The layout is schematically summarized in a flowchart in Figure 1.1.

Chapter Two is the literature review, which includes the general knowledge of nickel laterites mineralogy and occurrence; the current metallurgical processes and the general principles of the leaching of ores. Chapter Three (experimental design) describes the materials and methods used in the study. The subsequent chapters (Chapter Four through Seven) describe the laboratory tests, findings and conclusions. The dissertation concludes in Chapter Eight with a summary of the findings and

recommendations. Appendices of detailed laboratory test results and other important data are also included.

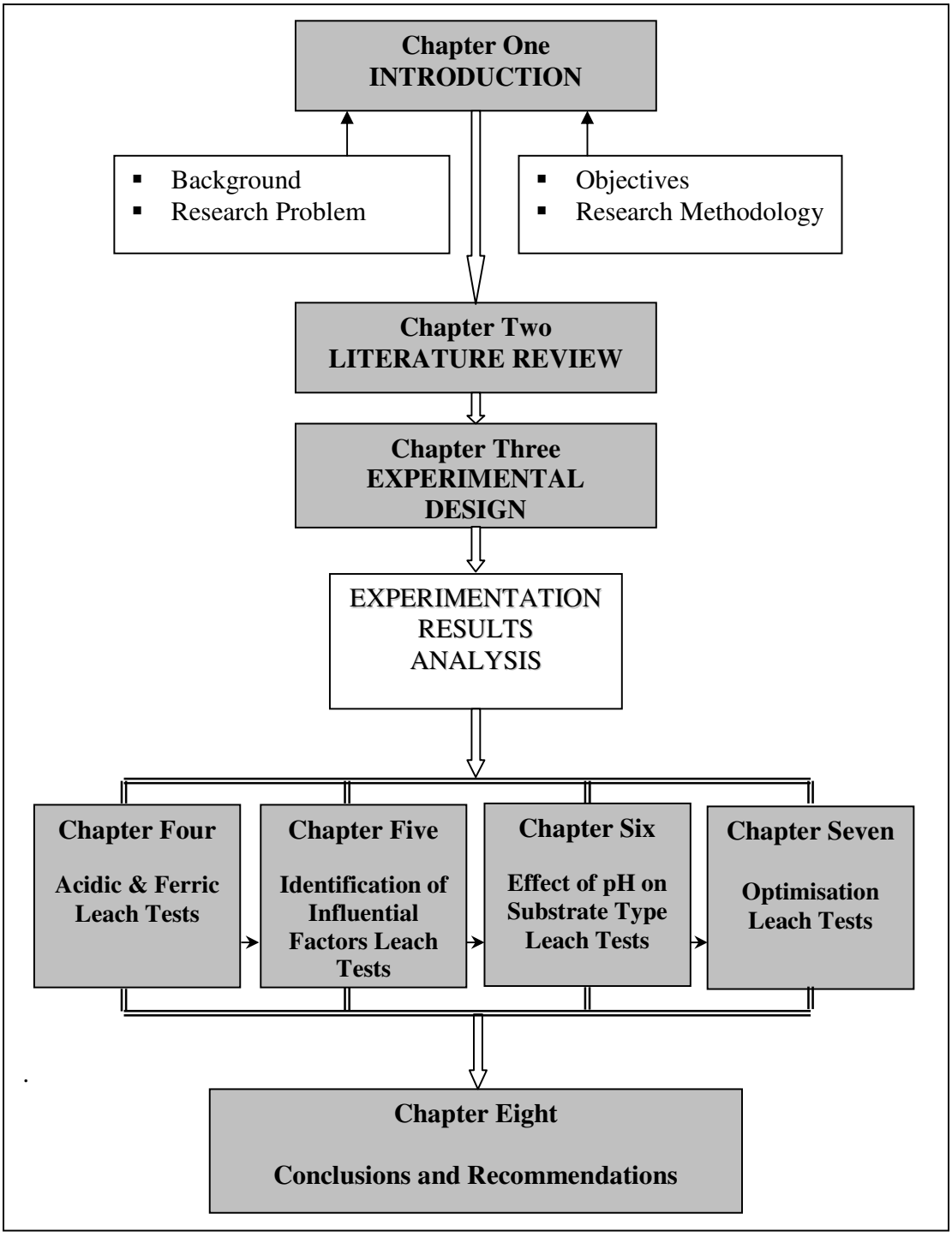


Figure 1.1. Dissertation layout

1.6 Summary

In this introductory chapter, the background, problem statement, and study objectives were discussed. The research methodology was then briefly described, followed by the dissertation layout.

CHAPTER TWO

LITERATURE REVIEW

"*For a research worker, the unforgotten moments of his (or her) life are the rare ones, which come after years of plodding work, when the veil over nature's secret seems suddenly to lift, and when what was dark and chaotic appears in a clear and beautiful light and pattern*".

- Gerty Cori (One of first few women to win the Nobel Prize)

2.1 General Introduction

Nickel is an important metal in human life and in the industry. In recent years, the world nickel demand has been driven by soaring steel production, particularly in China. With the rapid growing demand for nickel coupled with the depletion of high grade sulphide reserves, low grade nickel ores, which cannot be economically processed by conventional metallurgical processes, become increasingly important sources of nickel. Laterite ore, which is often considered as a low grade nickel ore, contains several kinds of metal elements including nickel, cobalt, iron, silicon, aluminium and chromium; and thus, constitutes an alternative source of nickel.

The aim of this literature review is to obtain a general knowledge of nickel laterites mineralogy and occurrence including the current metallurgical processes and the associated difficulties in the beneficiation of nickel laterites. The uses of nickel as the ultimate product are highlighted and discussed in the subsequent sections of this chapter. The general principles of the leaching process of ores are also discussed and include presentation of some of the chemical formulations for oxidation/reduction reactions of the elemental compounds. The importance of chemolithotrophic microorganisms in the oxidation of sulphur and reduced sulphur compounds, and subsequent production of sulphuric acid which can dissolve nickel laterites through protonation is also accentuated.

2.1.1 Nickel

Nickel (Ni) is a lustrous, silvery-white metal with atomic number 28 and atomic mass of 58.6934. Its electronic configuration is [Ar] $3d^8 4s^2$. It is both siderophile (i.e associates with iron) and chalcophile (i.e associates with sulphur). Some of its metallurgical advantages include high melting point of 1453℃, high resistance to corrosion and oxidation, good thermal and electrical conductivity, ferromagnetic

properties, catalytic behaviour, easy of electroplating and excellent strength and toughness at elevated temperatures.

Nickel is extracted from both sulphide and laterite (oxide) ores. Its final products are available in the form of cathode, powder, briquettes and pellet. Other products are ferronickel and nickel chemicals. The main markets for nickel are stainless steel, non-ferrous alloys and alloys which are used in building industries, cutlery, aerospace and military applications. Nickel is also used in batteries, fuel cells and coins. Additionally, nickel-alloys are a significant raw material in the chemical, petrochemical, and energy industries.

2.1.2 Nickel Laterites Mineralogy and Occurrence

The bulk of the mined nickel comes from two types of ore deposits – lateritic ores and sulphidic ores. These two ores are both of economic importance. The other two deposits in which nickel occurs are hydrothermal deposits and seafloor manganese nodules. Laterites represent approximately 70% of the world's onshore nickel resources (Elias, 2002; Gleeson et al., 2003; Dalvi et al., 2004; Watling, H. R., 2007) with the majority located in the tropical to subtropical climates. There are significant mineralogical differences with location (Krause et al., 1998). Lateritic deposits are often located very close to the surface (typically less than 50 m in depth depending on the age and degree of weathering), thus, they are easily mined by cheap open pit techniques.

Nickel laterites are residual products of a prolonged mechanical and chemical weathering of ultramafic rocks at the surface of the earth. The various original minerals unstable in the presence of water dissolve or breakdown and new minerals are formed that are more stable to the environment (Elias, 2002; Golightly, 1981;

Krause et al., 1998). This process results in the concentration by a factor of 3 to 30 times the nickel and cobalt content of the parent rock (Elias, 2002).

Nickel laterite formation, including type and grade is controlled by geological structure, tectonism, climatic and weathering history, regolith landform setting and topography (Elias, 2002; Gleeson et al., 2003). On the basis of mineralogy, nickel laterites are classified as oxide deposit, clay silicate deposit and hydrous silicate deposit (Brand et al., 1998; Elias, 2002). Nickeliferous limonite, $((Fe,Ni)O(OH).nH_2O$, is the oxide deposit consisting mainly of goethite with mean grades of 1.0-1.6% nickel. The hydrous silicate deposit is dominated by a mixed structure of hydrous magnesium-nickel silicates and is informally known as garnierite, $((Ni,Mg)SiO_3.nH_2O)$, with the highest global nickel grades averaging 1.8-2.5% (Brand et al., 1998; Gleeson et al., 2003). The clay silicate deposit is nontronite (Camuti and Riel, 1996) with mean grades averaging 1.0-1.5% nickel (Brand et al., 1998). The clay laterite is formed in less severe conditions when partially leached silica combines with iron, nickel and small amounts of aluminium (Elias, 2002). The mineralogical transformation involving the loss of magnesium and residual concentration of iron results in a familiar chemical trend in laterites; where magnesium decreases upwards and iron increases upwards through the laterite profile (Elias, 2002).

Nickel grade of sulphide ores typically ranges from 1- 4%. A major difference between laterites and sulphides processing is that sulphides are amenable to beneficiation processes such as flotation and magnetic separation, producing high grade concentrates that can be smelted. This is because in sulphide ores, most of the nickel is concentrated in sulphide minerals unlike the laterites where the nickel is dispersed through out the minerals. The most common nickel sulphide species is pentadlite ($(Fe, Ni)_9S_8$), which accounts for about 75% of the nickel production (Giaveno and Donati, 2001).

2.1.3 Currently Existing Nickel Laterites Processing Methods

Nickel laterites are mineralogically and chemically complex (unlike sulphides), which make their processing more complex and expensive. Nickel is present in the lateritic ores as a minor constituent of other minerals and, therefore, it is not amenable to concentration by any known conventional upgrading system (Valix et al., 2001a). A large volume of ore is, therefore, required to be treated in order to produce nickel from laterite ores (Elias, 2002). Recovery of nickel laterites is currently through conventional methods of pyrometallurgy and hydrometallurgy. The difference in mineralogy is the major factor controlling the choice of the treatment process; thus all the three classes of nickel laterite ore vary in processing requirements and economic value (Gleeson et al., 2003).

The concentration of iron, silica and magnesia which are the primary gangue elements define the most applicable treatment process. Smelting requires some magnesia for creating slag and, therefore, is not suitable for treating limonite with low magnesia and high iron while acid leaching cannot tolerate ores with high levels of magnesia due to the excessive high acid consumption (Taylor, 1997). In other words, in smelting, the silica to magnesium ratio in the feed is critical in controlling the melt temperatures and slag reactivity and viscosity (Elias, 2002). Table 2.1, gives an estimate of the global resources for nickel laterites, from the perspective of the processes employed to extract nickel (hydrometallurgical or pyrometallurgical), in millions of metric tonnes.

Table 2.1. Global resource for nickel laterites (Dalvi et al., 2004)

Processing method	Resource Mt	Assay % Ni	Ni content Mt	Distribution %
Pyrometallurgy	4,000	1.55	62	39
Hydrometallurgy	8,600	1.15	99	61
Total	12,600	1.28	161	100

Mt = Metric Tonnes; Ni = Nickel

As shown in Table 2.1, there is almost twice as much laterite resource that is amenable to hydrometallurgical processing (e.g. limonite, nontronite/smectite) compared to that amenable to pyrometallurgical processing (e.g saprolite and garnierite) (Elias, 2002; Dalvi et al., 2004). The higher source of laterite ore with a low nickel content that is more amenable to hydrometallurgical processing means that future plants will have to focus more on cheaper and environmental friendly hydro-processing routes.

Pyrometallurgy

This process treats the more nickel-rich silicate fraction (Elias, 2002). A minimum grade of 1.7% Ni (with low power cost) or 2.1% Ni (with high power cost) is required for an economic project (Dalvi et al., 2004). The two processes that are in practice are ferronickel smelting and matte smelting. The processes are very similar except that sulphur is added to the reduced ore in the kiln during matte smelting. Production of nickel matte is suited for low melting point slag in the range of 1.8 to 2.2 SiO_2/MgO ratio; whereas ferronickel is suited for high melting point slag in the range of either <2 or >2.5 SiO_2/MgO ratio (Dalvi et al., 2004). This process is an energy intensive process, which includes drying of the ore, calcination/reduction in a rotary kiln and smelting in electric furnaces in the presence of carbon and/or sulphur. The ferronickel (reduced Fe-Ni alloy) can be used directly for stainless steel production. The crude metal or matte can join the conventional sulphide route for further processing or refined to produce the final product (Dalvi et al., 2004).

Hydrometallurgy

There are a number of hydrometallurgical processes that are either in operation, are being piloted or evaluated. The two most common ones are discussed in the subsequent sections.

High Pressure Acid Leaching (HPAL): This process involves leaching ore at high pressure (4500 kPa) and elevated temperatures (≥250°C) in autoclaves. Pure oxide (limonitic laterite) is ideal for this process due to its lower magnesium and silica content and consequently, low acid consumption (Georgiou and Papangelakis, 1998; Elias, 2002). Magnesium and aluminium are strong acid consumers, and high levels of aluminium can cause the formation of alunite ($(H_3O)Al_3(SO_4)_2(OH)_6$) scale in the autoclave. A minimum process plant grade of 1.3% Ni is required for an economic project (Dalvi et al., 2004). In clayish laterites, the presence of colloidal silica in slurries and solutions released by breakdown of the clay can cause problems with high pressure pumping and solid-liquid separation (Elias, 2002) if used in HPAL. HPAL process has proven to be successful in extracting high levels of nickel and cobalt whilst minimizing extraction of iron and aluminium (Keyle, 1996; Reid, 1996; Georgiou and Papangelakis, 1998). However, HPAL requires sophisticated equipment, high degree of process control and skilled expertise to work properly (Dalvi et al., 2004). HPAL has a complicated solution and solids chemistry (Dalvi et al., 2004) which can lead to problems with engineering aspects and materials of construction.

Reduction roast-ammoniacal leach (Caron process): This can be used for processing high iron limonitic ores or a mixture of limonite and saprolite. However, excess silica decreases nickel recovery (Elias, 2002). The process involves drying and roasting in a reducing atmosphere followed by low pressure ammonia leaching (Elias, 2002; Gleeson et al., 2003).

This process has some disadvantages, which include lower nickel and cobalt recovery and, energy intensive pyrometallurgical steps at the front end of the processing cycle. The back-end, which is hydrometallurgical, requires various reagents (Dalvi et al., 2004).

2.2 Bacterial Leaching

2.2.1 Introduction

Many high-grade and easily exploited deposits of nickel and other minerals are becoming scarcer. Using biotechnology to study and recover low grade metallic values presents new business opportunities and has a significant impact on the metal industry. Among the biotechnologies, bacterial leaching is one of the most significant in the mining and minerals industry. Bacterial leaching or bioleaching is the extraction of metals from their mineral sources by using microorganisms. Bacterial leaching is now being used as an alternative approach to the high energy, capital intensive and environmental unfriendly conventional hydrometallurgical and pyrometallurgical methods. It is an acceptable practice considered as a successful and expanding area of biotechnology (Rawlings and Johnson, 2007).

2.2.2 Microorganisms Used in Leaching

The microorganisms which are important in the biohydrometallurgical processes concerned with metal extraction may be divided into two groups on the basis of nutritional requirements, i.e., chemolithotrophic and heterotrophic microorganisms. A review of these microorganisms is given here because the knowledge of their characteristics is important in the selection of suitable conditions during the bioleaching processes.

Chemolithotrophic microorganisms

Amongst the chemolithotrophic bacteria involved in bacterial leaching, the acidophilic, iron- or sulphur- oxidizing chemolithotrophic microorganisms have been studied most intensively and are the most important in commercial operations to date (Rawlings, 2005). Current worldwide biooxidation and bioleaching research and

operations utilising these organisms are focused essentially on gold (Brierley and Brierley, 2001; Nestor et al., 2001; Iglesias and Carranza, 1994) and copper production (Cancho, et al., 2007; Waitling, 2007; Sadowski et al., 2003; Gericke and Pinches, 1999). Some commercial bacterial leaching plants include the gold processing plants in Fairview in South Africa and Ashanti in Ghana; and the copper processing plants like Dos Amigos in Chile; Cerro Verde in Peru; and S & K Copper in Myanmar (Brierley and Brierley, 2001).

This particular study focuses on the use of a mixed culture of *Acidithiobacillus ferrooxidans, Acidithiobacillus caldus* and *Leptospirillum ferrooxidans* in the bacterial leaching of nickel laterites. These typically are acidophilic microorganisms because they can grow optimally at pH < 3 (Norris and Johnson, 1998).

Previous studies by Giaveno and Donati (2001) have shown that mixed cultures are more efficient than pure cultures because of the co-operation of the mechanisms involved in the mixed cultures. There is also a possibility of competition for oxygen by iron oxidising bacteria that could lead to reductive dissolution of ferric iron in nickel laterites, thus destabilizing the structure of the nickel literites (Bridge and Johnson, 1998). As indicated in the following equation, the reduction of soluble ferric iron by bacteria can result in the equilibrium between solid-phase iron (III) and soluble-phase iron (III) being shifted somewhat, accelerating the dissolution of the mineral: $Fe^{3+}_{\text{solid phase}} \leftrightarrow Fe^{3+}_{\text{soluble phase}} \rightarrow Fe^{2+}$ (by bacterial reduction).

Acidithiobacillus ferrooxidans. This is a motile, non-sporulating, Gram-negative, rod-shaped 0.3-0.5x1.0-1.7µm (Karavaiko et al., 2006) and has a physiology ideally suited for growth in an inorganic mineral environment (Mason and Rice, 2002). It is motile by means of a single polar flagellum (Torma, 1977; Jensen and Webb, 1995). It was originally isolated and characterized as being autotrophic and chemolithotrophic by Temple and Colmer (1951). It was renamed from *Thiobacillus*

ferrooxidans by Kelly and Wood (2000). It grows using CO_2 as the sole carbon source and obtains energy from the oxidation of sulphur and reduced sulphur compounds as well as that of the oxidation of ferrous ion. The bacterium thrives in an aerobic environment, though it is also able to grow anaerobically with ferric iron as terminal electron acceptor and reduced sulphur or metal sulphides or formate as electron donors (Pronk et al, 1991, 1992; Drobner et al., 1990).

Leptospirillum ferrooxidans. These are strictly aerobic, obligately chemolithotrophic, Gram-negative, motile vibrios, spirals, or pseudococci, 0.2-0.5x0.9-2.0µm. They are more acid resistant (Norris, 1983) and more tolerant of high temperatures (20-45°C) than *Acidithiobacillus ferrooxidans* (Rawlings et al., 1999). These microorganisms obtain the energy required for survival from the oxidation of reduced iron containing compounds (Rawlings et al., 1999).

Acidithiobacillus caldus. They are moderately thermophilic, aerobic, Gram-negative motile rods, 0.7-0.8x1.2-1.8µm (Karavaiko et al., 2006), each with a single polar flangellum (Hallberg and Lindström, 1994). This bacterium is capable of oxidizing a wide range of reduced inorganic sulphur compounds but not metal sulphides (Hallberg et al., 1996). However, this bacterium may be found with others associated with leaching because of the presence of reduced inorganic sulphur compounds (elemental sulphur and tetrathionate) resulting from leaching of sulphides. Tetrathionate ($S_4O_6^{2-}$) which occurs as a metabolic intermediate in the oxidation of some reduced sulphur compounds can be used as the sole energy source for acidithiobacillus caldus (Bugaytsova and Lindstrom, 2004).

Heterotrophic microorganisms

Several heterotrophic microorganisms, including both bacteria and fungus species are known for their leaching ability, especially of oxidic, siliceous or carbonaceous material (Willscher and Bosecker, 2003). Heterotrophic microorganisms have also

been studied in a quest to recover nickel from low grade nickel laterites (Tzeferis, 1994; Valix et al., 2001a, b; Tang and Valix, 2006). These microorganisms, in direct contrast to autotrophs, ingest biomass to obtain their energy and nutrition. The heterotrophs have an absolute dependence on the biological products of autotrophs. This is because they obtain their carbon for growth solely by feeding on the carbon produced by autotrophs (e.g., dead plants and dead organic matter). *Aspergillus* and *Penicillium* are the two widely studied strains of heterotrophic microorganisms that can be used in the bacterial leaching. The effectiveness of these strains was found to depend on their ability to produce hydroxycarboxylic acids, especially citric acid (Tzeferis, 1994). The acids produced usually have dual effects of increasing metal dissolution by lowering the pH, and that of increasing the load of soluble metals by complexion/chelating into soluble organic-metallic complexes (Tzeferis, 1992). Apart from nickel laterites, the use of heterotrophic micro-organisms have been tested in the bioleaching of zinc ores (Dave et al., 1981), extraction of lithium from spodumene (Ilgar et al., 1993), treatment of quartz sands (Ehrlich, 1988), biobeneficiation of bauxite to remove calcium and iron (Vasan et al., 2001), and recovery of aluminium from low grade bauxite ore (Ghorbani et al., 2007). However, currently there is no known commercial application of these microorganisms in the mining industry.

2.2.3 Bioleaching of Metal Sulphide Ores

Many studies on the leaching action of microorganisms have involved mainly sulphide ores of copper and /or iron (Ross, 1990). The bacterial oxidation of sulphide minerals by *Acidithiobacillus* bacteria is a well established phenomenon in the commercial industry for the recovery of copper, uranium and in the biooxidation pretreatment of refractory sulphidic gold ores before cyanidation (Acevedo, 2000; Brierley and Brierley, 2001; Nestor et al., 2001 ; Kodali et al., 2004; Ndlovu, 2008). In this process, the microorganisms are used to oxidize pyrites and arsenopyrites to expose the gold occluded within the sulphide mineral matrix.

Sulphide ores containing nickel and many other elements can also be bioleached using iron- and /or sulphur- oxidising bacteria such as *Acidithiobacillus ferrooxidans, Acidithiobacillus caldus* and *Leptospirillum ferrooxidans*. The nickel sulphide ores that have been studied with commercial interest include millerite (NiS), nickeline (NiS), violarite ($(Ni,Fe)_3S_4$), bravolite ($(Ni,Fe)S_2$) and Pentlandite ($(Fe, Ni)_9S_8$) (Giaveno and Donati, 2001). These ores are amenable to bacterial leaching because they contain ferrous iron and/or reduced sulphur which provide energy for the chemolithotrophic microorganisms. In particular, low grade nickel sulphide ores such as pyrrhotite ($Fe_{1-x}S$), where x=0-0.125, and the so-called Duluth Gabbro are suited for bioleaching (Watling, 2007). These ores cannot be subjected to the traditional high-temperature processing because they are considerably difficult to concentrate. Although bioleaching provides the possibility of recovering metals from low-grade deposits that would otherwise be considered waste, its application greatly depends on the value of the metal to be recovered. A major challenge is to find a suitable match between an ore body and bioleaching technology. For example although the bioleaching technology for nickel recovery using bacteria known as the the BioNIC™ process has been thoroughly tested, no ore body of a suitable concentration and size has been identified as yet to allow economic recovery at current nickel prices. There is thus, currently no known existing commercial application of the bioleaching of sulphide ores containing nickel in the mining industry.

2.2.4 The Mechanisms of Bacterial Leaching of Metal Sulphide Ores

The microbial effects of bacteria and fungi on minerals are based mainly on three principles, namely acidolysis, redoxolysis, and complexolysis (Tzeferis, 1992). Microorganisms are able to mobilize metals by the formation of organic or inorganic acids (protons); oxidation and reduction reactions; and the excretion of complexing agents. In particular, metal extraction from mineral ore by chemolithotrophic bacteria

is achieved through two main reactions: the oxidation of ferrous to ferric iron and that of sulphide/sulphur to sulfuric acid (Equation 2.1).

$$\left.\begin{aligned} 2Fe^{2+} + 0.5O_2 + 2H^+ &\xrightarrow{\text{bacteria}} 2Fe^{3+} + H_2O \\ H_2S + 2O_2 &\xrightarrow{\text{bacteria}} H_2SO_4 \\ S^0 + 1.5O_2 + H_2O &\xrightarrow{\text{bacteria}} H_2SO_4 \end{aligned}\right\} \quad (2.1)$$

Models of dissolution mechanisms of sulphur and iron bearing minerals

Previously, the leaching mechanism of sulphide bearing minerals was thought of as comprising of two or three different mechanisms (Fowler, et al., 2001; Eligwe, 1988; Boon et al, 1995). Firstly, the direct mechanism which assumes that bacteria attach onto the mineral particle surfaces, and directly oxidize iron and sulphur moieties in the mineral by biological means to release metal ions in solution (Equation 2.2). The second mechanism, the indirect mechanism, is assumed to involve the bacteria in solution oxidizing ferrous ion to ferric ion and elemental sulphur to sulphate ions (Equations 2.4 and 2.5 respectively). Ferric ion is a strong oxidizing agent and this in turn attacks the sulphide mineral producing metallic ions, ferrous ions in solution and elemental sulphur (Equation 2.3).

$$MS_x + (2X\text{-}0.5)O_2 + H_2O \xrightarrow{bacteria} M^{x+} + XSO_4^{2-} + 2H^+ \quad (2.2)$$

$$MS_x + Fe^{3+} \xrightarrow{Chemical} M^{x+} + XS^0 + Fe^{2+} \quad (2.3)$$

$$2Fe^{2+} + 0.5O_2 + 2H^+ \xrightarrow{bacteria} 2Fe^{3+} + H_2O \quad (2.4)$$

$$S^0 + 1.5O_2 + H_2O \xrightarrow{bacteria} SO_4^{2-} + 2H^+ \quad (2.5)$$

(where M is a metal)

The third mechanism, indirect contact mechanism, assumes that the bacteria attach themselves onto the mineral particle surfaces and excrete polymers forming an exopolymeric layer. The bacteria subsequently oxidize ferrous iron to ferric iron

within this exopolymeric layer, and the generated ferric iron leaches the mineral within this compartment (Equation 2.3 and 2.4, respectively).

The recent developments in the bioleaching of sulphide minerals have combined all facts about the 'indirect' and 'direct' leaching mechanisms with the following features (Sand et al., 2001):- cells have to be attached to the mineral and in physical contact with the surface; cells form and excrete exopolymers; these exopolymeric envelopes contain ferric iron compounds which are complexed to glucuronic acid residues. These are part of the primary attack mechanism; thiosulphate is formed as intermediate by-product during the oxidation of sulphur compounds; sulphur or polythionate granules are formed in the periplasmatic space or in the cell envelope.

Currently, the two postulated 'indirect' mechanisms with no evidence for a 'direct' enzymatically mediated process are termed the thiosulphate mechanism and the polysulphide mechanism (Hanford and Vargas, 2001; Schippers and Sand, 1999; Sand et al., 2001). The mineralogy and electronic structural configuration of sulphides determines the type of leach mechanism (Hanford and Vargas, 2001; Schippers and Sand, 1999; Sand et al., 2001). Metal sulphides with valence bands that are derived only from orbitals of the metal atoms cannot be attacked by protons (acid-nonsoluble). In contrast, metal sulphides with valence bands derived from both the metal and sulphide orbitals, are more or less soluble in acid (acid-soluble).The influence of mineralogy, in particular crystal orientation, was also observed in the bacterial leaching of pyrite (Ndlovu and Monhemius, 2005).

The thiosulphate mechanism involves solely the chemical reaction of ferric iron with acid-insoluble metal sulphides (FeS_2, MoS_2 and WS_2) producing thiosulphate (Schippers and Sand, 1999). Thiosulphate which is unstable in acidic liquors, particularly in the presence of ferric iron, reacts further with ferric iron in a series of

reactions via tetrathionate ($S_4O_6^{2-}$), disulphane-monosulphonic acid ($HSSSO_3^-$) and thionate with the final product being sulphate (Schippers et al., 1996).

The polysulphide reaction mechanism involves the attack of acid soluble sulphides (ZnS, NiS, CoS, $CuFeS_2$ and PbS) by ferric iron and protons. The proton mediated dissolution forms free metal ions and hydrogen sulphide (Equation 2.6) and the hydrogen sulphide formed is microbially oxidized to sulphuric acid (Equation 2.7) (Johnson, 2003).

$$MS_x + 2XH^+ \xrightarrow{chemical} M^{x+} + XH_2S \quad (2.6)$$

$$H_2S + 2O_2 \xrightarrow{bacteria} H_2SO_4 \quad (2.7)$$

(where X is a whole number).

The metal attack by ferric iron forms ferrous iron and polysulphide (Equation 2.8). Polysulphides are a general class of compounds in which sulphur is polymerized and reduced, generally of the form M_2S_n ($n > 2$) with typical value of *n* not being more than 6 (Klauber, 2008). The polysulphide is oxidised by ferric iron producing elemental sulphur (Equation 2.9). The sulphur produced is reasonably stable under experimental and environmental conditions and can only be degraded to sulphuric acid (Equation 2.10) by sulphur oxidizing microbes such as *acidithiobacillus thiooxidans* (Schippers and Sand, 1999). The sulphuric acid formed enhances the dissolution of sulphide metals by proton attack (Johnson, 2003).

$$MS_x + Fe^{3+} + 2H^+ \xrightarrow{Chemical} M^{x+} + H_2S_x + Fe^{2+} \quad (2.8)$$

$$H_2S_x + 2Fe^{3+} \xrightarrow{Chemical} 0.125XS_8 + 2Fe^{2+} + 2H^+ \quad (2.9)$$

$$0.125S_8 + 1.5O_2 + H_2O \xrightarrow{bacteria} SO_4^{2-} + 2H^+ \quad (2.10)$$

The role of the bacteria in both the thiosulphate and polysulphide mechanisms is to regenerate the ferric iron and protons consumed by the leach reactions (Hanford and Vargas, 2001).

In summary, the oxidation of biological relevant reduced sulphur compounds (sulphides, comprising aqueous (hydro) sulphide as well as insoluble metal sulphides, polysulphides, elemental sulphur, sulphite, thiosulphate and polythionates (such as tri-, tetra-, and pentathionates) and the subsequent acid generation can be of great importance for the bioleaching of nickel laterites.

2.2.5 Bacterial Leaching of Nickel Laterite Ores

Although several processes have been proposed for the treatment of nickel laterites by conventional pyrometallurgical and hydrometallurgical routes, none of the processes have gained general acceptance in the industry because of high capital cost and technological outlay. However, biohydrometallurgical processes such as bioleaching have been long since accepted as simple to use, of low capital cost and of minimum environmental impact. The possibility to employ heterotrophic organisms to treat non-sulphide ores such as nickel laterites has been described by several authors (Bosecker, 1986; Groudev, 1987; Tzeferis et al., 1991; Tzeferis and Agatzini-Leonardou, 1994; Valix et al, 2001a,b). Heterotrophic microorganisms have the potential of producing organic acidic metabolites from carbohydrates that are able to solubilise oxide, hydroxide, silicate and carbonate minerals; thus yielding nickel as the required by-product.

Organic acids produce protons which contribute to proton promoted mineral dissolution. Organic acids can also complex with metal ions in solution, lowering metal activity and increasing the apparent solubility of the mineral (McKenzie et al., 1987). The major impact of organic acids may be that metal-organic complexes can form at the solid-solution interface, weakening cation-oxygen bonds, thus catalyzing

the dissolution reaction. Dissolution is in this case enabled by redox reactions in which the organic acid reduces the metal ion at the surface (McBride, 1989).

The following are some of the possible reactions described above that can take place to finally produce nickel ions (Tzeferis, 1992):-

Proton attack

$$\left.\begin{aligned} NiO + 2H^+ &\rightarrow Ni^{2+} + H_2O \\ CaCO_3 + 2H^+ &\rightarrow Ca^{2+} + H_2O + CO_2 \end{aligned}\right\} \quad (2.11)$$

Reduction

$$MnO_2 + 2e^- + 4H^+ \rightarrow Mn^{2+} + 2H_2O \quad (2.12)$$

Complexation / Chelation

$$Ni^{2+} + C_6H_8O_7 \rightarrow Ni\,(C_6H_5O_7) + 3H^+ \quad (2.13)$$

However, the use of these heterotrophic organisms poses a danger of possible contamination by undesirable organisms under commercial scale condition. In addition commercial mineral biooxidation processes using heterotrophic microorganisms are unlikely to be viable because of the vast amount of carbon sources, for example molasses, required for metabolism (Rawlings, 2005).

The use of chemolithotrophic bacteria in the treatment of sulphide ores is a well established and commercial viable technology in the mineral processing industry. However, non-sulphide ores or minerals low in sulphur such as nickel laterites are difficult to effectively solubilise using chemolithotrophic microorganisms. This is because non-sulphide ores do not contain sufficient reduced sulphur to provide energy for the chemolithotrophic microorganisms. The oxidation of reduced sulphur

to sulphuric acid by chemolithotrophic microorganisms is essential in the solubilisation of non-sulphide ores. Alternatively, the metal value in the nickel laterites may be recovered by allowing the primary oxidation of pyrite, or similar iron/sulphur minerals to provide sulphuric acid solutions, which then solubilises the metal content. This can be made possible by employing chemolithotrophic bacteria such as *Acidithiobacillus ferrooxidans, Acidithiobacillus caldus* and *Leptospirillum ferrooxidans*. These microorganisms, unlike heterotrophs, use CO_2 as their sole source of carbon and derive their energy from the oxidation of reduced sulphur and/or ferrous iron, ultimately producing sulphuric acid (Rossi, 1990; Hanford and Vargas, 2001; Schippers and Sand, 1999) as shown in Equations 2.8 – 2.10.

The sulphuric acid produced maintains the pH at levels favourable to the bacterial activities (Rossi, 1990) and can help in the effective leaching of nickel laterite ores. The hydrogen ions can displace metal cations (Equation 2.11) from the ore matrix, thus inducing the dissolution of the metals (Tzeferis, 1992).

Chemical tests carried out on nickel laterites have indicated that sulphuric acid leached the metals more rapidly and extensively than the organic acids (Alibhai et al., 1993). Sulphuric acid is also preferred in terms of cost, corrosion, wear and can easily be regenerated in solvent extraction and electrowinning plants (Davenport et al., 2002); thus making it easy for the bacterial leaching to be retrofitted into the existing plants.

Due to the problems associated with high pressure acid leaching during operation and commissioning of nickel laterites plants (e.g, Murrin Murrin plant, Australia), sulphuric acid leaching at atmospheric pressure is now receiving more attention. Agitation and column tests have shown that the Greek serpentinic nickeliferrous ore could be leached with sulphuric acid at atmospheric pressure with recoveries of up to 74% and 60%, respectively (Agatzini-Leonardou and Zafiratos, 2004).

In summary, the generation of sulphuric acid and its subsequent use can be of great importance for the leaching of nickel laterites.

2.2.6 The Kinetics of Leaching Reactions

Both the kinetics and the final metal recoveries depend on the mineralogical type of the ore (Tzeferis and Agatzini-Leonardou, 1994; Valix et al., 2001b). The difficulty in mobilizing metals, e.g. nickel, from various minerals phases is different and this difference is generally reflected on the leaching effectiveness (Tzeferis and Agatzini-Leonardou, 1994).

Thermodynamic data can only indicate the tendency of a reaction but not the rate of reaction or detailed mechanism. This is particularly so in the case of leaching reactions which are heterogeneous in nature and comprise several sequential stages (Jackson, 1986). For heterogeneous systems, the reaction kinetics are based on the shrinking core model (Levenspiel, 1972; Smith, 1981; Han, 2002). This is the most widespread and realistic model describing fluid-solid reaction kinetics of dense (non-porous) particles. Examples of the fluid-solid reactions include, the oxidation of sulphide minerals to yield oxides by reducing gases, and the extraction of metals from ores using acids (Levenspiel, 1972).

In hydrometallurgy, the uses of the shrinking core model for the solid-liquid systems have been extensively examined (Crundwell, 1995; Veglio et al., 2001). They are generally applied to describe the shrinkage of ore particles during mineral leaching reactions which are a central unit operation in the hydrometallurgical ore treatment. Although there is also literature data on the use of shrinking core model for modeling the bacterial leaching process (Brochot et al., 2004; Leahy, 2005), most of the data concern the bioleaching of sulphide ores. The bioleaching of sulphide ores also follow the same principles of the shrinking core model as described below (i.e., the

establishment of a link between the leaching kinetics and the changes in the particle sizes).

Based on the shrinking core model, the mechanism of the non-catalysed heterogeneous reaction may take place as follows. Initially the reactants diffuse from the bulk of the first phase to the interface between the phases.

If an additional layer of solid products and inert material is present at the interface the reactants would have to overcome the resistance of this layer before reaching the surface of the second layer. Then, diffusion of reactants from the interface to the bulk of the second phase takes place. Furthermore, chemical reactions between the reactants in phase one and those in phase two occur. Finally, the products diffuse within the second phase and/or out of phase two into the bulk of phase one (Levenspiel, 1972; Smith, 1981; Han, 2002).

It must be pointed out here that at times some of these steps do not exist. In addition, the resistances of the different steps usually vary greatly from one another. Depending on which step is the slowest, that step would consequently be limiting to the overall reaction; therefore, identifying this step is of utmost importance (Smith, 1981).

For spherical particles involving the quasi-steady state diffusion of the reactant through the previously reacted portion of the particle, followed by the chemical reaction at the surface of the unreacted core, it is useful to express the reaction rates in terms of fractions reacted (i.e., particle conversion). Derivation of equations governing these rate controlling regimes (Table 2.2) can be found in the literature (Levenspiel, 1972; Smith, 1981; Han, 2002).

Tests of these model equations against the rate data are not convincing evidence of a particular mechanism (Prosser, 1996; Gbor and Jia., 2004). A review by Prosser

(1996) indicated a lot of variables and phenomenon that may affect the rate and reaction regime of a leaching process. Gbor and Jia (2004) indicated that some researchers have commented that the ash layer diffusion controlled equation of the shrinking core model may not be applied to liquid-solid reactions (e.g leaching) because it was derived using the pseudo-steady state approximation; that is, the rate of movement of the interface (between the un-reacted core and the ash/inert layer) is much slower than the rate of diffusion.

Table 2.2. Shrinking core models

Regime	Equation
Film diffusion control	$X = kt$
Chemical reaction control	$1-(1-X)^{1/3} = kt$
Ash diffusion control	$1-3(1-X)^{2/3}+2(1-X) = kt$

X= fractional conversion; t = time (days); k = rate constant (day^{-1})

One major factor that can affect the interpretation of the leaching data is the particle size distribution (PSD) of the solid material (Gbor and Jia, 2004). Neglecting the PSD would shift the kinetic control regime to the other reaction regime depending on the coefficient of variation (CV). CV is the ratio between the standard deviation of the particle size range and the mean of that particle size range. Gbor and Jia (2004) came up with the conclusions that, (1) neglecting PSD would shift control regime from chemical reaction to inert/ash layer diffusion when CV is between 0.7 and 1.2; (2) for systems controlled by liquid film diffusion, neglect of PSD would shift control regime to chemical reaction when CV is between 0.3 and 0.7 or to inert/ash when CV is greater (0.9-1.5); (3) an inert/ash layer diffusion controlled process was insensitive to neglect of PSD, and that when CV is less than 0.3, neglect of PSD would not cause any erroneous shift. Veglio et al (2001) also found significant differences between the

kinetic models that ignored the particle size effect and the one that incorporated the particle size effect.

One of the convincing ways of finding out the mechanism controlling the shrinkage processes is the use of activation energies. In other words, the magnitude of the activation energy can provide a more positive evidence for the reaction and diffusion controlled regimes (Gbor and Jia, 2004). In the case of the reactant diffusion through the fluid surrounding the particle control, the activation energy is $\leq$ 25kJ/mol; if the process is controlled by ash diffusion, the activation energy is $\leq$ 25kJ/mol; for chemical reaction control, the activation energy is either high or low (Prosser, 1996). However, the most consistent and more acceptable argument is that chemical controlled reactions have very high activation energies in excess of 40kJ/mol (Gbor and Jia, 2004). It must be noted, though, that different parameters of the rate data have been used in Arrhenius plots. Two common versions are the slope of the line, k, drawn through equations like those in Table 2.2, and the initial rate; that is, the slope of the data locus at small values of time. The third version uses a parameter calculated by numerically fitting a polynomial equation (e.g., $y = a + bt + ct^2$) to data, and calculating the slope at $t = 0$. The three versions yield different values for the activation energy (Dutrizac, 1981; Antonijevic et al., 1994). One disputed assumption when using the Arrhenius equation states that the pre-exponential factor, A, in the Arrhenius equation is independent of temperature. That implies that every variable which has an effect on the rate of reaction is unchanged when the temperature of the system is changed. There are some systems for which such assumption is clearly incorrect.

2.3 Summary

This study is aimed at establishing the potential for the bacterial leaching of nickel laterites using chemolithotrophic microorganisms with an external supply of sulphur

containing material for energy purposes. Bacterial leaching is a process in which microorganisms are utilised to help in the recovery of metals from their ores/concentrates. The literature review contained in this chapter has shown the difficulty involved in the processing of nickel laterites using conventional methods (section 2.1.3). Nickel laterite contains metal values, but is not capable of participating in the primary bacterial oxidation because it contains neither ferrous iron nor substantial amount of reduced sulphur. However, its metal value can be recovered by allowing the primary oxidation of pyrite, or similar iron/sulphur minerals to provide sulphuric acid solutions, which solubilise the metal content.

The oxidation of the sulphur moiety and ferrous iron can be made possible by the use of chemolithotrophic bacteria. These chemolithotrophic bacteria require their substrates to contain ferrous iron or reduced sulphur (including sulphides, disulphides or arsenosulphides) or both, depending upon the bacterial species, in order to gain energy for cell maintenance and growth. It is also indicated that organic acids can act as chelating agents in complex formation with metal ions. In this review, therefore, the potential of elemental sulphur (S_8) or pyrite (FeS_2) addition and subsequent biological acid generation for the bioleaching of nickel from nickel laterites was investigated and postulated to be a possible nickel recovery process.

CHAPTER THREE

MATERIALS AND METHODS

"*If you don't learn from mistakes, there's no need making them*".

-Herbert V. Prochnow

3.1 Introduction

This chapter discusses the preparation of the materials as well as the experimental and analytical methods employed in the study. Data analysis is also discussed. A summary is subsequently provided to wrap-up the chapter.

3.2 Materials

3.2.1 Nickel Laterite Ore

The nickel laterite ore used throughout this study was provided by Mintek, South Africa. The ore was crushed and finely ground in a ball mill. The ground material was dry sieved using standard sieve plates and was classified into different size fractions depending on the nature of the experiment. Dry sieving was chosen over wet sieving because (i) dry sieving may reduce the disruption of physical structures of nickel laterite ore compared with wet sieving, (ii) water-soluble components of nickel laterites can be determined on aggregates separated from dry sieving which are not possible in wet sieving, (iii) aggregates separated by dry sieving may represent more closely those in the field during the absence of rain or irrigation, and (iv) very small samples could be utilised.

Representative samples were prepared by coning and quartering. Prior to experimentation, the percent nickel composition in the laterite was calculated as a percentage of the total mass of the nickel laterite ore (see example in Appendix A). This % nickel composition in the laterite was determined using the Varian SpectrAA-55B atomic absorption spectrophotometer after digestion of ore with aqua regia (3:1 ratio of HCl and HNO_3 mixture). The composition of nickel laterite ore is given in Appendix B.

3.2.2 Reagents

All reagents used in this study were of analytical grade obtained from Merck, South Africa (unless stated otherwise), and were used as obtained without further purification. The chemically pure elemental sulphur assayed 98.0-102.0%. Sulphur was used as obtained with the particle sizes of < 38 μm.

3.2.3 Pyrite

Pyrite used in this study was obtained from African Gems and Minerals, South Africa. Pyrite was chosen because it is the most widespread and represents the highest composition of sulphur over the other types of sulphide ores. It was crushed and finely ground to <38 μm (i.e same as that of sulphur substrate). The chemical composition of the pyrite as given by the supplier was: Fe = 45.9%, S = 53.7%, other elements = 0.4%.

3.3 Bacterial Growth and Maintenance

3.3.1 Standard 9K Medium (Silverman and Lundgren, 1959)

The standard 9K media composition used for the growth of the bacteria was as follows (in gpl):- $(NH_4)_2SO_4$,3.0; K_2HPO_4,0.5; $MgSO_4$,0.5; KCl, 0.1, $Ca(NO_3)_2$,0.01; $FeSO_4.7H_2O$,44.22; 0.5M H_2SO_4 for desired pH and distilled water for desired volume make up, appropriate energy sources (pyrite or elemental sulphur).

3.3.2 Bacterial Growth

The microorganisms used through out this study were a mixed culture of bacteria (*Acidithiobacillus ferrooxidans, Acidithiobacillus caldus* and *Leptospirillum*

ferrooxidans). The original bacteria were provided by Mintek, South Africa. The bacteria were grown in standard 9K medium with the composition specified in section 3.3.1. The medium was first adjusted to an appropriate pH (1.8-2.0) and then sterilised by autoclaving at 121℃ for 20 minutes. An appropriate amount of sterilised energy source (pyrite or sulphur) was then added. The medium was then inoculated with 10% v/v of bacteria and incubated at 30-35℃ at a pH of 1.8-2.0 on a platform shaker. Growth was monitored by monitoring the apparent bacterial population using the UV-Visible spectrophotometer shown in Figure 3.1.



Figure 3.1. The UV-Visible spectrophotometer

3.3.3 Bacterial Cell Harvesting

After the bacteria have been grown in accordance with the procedure mentioned in section 3.3.2, the culture was harvested after five to seven days (Mason and Rice, 2002; Mehta et al., 2003) according to the procedures described by Silverman and Lundgren (1959), and Nestor et al (2001). The bacterial culture was filtered to remove precipitates using Whatman filter # 1 and the filtrate was then centrifuged for 60 minutes. The mixture was then transferred to acidified distilled water at pH of 1.8-2.0 and shaken for about a minute and then put in a fridge and allowed to settle for 6hrs.The turbid supernatant was then recovered. The cells were then removed from the supernatant by centrifuging and then washed with acidified distilled water until

the cells were clean. The cells were then suspended in acidified water at pH of 1.8-2.0 and stored at 4˚C, and kept for use in the bioleaching experiments.

3.3.4 Determination of Bacterial Population using UV-Visible Spectrophotometer

The bacterial population was determined by measuring turbidity or optical density of the bacterial suspension using a UV-Visible double beam spectrophotometer (Model 4802). Since turbidity is directly proportional to the number of cells, this property was used as an indicator for bacterial concentration. The cells suspended in the suspension interrupt the passage of light allowing less light to reach the photoelectric cell and the amount of light transmitted through the suspension was measured as percentage transmission (or %T). The turbidity for cell suspension was measured at 550 nm (Plumb et al., 2008) against sterile 9K media as a reference. The wavelength of 550 nm is chosen because at this wavelength changes in both size of the cells as well as changes in the total nucleotide concentrations are reflected (Alupoaei and García-Rubio, 2004).

Note that the relationships among absorbance (A), transmittance (T) and optical density (OD) are as follows; T = , where I is the light passing through the sample and I0 is the light hitting the sample. A = . Optical density is a measure of absorbance and is related to transmittance by the following expression; OD = 2 – log (%T).

Other available methods based upon measurement of nitrogen or protein content or ammonia consumption, and that of using the phase contrast microscope were less convenient and slower than the UV-Visible double beam spectrophotometer. On the other hand, the UV-Visible spectrophotometer is a versatile, quantitative, rapid, and reliable analytical tool (Alupoaei and García-Rubio, 2004). It must be noted, however, that this method measures both the dead and active bacteria as it does not differentiate between the two states. However the results obtained used in conjunction

with pH and redox potential changes would reasonably outweigh the disadvantages of counting the dead bacteria. Prior to reading the samples were filtered through Whatman filter number 1 to remove any solid particles.

3.4 Experimental Methods

3.4.1 Design of Experiments

Two of the aims of this study can be summarised as; (1) screening and identification of important factors, and (2) optimization of important factors. The design of experiments methodology (DOE) was employed in executing these two objectives. The greater advantage of DOE is that it provides an organized approach in which an appropriate experimental objective can be selected. Thus, by using DOE, one obtains more useful and more precise information about the studied system, because the joint influence of all factors is evaluated.

Screening of factors (Chapter 5) was done at the beginning so as to explore some factors in order to reveal whether they have any influence on the response (nickel recovery), and to identify their appropriate ranges. A quarter basic fractional factorial designs 2^{5-2}_{III} with a fold-over were used in determining the influential factors. The experimental results were analysed statistically for the significance of the factors using the probability plots.

Optimisation of factors (Chapter 7) was done after screening so as to predict the response values for all possible combination of factors within the experimental region, and to identify an optimal experimental point. The response surface methodology (RSM) was used in the optimisation of important factors. The design procedure for the RSM was as follows (Gunaraj and Murugan, 1999): (1) designing and performing a series of experiments for the adequate and reliable measurement of

the response (nickel recovery), (2) developing a mathematical model, (3) finding the optimal set of experimental parameters and, (4) representing the effects of process parameters through three dimensional (3-D) plots.

The optimisation experiments were designed using central composite design, and the optimal set of parameters was determined using ridge analysis method (see Appendix H). In central composite designs, the factorial designs are augmented with axial designs. The term "central composite design" arises because the centres of the factorial and axial designs coincide (Öberg and Deming, 2000). A quadratic response surface model of the form,

$$y = \beta_0 + \sum_{i=1}^{k} \beta_i X_i + \sum_{i=1}^{k} \beta_{ii} X_i^2 + \sum_{i=1}^{k} \sum_{j=i+1}^{k} \beta_{ij} X_i X_j + \varepsilon \qquad (3.1)$$

was fitted and solved using the method of least squares. In Equation 3.1, y is the predicted response, β_0 is the coefficient for intercept, β_i is the coefficient of linear effect, β_{ii} is the coefficient of quadratic effect, β_{ij} is the coefficient of interaction effect, k is the number of variables, and X_i and X_j are coded independent variables.

Following the program of experimentation and after the regression coefficients have been obtained, the adequacies of the models were checked using the analysis of variance (ANOVA) technique (Khuri and Cornell, 1987). Fisher's variance ratio test (*F-test*), standard errors of model coefficients (*t-test*), the coefficient of determination (R^2) and, the absolute average deviation (*AAD*) are the methods that were employed in the ANOVA.

Appendix H gives details of the statistical and mathematical methods used.

3.4.2 Apparatus and Experimentation

All leaching experiments were carried out in either 250-ml or 500-ml Erlenmeyer flasks placed in the Labcon shaking incubator (Model FSIM-SPO16) as shown in Figure 3.2 with speed and temperature adjustments made according to specific experiements. All tests and controls were duplicated.



Figure 3.2. Agitation leaching test equipment (Labcon shaking incubator)

3.4.3 Experimental Design

Table 3.1 shows the experimental design indicating test conditions, materials and/or samples tested, and the number of replicates in each experimental test in this study.

Table 3.1. Experimental design

Test type	Test conditions	Material/Samples tested	Replicates
Acidic and ferric leaching	-lixiviant concentrations -pH -temperature	-H_2SO_4 -Citric acid - $Fe_2(SO_4)_3$, -Acidified $Fe_2(SO_4)_3$, -Nickel laterite	2
Identification of influential factors	-pH -particle size -pulp density -substrate type -inoculum size	-bacteria -pyrite/sulphur -standard 9K media -nickel laterite	2
Effects of initial pH on substrate type	-pH -redox potential -substrate type	-bacteria -pyrite/sulphur - standard 9K media -nickel laterites	2
Optimisation of influential factors	-pH -particle size -pulp density	-bacteria -sulphur - standard 9K media -nickel laterite	2

3.5 Analytical Techniques

3.5.1 Nickel Concentration

The Varian SpectrAA-55B atomic absorption spectrophotometer (AAS) with an air/acetylene flame was used to determine the nickel concentration of all samples using the conditions in Table 3.2 (Varian Techtron (Pty) Ltd., 1989).



Figure 3.3. The Varian SpectrAA-55B atomic absorption spectrophotometer

Table 3.2. Operating conditions for nickel analysis by AAS

Metal	Wavelength (nm)	Slit width (nm)	Lamp current (mA)	Range (ppm)
Nickel	352.4	0.5	4	1-100

The 352.4 nm line was preferred to the more sensitive 232 nm line for nickel because the calibration is less curved over the working range and the signal is less susceptible to non atomic absorbance (Varian Techtron (Pty) Ltd., 1989). Aqueous metal standards were 1000 ppm (from Associated Chemicals Enterprises Ltd, South Africa) and were diluted using distilled water to the required concentrations of 20, 40, 60 and 80 ppm for calibration of the atomic absorption spectrophotometer (AAS). All samples were diluted to the correct concentration range and were measured in duplicate. The atomic absorption spectrophotomter was statistically validated for accuracy at 99% confidence level (see Appendix G). The AAS is shown in Figure 3.3.

3.5.2 pH and Oxidation Reduction Potential

The pH profiles and redox potentials of the leach solution were measured using the 744 pH meter Metrohm. The redox potentials readings were obtained using the Ag/AgCl/3M KCl reference electrode and subsequently converted to the standard hydrogen electrode (SHE) by adding 210 mV (Friis et al., 1998). The measurements

were standardised with Metrohm buffer solutions at pH = 4 and 7. After use the electrode was washed with distilled water and then dried. The electrode was then stored in 3M KCl solution to prevent desiccation. The pH meter was statistically validated for accuracy at 99% confidence level (see Appendix G).

3.6 Data Analysis

The data was obtained as described in the previous sections of this chapter. The data collected was used to develop relationships between nickel recovery and the parameters tested (e.g., pH, temperature, substrate type, etc). These relationships and the observed results are discussed in the subsequent chapters of this dissertation. The recovery during the leaching of nickel laterites was calculated as a percentage of nickel in the liquid phase to that in the nickel laterite ore (see example in Appendix A). Some data as in Chapter 5 and 7 were statistically analysed.

3.7 Summary

This chapter presented and discussed the materials and methods used in the study. In particular, the focus of the chapter was on the following activities that constitutes the laboratory testing aspect of the study:

- Reagents preparations.
- Sieving of nickel laterites into different sizes depending on the nature of test works.
- Bacterial growth and harvesting.
- The choice of designs for the DOE.
- Agitation leach test works.
- Determination of the concentration of nickel in the leach solution.

- Data analysis and interpretation. All results from the test works were recorded. Correlations between process variables and nickel recovery were determined graphically, analytically and empirically.

CHAPTER FOUR

ACIDIC AND FERRIC LEACHING

"*It is a great nuisance that knowledge can only be acquired by hard work*".

- W. Somerset Maugham

4.1 Introduction

The constant increase in demand for metals has motivated intensive studies into the recovery of metals from low grade ores. Recently, relatively great attention has been paid to the research connected with the recovery of nickel from nickel laterites using commercial acids (Bosecker, 1986; Valix et al., 2001a,b; Alibhali et al., 1993). This is so because an economical process for recovering nickel from large quantities of low grade laterite is needed.

The possibility to employ microorganisms to treat non-sulphide ores such as nickel laterites has been described in Chapter 2 (Section 2.2.5). These microorganisms either produce organic acids such as citric acid (i.e., heterotrophic microorganisms) or inorganic acids such as sulphuric acid (i.e., chemolithotrophic microorganisms).

In order to have an insight on the use of chemolithotrophic bacteria in this process, it is important to understand the role and effects of sulphuric acid. Its effect can be easily understood by comparing it to the previously well researched citric acid (Tzeferis and Agatzini-Leonardou, 1994; Tzeferis, 1994). On the other hand, the use of the ferric sulphate as one of the lixiviant will act as a basis for the provision of using ferrous iron or pyrite as a substrate in the bacterial leaching process. The oxidation of ferrous iron and/or pyrite produces ferric iron. Ferric cations hydrolyse in the presence of water generating acid, which can be consumed by nickel laterites; thus facilitating the leaching and nickel extraction processes.

Determination of the acid conditions, i.e., concentration and pH required to maximize nickel extraction will lay a foundation for the subsequent bioleaching studies (Chapter Five through Seven). In addition, in this experimental study of nickel laterites dissolution using sulphuric acid, citric acid and ferric ions, it is also

attempted to fit the kinetic data into a shrinking core model so as to compare the reaction kinetic models for the lixiviants under the same experimental conditions.

4.2 Materials and Methods

This study deals with the effects of three parameters, concentration, pH and temperature, on nickel laterite dissolution using sulphuric acid, citric acid and ferric sulphate. Therefore, the study was divided into three parts dealing with varying the concentrations, pH and temperature.

4.2.1 Ore Samples and Preparation

The nickel ore was crushed and using standard sieve plates was classified into +63-75μm size fraction. This size range was used because it represented most of the nickel laterite material in terms of mass (Table B3). The chemical composition of nickel was determined prior to chemical leaching experiments. The typical chemical composition of various oxides in the laterite ore used is given in Appendix B.

4.2.2 Chemical Leach Tests at Different Concentrations

Chemical leach tests were carried out using analytical grade citric acid ($C_6H_8O_7$), sulphuric acid (H_2SO_4), ferric sulphate ($Fe_2(SO_4)_3$) and acidified ferric sulphate. In each experiment, 5g of ore was added to 100mL of lixiviant having a specified concentration (Table 4.1) and a temperature of 30°C. A pulp density of 5% w/v was chosen because it had shown higher recoveries in previous microbial studies, and a temperature of 30°C is hypothetically optimum for chemolithotrophic bacteria used in this study (Karavaiko et al., 2006). To rule out the diffusion control of dissolution, the tests were stirred at a rate ≥ 200 rpm so as to ensure that particles are suspended in solution (Levenspiel, 1972). The solution was sampled every two days and the total

concentration of nickel was determined by the Varian SpectrAA-55B atomic absorption spectrophotometer. The pH profiles were measured but not controlled through out the leach period. Solution loss through sampling and evaporation was compensated by the addition of distilled water. However, the extent of solution loss through evaporation and sampling is negligible compared to the solution volume of 100mLs for it to have a measurable effect on the concentration.The recovery during the leaching of nickel laterites was calculated as a percentage of nickel in the liquid phase to that in the nickel laterite ore (see example in Appendix A). All experiments were performed in a platform shaking incubator, and flasks were covered with pieces of aluminium foil to reduce evaporation.

4.2.3. Chemical Leach Tests at Same Initial pH

In each experiment, 5g of ore was added to 100mL of lixiviant having an initial pH of 0.5, 1.0, 1.5 and 2.0, and a temperature of 30°C. These pH ranges (i.e. pH < 3) were chosen to simulate conditions in which acidophilic microorganisms can grow optimally (Norris and Johnson, 1998). The pH profiles were measured but not controlled through out the leach period. All other test conditions remained the same as in section 4.2.2 above.

4.2.4. Chemical Leach Tests at Different Temperatures

In each experiment, 5g of ore was added to 100mL of lixiviant having a concentration of 0.5M and temperatures of 30°C, 40°C, and 45°C, respectively. The highest temperature of 45°C was chosen to simulate the optimum temperature in which the more thermo-tolerant *Acidithiobacillus caldus* bacteria in the mixed culture can survive (Rawlings et al., 1999). Ferric sulphate was acidified with 0.5M sulphuric acid. This was done because acidified ferric sulphate performed better (Table 4.1) in

the tests performed in section 4.2.2. All other test conditions remained the same as in section 4.2.2 above.

4.3 Results and Discussion

4.3.1 Effect of Initial Lixiviant Concentration

For the results discussed in this section, reference should be made to the experimental data in Appendix C (Tables C1-C3). The results discussed are an average of the runs conducted under similar experimental conditions.

Table 4.1 shows the leaching conditions of various chemical tests and nickel recovery over a leaching period of 10 days. The dissolution rate of nickel laterite as shown in Table 4.1 depends on the leaching media (H_2SO_4, $C_6H_8O_7$, $Fe_2(SO_4)_3$, acidified $Fe_2(SO_4)_3$).

[a]Table 4.1. Leaching conditions and solubilisation of nickel by H_2SO_4, $C_6H_8O_7$, $Fe_2(SO_4)_3$ and acidified $Fe_2(SO_4)_3$ at 30°C over a 10 day leaching period

Leach media	Initial pH	Final pH	Recovery (%)
0.5 M [H_2SO_4, $C_6H_8O_7$]	0.36	0.63	79.6
0.5 M [$C_6H_8O_7$, $Fe_2(SO_4)_3$, H_2SO_4]	0.23	0.41	74.7
0.5 M H_2SO_4	0.39	0.74	71.9
1 M $C_6H_8O_7$	1.29	1.70	57.4
0.5 M $Fe_2(SO_4)_3$, 0.5M H_2SO_4	0.33	0.57	50.3
0.5 M $C_6H_8O_7$	1.45	2.02	46.6
0.5 M $Fe_2(SO_4)_3$, 0.1 M H_2SO_4	0.74	0.96	37.4
0.5 M $Fe_2(SO_4)_3$	0.93	1.13	20.3
Distilled water	5.88	8.39	0.5

[a]All values given here are the average of two separate runs carried out under the same experimental conditions (i.e. Tables C2 and C3).

The results shown in Table 4.1 indicated that H_2SO_4 was more effective in nickel dissolution than ferric sulphate and citric acid at the same starting concentration. Citric acid is a weaker acid than sulphuric acid, hence, the lower recoveries. The acidity constant of sulphuric acid is $pK_1 = -1.7$; $pK_2 = 1.96$ at 25°C (Perrin, 1982) and that of citric acid is $pK_1 = 3.14$; $pK_2 = 4.77$; $pK_3 = 6.39$ at 20°C (Albert and Sergent, 1962). The higher the acidity constant is, the weaker the acid. Nickel recovery with 1M citric acid was still lower than that of 0.5M H_2SO_4. However, higher nickel recovery was obtained in a mixture of $C_6H_8O_7$ and H_2SO_4, thus showing the positive synergic effect of sulphuric acid in the leaching process. These results also confirm the findings of other researchers (Alibhai et al., 1993) who noted, in chemical tests, that hydrogen ions concentration is the main factor affecting chemical leaching.

The recoveries as shown in Table 4.1 suggest that leach rates are highly dependent on the initial pH of the solution and the type of lixiviant. The low initial pH (at same initial concentration) as seen from ferric sulphate (Table 4.1) is as a result of hydrolysis reactions (Equation 4.1).

$$\left.\begin{aligned} Fe^{3+} + H_2O &\rightarrow FeOH^{2+} + H^+ \\ Fe^{3+} + 2H_2O &\rightarrow Fe(OH)_2^+ + 2H^+ \\ Fe^{3+} + 3H_2O &\rightarrow Fe(OH)_3 + 3H^+ \end{aligned}\right\} \qquad (4.1)$$

Furthermore, there is a reaction (Equation 4.2) in competition with the hydrolysis reactions giving products of basic ferric hydroxysulphate with the formula $MFe_3(SO_4)_2(OH)_6$, where M = H_3O^+ or K^+ or Na^+. These hydroxysulphates precipitates are known as jarosite. Jarosite is a member of the jarosite-alunite group of isostructural minerals described by the general formula $AB_3(SO_4)_2(OH)_6$, where the B site is occupied by Fe^{3+} (jarosite) or Al^{3+} (alunites) and the A site is occupied

most commonly by K^+, Na^+ and H_3O^+ (hydronium). The following is a formula for jarosite precipitation:

$$M^+ + 3Fe^{3+} + 2HSO_4^- + 6H_2O \rightarrow MFe_3(SO_4)_2(OH)_6 \downarrow + 8H^+ \qquad (4.2)$$

The acid produced in the hydrolysis and jarosite precipitation reacts with the metal values present in the ore.

Jarosite formation is temperature, pH and electrode potential (Eh) dependent and characteristically, the rate of formation increases dramatically with temperature; the rate is very slow below 60°C; the rate is at maximum at pH ≅ 2; the formation of jarosite is increasingly decreased at pH < 1, pH > 3, i.e., outside of a narrow pH range (Klauber, 2008). Basic ferric hydroxysulphate formation is also favoured by high sulphate contents (Georgiou and Papangelakis, 1998).

Table 4.1 also shows that ferric sulphate had a negligible effect on leaching. The negligible influence of ferric sulphate on leaching was attributed to the formation of the insoluble basic ferric hydroxysulphate layer (Equation 4.2). The insoluble layer causes a mass transfer barrier to mineral-H^+ contact. Precipitated jarosite is also known to have the ability to scavenge elements from solutions (Dutrizac, 1983). The gradual increase in pH during leaching in all the tests was caused by the progressive acid dissolution of nickel laterite.

Considerable variability in nickel recoveries can also be observed when leaching with different laterite ores due to their different mineralogical make-ups (Tzeferis and Agatzini-Leonardou, 1994; Valix et al., 2001b).

4.3.2 Effect of Initial Lixiviant pH

For the figures discussed in this section reference should be made to the experimental data in Appendix C (Tables C4-C6). The results discussed are an average of the runs conducted under similar experimental conditions.

Figure 4.1 shows the nickel recoveries with different lixiviants at the same initial pH of 0.5, 1.0, 1.5 and 2.0. As seen from the figure, citric acid had a higher recovery than sulphuric acid and ferric sulphate of the same initial pH of 1.0, 1.5 and 2.0. The higher recovery with citric acid than sulphuric acid can be attributed to the chelating of nickel ions by organic acid at these pHs while H^+ ions in sulphuric acid do not act as chelators (McKenzie et al., 1987).

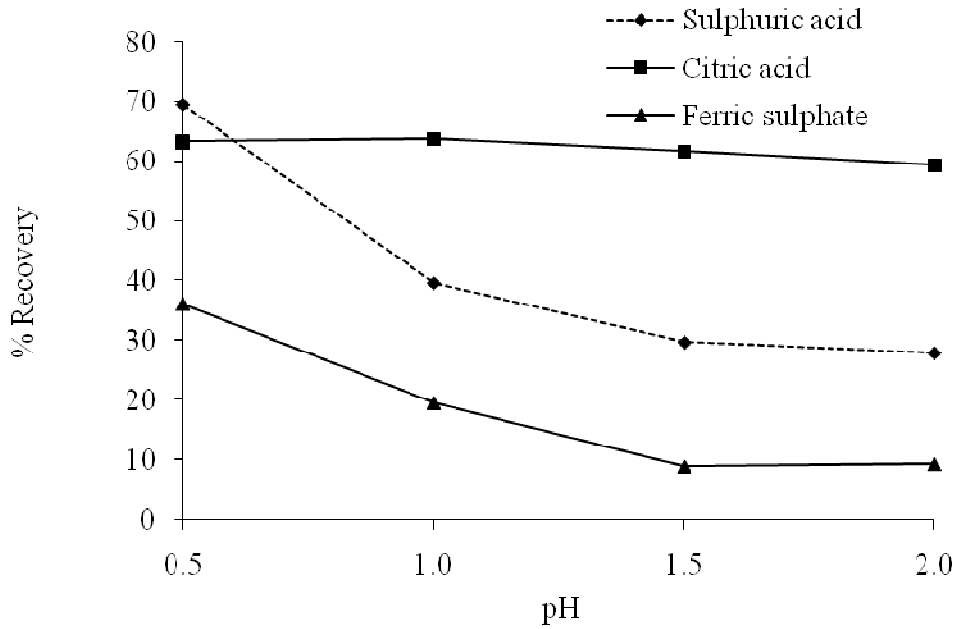


Figure 4.1. Nickel laterite recoveries at same initial pH for different lixiviants

It is also seen from the graph that at a starting pH of 0.5, sulphuric acid had a higher recovery than citric acid and ferric sulphate. This shows that chelation is not very

effective at a low pH of 0.5. This is because lowering pH protonates citrate anion converting it to citric acid according to Le Chaterlier's principle (Equation 4.3).

$$(C_6H_5O_7)^{3+} + 3H^+ \rightleftharpoons C_6H_8O_7 \qquad (4.3)$$

The figure also shows that there is very little step change in recoveries within the pH range studied for citric acid, whereas, there is a high step change in recovery for sulphuric acid and ferric sulphate.

As can be seen from Figure 4.1, the recoveries were generally higher at low pHs irrespective of the leaching media. There is higher acid activity at lower pH values, which promotes the leaching process and, hence higher recoveries.

4.3.3 Effect of Temperature

For the figures discussed in this section reference should be made to the experimental data in Appendix C (Tables C7-C9). The results discussed are an average of the runs conducted under similar experimental conditions.

The influence of temperature was studied at three different temperature values for each of the lixiviant. Figure 4.2 shows nickel recovery at different temperatures during the leaching period under study. The results show that the recoveries of nickel are high when the temperature is high irrespective of the lixiviant, i.e., temperature had a positive effect on leaching kinetics. Thus, it can be inferred that nickel recovery is proportionally related to temperature, within the range of 30 to 45°C.

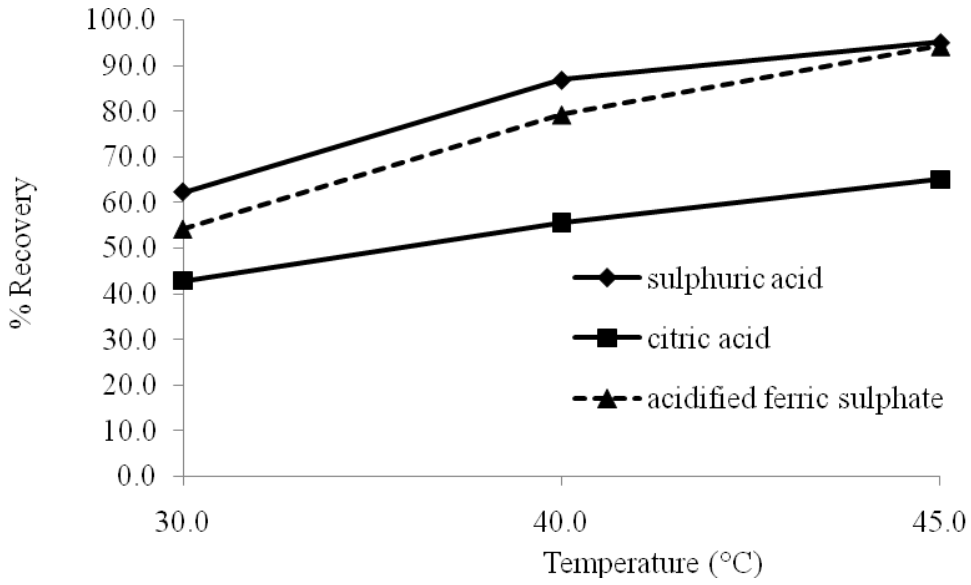


Figure 4.2. Nickel laterite recovery at different temperatures for different lixiviants

4.3.4 Kinetic Analysis

Rate controlling regimes

The dissolution rates of nickel laterites were analysed on the basis of the extraction type core model under the assumption that the ore consists of homogeneous spherical solid particles that react with the fluid isothermally. In addition, the concentration of the reacting fluid is assumed to be constant or in excess (Levenspiel, 1972). The essential premises of the shrinking core model are that, the rate is controlled by mass transport of a dissolved reactant or product from (or to) the bulk solution to (or from) the solid-solution interface via a boundary layer in which there is near laminar flow; the rate is controlled by some chemical reaction occurring at the solid-solution interface; the rate is controlled by mass transport of a dissolved reactant or product through the adhering layer of inert mineral or solid product formed during the reaction.

To determine the rate controlling regime, the experimental results at different temperatures were plotted in terms of the standard equations of the shrinking core model as shown in Figures 4.3, 4.4, 4.5 and 4.6 assuming a mono-sized particle size distribution.

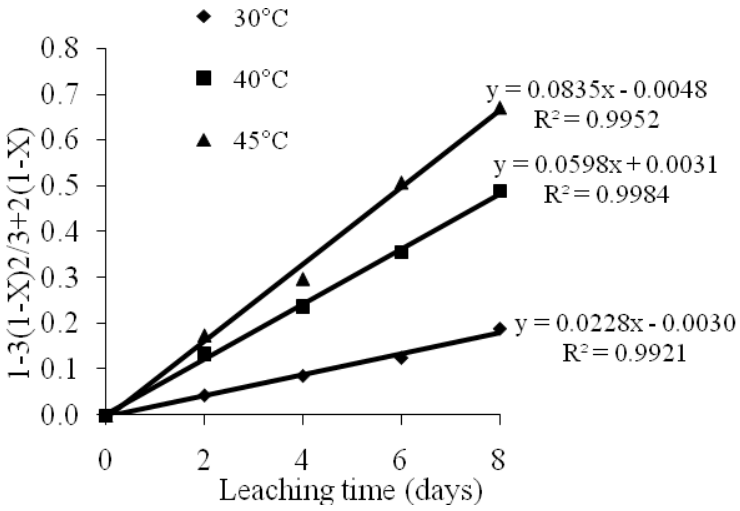


Figure 4.3. Plot of 1-3(1-X)$^{2/3}$+2(1-X) versus time for sulphuric acid

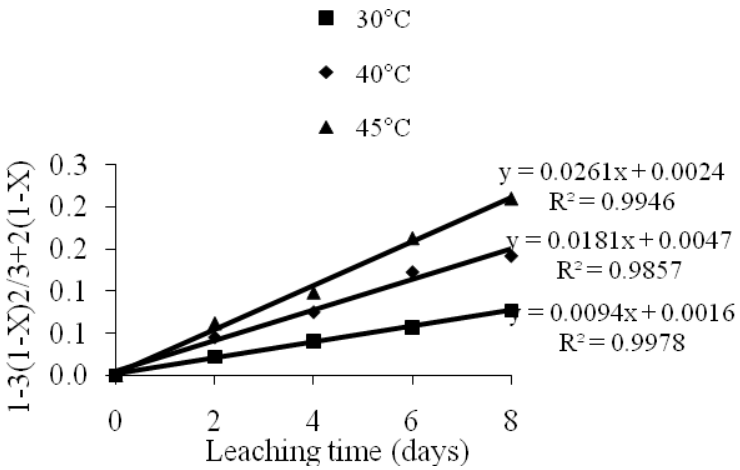


Figure 4.4. Plot of 1-3(1-X)$^{2/3}$+2(1-X) versus time for citric acid

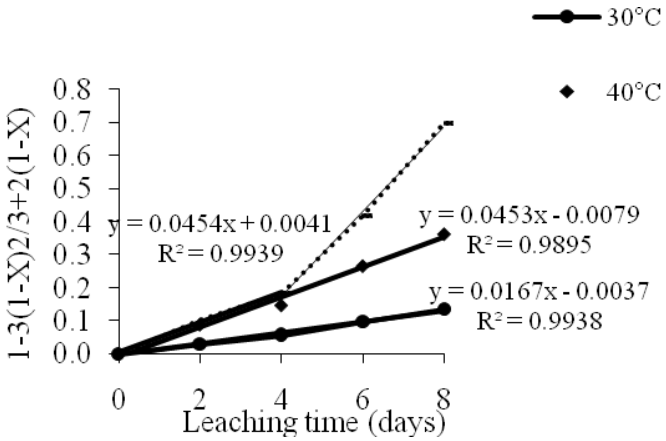


Figure 4.5. Plot of 1-3(1-X)$^{2/3}$+2(1-X) versus time for acidified ferric sulphate

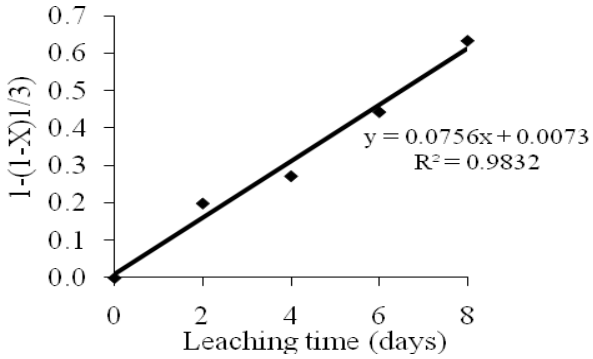


Figure 4.6. Plot of 1-(1-X)$^{1/3}$ versus time for acidified ferric sulphate at 45°C

From Figures 4.3 and 4.4, the kinetic model for diffusion through the product layer was assumed to control the rate of reaction for the nickel laterite with sulphuric acid and citric acid in the range of temperatures studied. It followed the kinetic equation given below:

$$1-3(1-X)^{2/3}+2(1-X)=kt \qquad (4.4)$$

where X is the conversion, t is the time in days and k is the apparent reaction rate constant (day^{-1}).

Examination of plots of other kinetic equations as functions of time did not give perfectly straight lines meaning that the dissolution reactions were not controlled by such regimes. From the analysis of the core-model, it was found that the dissolution rate at temperatures of 30°C and 40°C (Figure 4.5) were well expressed by the rate equation based on diffusion of the metal ions through a product layer of the ore for acidified ferric sulphate. Figure 4.5 also shows that the rate determining step changed at a temperature of 45°C after 4 days from that of diffusion through a product layer as can be seen from the change in slope (Figure 4.5). This was attributed to an increase in the activation energy of leaching perhaps as a result of the gradual built up of a passivating layer with time. The steeper the slope in Figure 4.5, the higher the activation energy required. Figure 4.6 shows that the rate determining step of the surface chemical reaction described by $1-(1-X)^{1/3} = kt$, was controlling. That is to say, the diffusion through the product layer at 45°C became so fast that the dissolution rate was limited by surface chemical reaction. Figures 4.5 and 4.6 also show that in the first 4 days the rate control was mixed for acidified ferric sulphate at 45°C (i.e., diffusion through a product layer and surface chemical reaction). This was attributed to the effect of higher temperature on the passivating layer. These results are similar to the observed effect of temperature on the passivating layer formed during leaching of chalcopyrite (Hackl et al., 1995).

Prosser (1996) and, Gbor and Jia (2004) have shown that plots such as figures 4.3-4.6 offer less convincing evidence of a particular mechanism. Prosser (1996) mentions several uncertainties pertaining to the determination of mechanisms of mineral leaching reactions. One major factor that can affect the interpretation of the leaching data is the particle size distribution (Gbor and Jia, 2004).

In the section below, it was also attempted to use activation energy to indicate the reaction control regimes. The magnitude of the activation energy can provide a more

positive evidence for the reaction and diffusion controlled regimes (Gbor and Jia, 2004).

Determination of activation energies

The apparent rate constant, *k*, obtained from the slopes of the straight lines in Figures 4.3, 4.4, 4.5 for sulphuric acid, citric acid and acidified ferric sulphate, respectively, at their respective temperatures was used to determine the activation energies. For acidified ferric sulphate, *k* was only determined for the first 4 days when the rate was assumed to be controlled by diffusion through the product layer.

Using the Arrhenius equation, $k = Ae^{-Ea/RT}$, the natural logarithm of *k (ln k)* is then plotted against the inverse of their respective temperatures (*1/T*) as shown in Figure 4.7. In the Arrhenius equation, *k* is the apparent reaction rate constant (day^{-1}), *A* is the frequency factor (day^{-1}), *Ea* is the activation energy ($Jmol^{-1}$), *R* is the universal gas constant (8.314 $JK^{-1}mol^{-1}$) and *T* is the reaction temperature (K). The slopes of this plot give *–Ea/R* from which *Ea* is obtained.

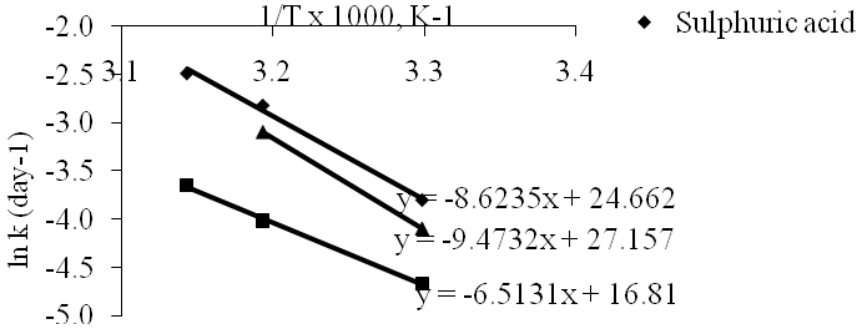


Figure 4.7. Arrhenius plot for nickel laterite dissolution with various lixiviants

The calculated activation energies were 70.4 kJ mol^{-1} (16.8 kcal mol^{-1}) for sulphuric acid, 54.1 kJ mol^{-1} (12.9 kcal mol^{-1}) for citric acid and 78.8 kJ mol^{-1} (18.8 kcal mol^{-1}) for acidified ferric sulphate. The activation energy for acidified ferric sulphate was only calculated for 30°C and 40°C (Figure 4.7) because acidified ferric sulphate indicated a reaction controlled at 45°C, and no further temperature was tested.
These values (derived from Figure 4.7) for activation energy are clearly too high for product layer diffusion as reported in the literature. The activation energy for product layer diffusion controlled process can be between 1 to 6 kcal mol^{-1} (Habashi, 1969). The activation energy for chemically controlled processes is usually greater than 10 kcal mol^{-1} (Habashi, 1969). The reactivity of the reacting substances is depended on the resulting activation energy.

The inconsistence in reaction regimes can be attributed to the high coefficient of variation (CV) in particle size distribution (Gbor and Jia, 2004) resulting from poor separation during dry sieving. In other words, poor separation results in having a sample with various sizes (i.e., CV is high). For this study, CV was defined as the ratio between the standard deviation of the particle size range and the mean of that particle size range. When the particle size distribution of a sample is not consistent, but varies, it results in varying reaction rates thus deviating from the actual reaction regime. On the other hand, wet sieving can lower the coefficient of variation (CV) of particles and make the shrinking core model for monosized distribution applicable (Gbor and Jia, 2004). This is because wet sieving removes the finer fractions resulting in a consistent size range. For the reasons given in section 3.2.1, this study did not consider wet sieving. However, on the other hand, Peters (1991) and Cusslers (1997) associate high activation energy with solid state diffusion or surface diffusion through very fine pores.

4.4 Summary and Conclusions

In order to provide useful insights into the process of leaching nickel laterites with chemolithotrophic microorganisms, chemical leach tests were initially instigated. In particular, this study looked at the leaching kinetics of nickel laterite in sulphuric acid, citric acid and ferric sulphate solutions. It has been deduced from this chapter that the dissolution rate of nickel laterite depends on the leaching media (H_2SO_4, $C_6H_8O_7$, $Fe_2(SO_4)_3$) and possibly the effect of chelation at certain pH ranges. Sulphuric acid leaching had a higher recovery (71.9%) than citric acid (46.6%) and ferric sulphate (20.3%), respectively, of the same concentration of 0.5M in two weeks. Although, an increase in the concentration of citric acid from 0.5M to 1M had a positive effect on the recovery of nickel, the recovery was still lower than that recorded for sulphuric acid alone at similar concentrations. However, combinations of sulphuric acid and citric acid gave a higher extraction (79.6%) than when citric acid was used alone indicating the positive effect of sulphuric acid on leaching. In the presence of ferric sulphate, dissolution was seen to increase with sulphuric acid concentration within the range 0.1 - 0.5 M studied.

Citric acid had a higher recovery than sulphuric acid and ferric sulphate of the same initial pH of 1.0, 1.5 and 2.0. The higher recovery with citric acid than sulphuric acid was attributed to the chelating of nickel ions by the organic acid anions (McKenzie et al., 1987). At an initial lower pH of 0.5, sulphuric acid had a higher recovery than citric acid and ferric sulphate.

The effect of temperature was modeled by the Arrhenius equation. The activation energies were calculated as 70.4 kJ mol^{-1} for sulphuric acid, 54.1 kJ mol^{-1} for citric acid and 78.8 kJ mol^{-1} for acidified ferric sulphate signifying lower reactivity between nickel laterites and the lixiviants. The higher activation energies are characteristic for processes controlled by chemical reactions on the surface.

In contrast, the shrinking core model indicated the diffusion through the product layer as rate controlling. Plots of various shrinking core model equations alone do not provide convincing evidence for the rate control regimes. This inconsistence is attributed to the large CV in particle size distribution resulting from poor separation during dry sieving.

The next chapter focuses on identifying factors that are influential in the bacterial leaching of nickel laterites using chemolithotrophic microorganisms and external supply of sulphur containing material.

CHAPTER 5

IDENTIFICATION OF INFLUENTIAL FACTORS

"*Theory is the general; experiments are the soldiers*".

- Leonardo Da Vinci

5.1 Introduction

One-factor-at-a-time experimental designs where a single factor is varied while others are kept constant are often expensive and time consuming, and do not often consider the interactive nature of various independent factors that would otherwise impact the results (Box et al, 1978; Montgomery, 2005). Factor interaction is a situation where the effect of one factor on the response depends upon the level of another factor. In fact, a different effect might be observed if one or more of the factors were held constant at another value. The objective of the study in this chapter was to investigate the factors that influence the dissolution of nickel laterites using a mixed culture of chemolithotrophic bacteria (*Acidithiobacillus ferrooxidans, Acidithiobacillus caldus* and *Leptospirillum ferrooxidans*). The significance of each factor and their interactive effects were evaluated using a statistical design of experiments by way of quarter fractional factorial designs (i.e., 2^{5-2}_{III}) and dissolved nickel was taken as the measured response. Knowing the significance that a factor has in influencing the measured response is paramount for process/product optimisation and cost control. The significant factors can be optimised while the insignificant ones can be set at levels where the least cost is incurred.

5.2 Materials and Methods

5.2.1. Ore Samples and Preparation

Using standard sieve plates, the mineral was classified into three different size fractions (-38µm, +53-63µm and +100-150µm). The choice of particle size in the range of -38µm and 100-150µm for high and low level, respectively, was meant to give a relatively broader range so as to increase the chance of detecting its statistical significance. The centre point of +53-63µm was chosen as it was similar to what

some researchers used in previous similar studies (Valix et al., 2001b; Tang and Valix, 2006).

Using the centre point (i.e., +53-63μm) as the reference bench mark and to optimize the statistical analysis; one standard fractional size (+100-150μm) was selected above this size and one below (-38μm); thus bringing the total fractional sizes evaluated to three. The chemical composition and the particle size distribution of each fraction were determined prior to bioleaching experiments.

The typical chemical composition of various oxides in the laterite ore, and the distribution of particle size for different fractions of nickel laterites used and their specific elemental composition are given in Appendix B.

5.2.2. Microbes

The bacteria and growth media used were described previously in sections 3.3.2 and 3.3.1 of Chapter 3, respectively.

5.2.3 Experimental Plan for Statistical Design of Experiments (DOE)

Design of experiments is the simultaneous study of several process variables (Barrentine, 1999; Montgomery, 2005). A quarter basic fractional factorial designs 2^{5-2}_{III} with a fold-over were used for this study to identify statistical significant factors. Previous researchers, though using heterotrophic microorganisms, did identify some factors that may be significant in the dissolution of nickel laterites (Tang and Valix, 2006). Therefore, the choice of factors and levels was based on past experience of bacterial leaching.

This study was designed to determine the influence of some of the factors in the bacterial leaching of nickel laterites using chemolithotrophic bacteria and quantify them to ensure that the influence is measurable. In this study, the potential design factors were classified as controlled factors and held constant factors. The controlled factors were the factors that were actually selected for study (Table 5.1). The held constant factors (temperature at 30°C and 190 rpm agitation speed) were those which may exert some effect on the response, but for the purpose of this study were not of interest; so they were held constant at a specific level.

Apart from substrate type that was a qualitative factor, the rest of the factors were quantitative factors because they were measured on a numerical scale. Different levels of qualitative factors are represented by indicator variables, for example, in this study, sulphur was arbitrarily represented as level 1 and pyrite as level 2 (Table 5.1). Sulphur was chosen as a centre point because of its ability to produce sulphuric acid directly upon oxidation.

Table 5.1. Experimental factors and levels for controlled factors

Controlled factors	Level 1	Centre Point	Level 2
pH	1.5	2.0	2.5
Particle size (µm)	-38	-63+53	-150+100
Pulp density (%w/v)	5	10	15
[a] Substrate type	5% Sulphur	5% Sulphur	5% Pyrite
Inoculum dosage (%v/v)	5	10	15

At the screening stage, the use of two levels for each factor allows for simplification of the analysis and provides substantial reduction in the number of runs required (Montgomery, 2005). This is normally significant for most experimental work until the final refining or optimization stage (Montgomery, 2005).

To simplify the calculations and for uniform comparison, factors were studied with their codified values. The physical and coded levels are given in Table 5.2 and 5.3, respectively.

In general, coded values were obtained as follows:

Quantitative variables; coded value = [physical value – ½(highest value + lowest value)]/½(highest value-lowest value).
Qualitative variables; coded variables were assigned at random.

Table 5.2. Nickel recovery results for the 2^{5-2}_{III} fractional factorial design (basic)

Standard run order	Random run order	[c] Control factors					% Ni recovery (Average)
		A	B	C	D	E	
1	3	-1	-1	-1	+1	-1	24
2	8	+1	-1	-1	+1	+1	20
3	7	-1	+1	-1	-1	+1	30
4	6	+1	+1	-1	-1	-1	26
5	1	-1	-1	+1	-1	+1	17
6	4	+1	-1	+1	-1	-1	14
7	5	-1	+1	+1	+1	-1	30
8	2	+1	+1	+1	+1	+1	26

[c] The actual factor levels, coded as values of -1 and +1 in the table were as follows: for pH (A):1.5 (-1) and 2.5 (+1); particle size (B): -38µm (-1) and -150+100µm (+1); pulp density (C):5% w/v(-1) and 15% w/v(+1); substrate type (D): sulphur (-1) and pyrite (+1); inoculum size (E):5% v/v (-1) and 15% v/v (+1).

Table 5.2 shows the experimental layout and standard runs for the 2^{5-2}_{III} basic design. In general, the n^{th} column consists of 2^{n-1} minus signs followed by 2^{n-1} plus signs (Box et al, 1978). However, in this 2^{5-2}_{III} fractional factorial design, the column for

substrate type was obtained by combining the particle size and pulp density columns, and the inoculum size column was obtained by combining the pH, particle size and pulp density columns.

There is a confounding pattern of effects when using fractional factorial designs. This really means that (assuming that three-factor and higher interactions are insignificant) the estimated effect of a factor is a combination of the actual values of the effects of that factor and its two factor interactions (Barrentine, 1999). To separate the main effects and the two factor interactions, the fold over technique is used, and it is run with all the signs of the basic designs reversed (Montgomery, 2005; Barrentine, 1999). This is given in Table 5.3. Refer to Appendix A for a sample example.

Table 5.3. Nickel recovery results for the 2^{5-2}_{III} fractional factorial design (fold-over)

Standard run order	Random run order	[d] Control factors					% Ni recovery (Average)
		A	B	C	D	E	
1	6	+1	+1	+1	-1	+1	26
2	1	-1	+1	+1	-1	-1	29
3	8	+1	-1	+1	+1	-1	16
4	4	-1	-1	+1	+1	+1	20
5	3	+1	+1	-1	+1	-1	32
6	2	-1	+1	-1	+1	+1	35
7	5	+1	-1	-1	-1	+1	15
8	7	-1	-1	-1	-1	-1	23

[d] The actual factor levels, coded as values of -1 and +1 in the table were as follows: for pH (A):1.5 (-1) and 2.5 (+1); particle size (B): -38µm (-1) and -150+100µm (+1); pulp density (C):5% w/v(-1) and 15% w/v(+1); substrate type (D): sulphur (-1) and pyrite (+1); inoculum size (E):5% v/v (-1) and 15% v/v (+1).

5.2.4 Methodology for Data Analysis

Normal probability plots of effects

When analyzing data from unreplicated factorials, occasionally high order interactions occur and as such normal probability plots are used (Daniel, 1959) to estimate the significant factors. This is the plot of the actual value of the effect estimates against their cumulative normal probabilities (Daniel, 1959). The effects that are negligible are normally distributed, with mean zero and variance (σ^2) and will tend to fall along a straight line, whereas significant effects will have nonzero means and will not lie along the straight line. Effects in the statistical design are done by averaging the responses that are applicable to the level of each factor. The difference between the average responses at the two levels of each factor is an indication of the significance of that factor in influencing the response that is measured. Expressed mathematically, the single effects caused by the variation of the input parameters are calculated with the following formula:

$$\text{Effect} = \frac{2}{m} \sum_{i=1}^{m} (\text{algebraic sign of contrast constant x } R_{i,\text{observed}}) \qquad (5.1)$$

where $R_{i,\text{observed}}$ is the ith observation (recovery) in the experimental data, *m* is the number of runs (experiments).

In the probability plots, all effects have to be graded from low to high and numbered in this order. Afterwards, the numbered effects (i) get a value of percentage based on the following equation:

$$\text{Value} = \frac{i - 0.5}{n} \text{ x } 100\% \qquad (5.2)$$

where *n* is the number of values.

Graphical residual analysis

The normal plotting of residuals provides a diagnostic test for any tentatively entertained model (Montgomery, 2005; Box et al, 1978). The normal probability plots of the residuals for the data tests the hypothesis that the residuals have a normal distribution. This should be a straight line if the residuals have a normal distribution. A plot of residuals versus the fits (fitted model values) is a test of the assumption or hypothesis that the variations are the same in each group. Because outliers may have undue influence, studentised 'deleted' residuals were calculated for each run, based on the predicted value when that run was excluded from the analysis (Miles and Shevlin, 2001). The residuals were then calculated from the following equation:

$$\text{Residual} = \frac{R_{i,observed} - R_{i,predicted}}{\sigma_{i,residual}} \qquad (5.3)$$

where $\sigma_{i,residual}$ is the standard deviation of all residuals from the regression analysis that deleted the *i*th observation, $R_{i,predicted}$ is the predicted value of response from fitted model, $R_{i,observed}$ is the ith observation (recovery) in the experimental data.

Test for curvature using centre points

Adding centre points (Table 5.4) to the design provide protection against curvature from second order effects as well as allowing an independent estimate of error to be obtained (Montgomery, 2005).

Table 5.4. Nickel recovery results for the 2^{5-2}_{III} fractional factorial design (centre point replicates)

Run	[e] Control factors					% Ni recovery
	A	B	C	D	E	(Average)
1	0	0	0	0	0	20
2	0	0	0	0	0	21
3	0	0	0	0	0	25
4	0	0	0	0	0	22

[e] The actual factor levels, coded as values of 0 in the table were as follows: for pH (A):2.0; particle size (B): -63+53µm; pulp density (C):10% w/v; substrate type (D): sulphur; inoculum size (E):10% v/v.

The estimate of error, σ^2, is calculated as,

$$\sigma^2 = \frac{\sum_{\text{centre-points}} (Y_{c,i} - \bar{Y}_c)^2}{n_c - 1} \qquad (5.4)$$

where $Y_{c,i}$ are the observations at the centre, $\bar{Y}_C$ is the average of the observations of the n_c runs at the centre.

The pure quadratic curvature, $\sum_{i=1}^{k} \beta_{ii}$, can be estimated from $\bar{Y}_F - \bar{Y}_C$. The single-degree-of-freedom sum of squares associate with the null hypothesis, $H_0: \sum_{i=1}^{k} \beta_{ii} = 0$, is,

$$SS_{\text{pure quadratic}} = \frac{n_F n_C (\bar{Y}_F - \bar{Y}_C)^2}{n_F + n_C} \qquad (5.5)$$

where $\bar{Y}_F$ is the average of the observations at the factorial points under the study, n_F is the number of the factorial points, k is the number of factors.

If the ratio of Equation (5.4) and Equation (5.3) is small, then the centre points lie on or near the plane passing through the factorial points and hence, there is no quadratic effect (curvature). On the other hand, if the ratio is large, then quadratic curvature is present.

5.2.5 Experimentation

All the bacterial leaching tests (runs) of the quarter fractional factorial design 2^{5-2}_{III} were performed in 500-ml Erlenmeyer flasks (leaching vessel). A 200-ml mixture of sterilized standard 9K medium together with an appropriate amount of sterilised energy source, a predetermined amount of bacterial inoculum and an appropriate quantity of nickel laterite was added to the leaching vessel and maintained in a platform shaking incubator at 30°C and 190 rpm. The leaching vessels were covered with pieces of aluminium foil to reduce evaporation and prevent contamination; but allow free supply of air. An appropriate pH level was controlled and maintained using 1M sulphuric acid and 1M sodium hydroxide. The experiment was monitored every two days and a sample was taken using a pipette (1.5-ml) while agitating and was immediately filtered. The liquid extract was compensated by the addition of distilled water (or the standard 9K medium). The filtrate was analysed for nickel using the Varian SpectrAA-55B atomic absorption spectrophotometer. All experiments were randomly run and were carried out until there was stability in the nickel recovery.

5.3 Results and Discussion

5.3.1 Significant Factors

For the results discussed in this section, reference should be made to the experimental data in Appendix D (Table D1-D6).

The data given in Tables 5.2 and 5.3 were used to estimate the main and interaction effects as plotted in Figure 5.1.

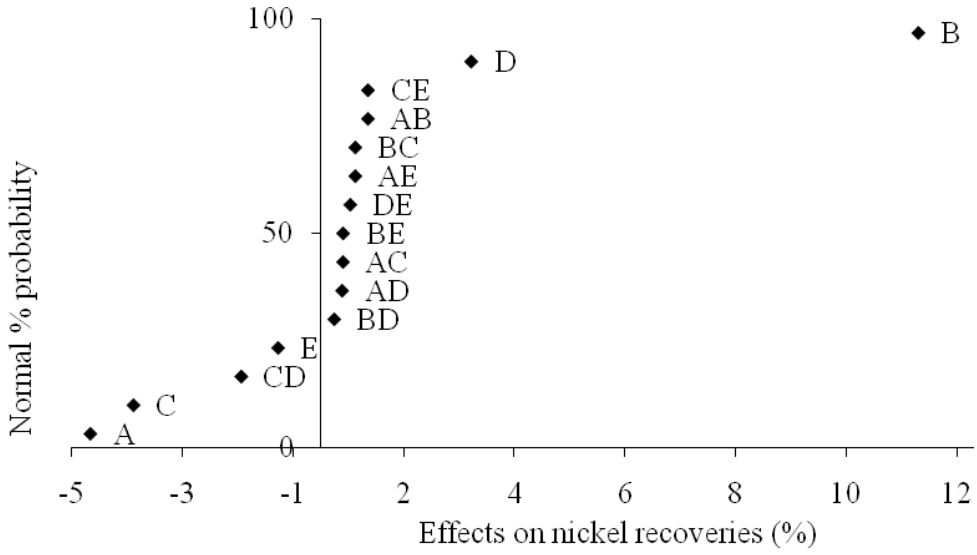


Figure 5.1. Normal plot of effects of main and two factor interactions (combined designs); A, B, C, D, E are factors (Table 5.2); AB, AC, AD, AE, BC, BD, BE, CE, CE are interaction of factors

The recoveries during the bacterial leaching of nickel laterites given in Tables 5.2, 5.3, and 5.4 were calculated as a percentage of nickel in the liquid phase to that in the original nickel laterite ore (see example in Appendix A). Table 5.3 is a fold- over design which was the exact opposite of the basic design (Table 5.2) in signs. The two

designs were combined to estimate all of the main effects clear of any statistically insignificant two factor interactions as shown in Figure 5.1.

The determination of the significant effects as analysed by the probability plots are shown in Figure 5.1. In Figure 5.1, when the effects of individual factors were assessed using the combined design of the basic and fold-over designs, A (pH), B (particle size), C (pulp density) and D (type of substrate) showed that they were statistically significant factors since they have nonzero means. E (inoculum size) was not a statistically significant factor because it does not differ much from normal distribution (zero mean). There was a significant interaction effect between pulp density and type of substrate. This means that the interactive nature of pulp density and substrate (sulphur and pyrite) has an effect on the nickel recovery process.

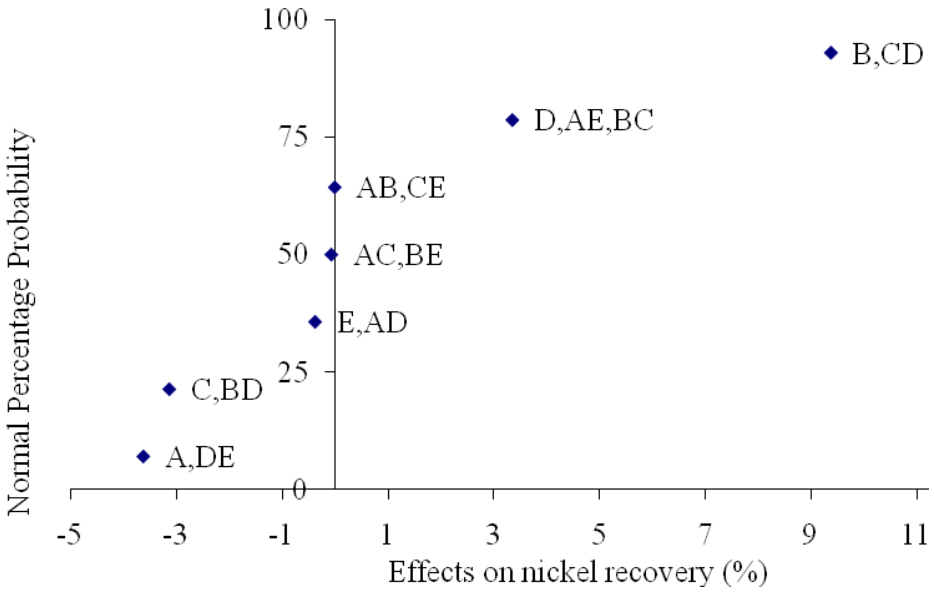


Figure 5.2. Normal plot of effects of main and two factor interactions (basic design)

When the effects of the main and two factor interactions of the basic design alone were plotted it was not possible to distinguish the main effects from the two factor

interactions in the confounding pattern (Figure 5.2). This can be seen, for example, an effect of factor 'A' was confounded by an effect of interaction between factors 'D' and 'E'. A first order polynomial model (prediction or fitted model) between significant factors and response was developed to illustrate the dependence of response on the significant factors. This model is expressed below:

$$R = 24.03 - 2.08A_a + 5.40B_b - 1.69C_c + 1.36D_d \quad + 0.71C_cD_d \quad (5.6)$$

where R is the recovery, A_a, B_b, C_c and D_d are the contrast constants (+1 and -1) for the factors A, B, C, D respectively.

In Equation 5.6, the negative signs in some of the variables of the prediction model equation indicate that in order to maximize bioleaching of nickel laterites, these factors must be kept in low levels. The positive signs mean that the factors must be kept at high levels.

The observed nickel recoveries at the four centre points were 20%, 21%, 25% and 22% (Table 5.4). The average of these four centre points is 22%; with a coefficient of variation of 9.8%. The average of the 8 runs for the base design (Table 5.2) and 8 runs for the fold-over design (Table 5.3) is 24%. Using the centre points, the error is estimated from Equation (5.4) as 5.0 and, the sum of squares for pure quadratic modeling from Equation (5.5) is 10.7. The ratio of the sum of pure quadratic (SS_{PE}) and error (σ^2) is 2.0. Since this ratio is large, it is suspected that there is a curvature present. The test for nonlinearity, however, does not tell which factor(s) contain the curvature, only that it exists (Barrentine, 1999). However, for the purpose of this study (screening of factors), it was assumed that the linearity assumption holds very approximately (Montgomery, 2005). In fact, since Equation (5.6) contains some interaction term, the model is, therefore, capable of representing some curvature in the response function (Montgomery, 2005).

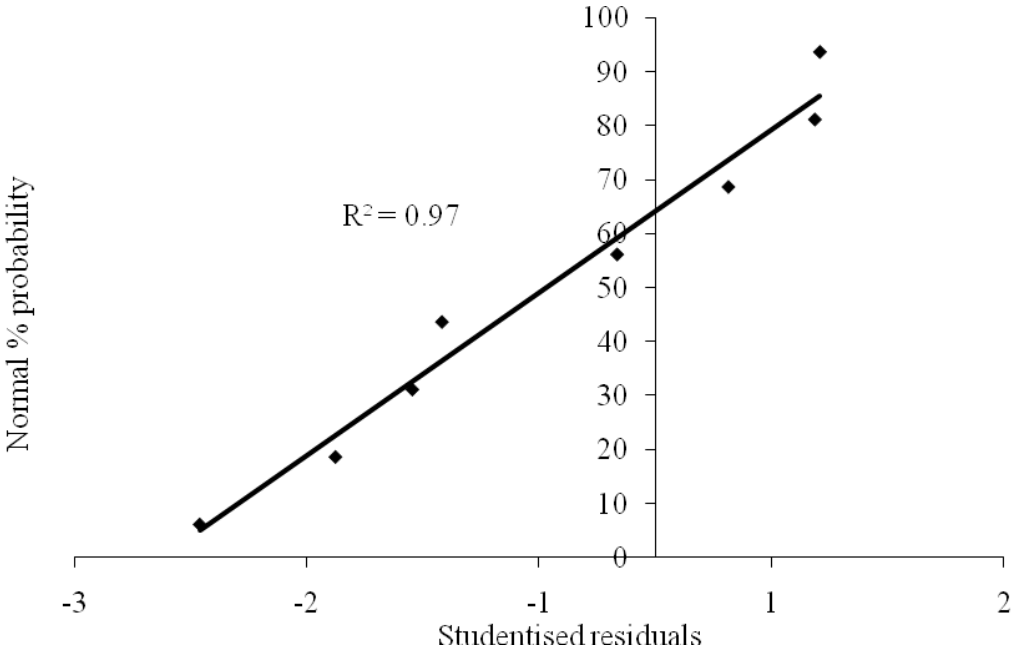


Figure 5. 3. Normal plot of residuals

Figure 5.3 is a normal plot of residuals. As can be seen, all residuals lie on a straight line with a linear correlation coefficient of 97%, which shows that the residuals were distributed normally. A plot of residuals versus the fits (fitted model values or predicted recovery) is a test of the assumption or hypothesis that the variations are the same in each group (Figure 5.4) i.e., the random errors are distributed with mean zero and constant variance. All residuals were distributed between -2 and +1 without any systematic structure. Since, the residuals were distributed normally with constant variance, mean zero and independently (Figures 5.3 and 5.4), it can be concluded that Equation (5.5) was good to fit the experimental data. In other words, the underlying assumptions about the errors were satisfied.

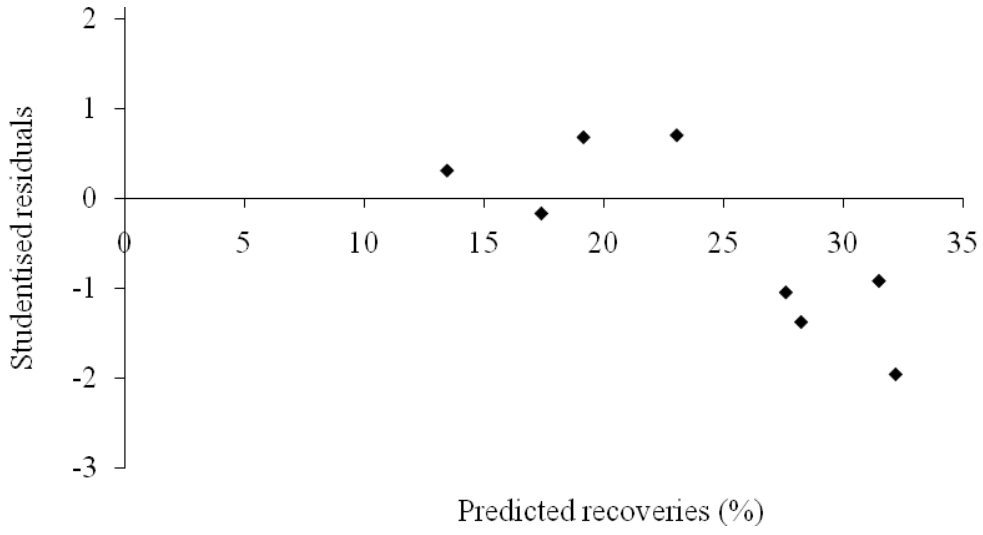


Figure 5.4. Plot of residuals versus predicted recoveries

5.3.2. Influence of Factors on Recovery

Effects of pH

The effect of pH is shown in Figure 5.5. The figure shows that higher recovery of nickel is obtained at lower pH under the conditions tested. A pH of the growth medium significantly affects the growth and activity of acidophilic microorganisms. Due to the high bacterial activity at lower pH, the concentration of acid (H^+ ions) is also expected to be high ($pH = -\log_{10}[H^+]$) . It is the H^+ ions that are assumed to induce nickel dissolution as indicated in Equation (2.11) of Chapter 2; and hence more nickel recovery at low pH levels.

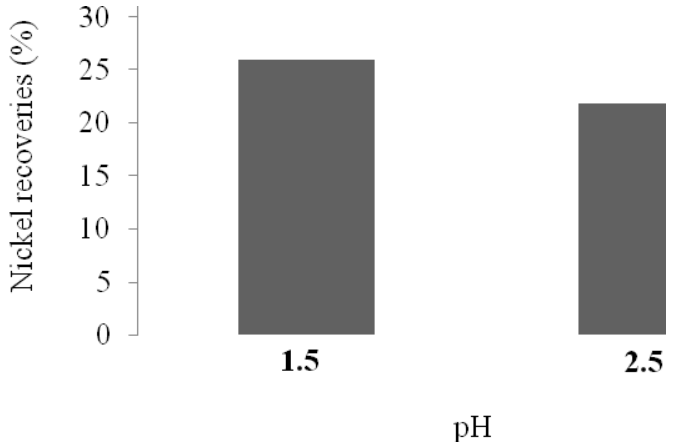


Figure 5.5. Effect of pH on nickel recovery (combined designs)

Effect of particle size

The effect of particle size is shown in Figure 5.6. The figure shows that, in the range studied, particles of less than 38μm had a negative influence on nickel recovery. This is in contrast to the expectation that a greater exposed surface area (of the smaller particles) would reflect an increase of the nickel dissolution. It also contrasts the fact that smaller particle sizes were found to have higher nickel content compared to larger particles (Appendix B). It is likely that the rate of collision between nickel particles and, that between nickel particles and bacteria increases as nickel particle size reduces (Acevedo et al, 2004), such that bacterial attachment to the pyrite or sulphur substrate is constrained. The apparent physical attrition, due to the presence of small particles, could have disrupted the structure of the cells (Nemati et al, 2000), thus rendering them inactive to produce lixiviant through oxidation of the respective substrates.

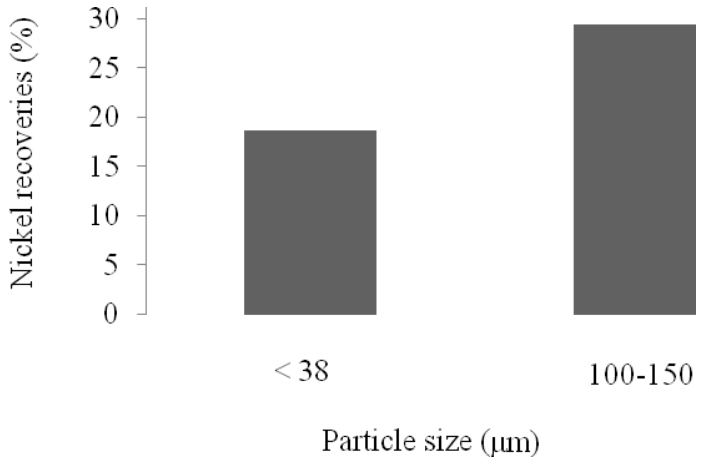


Figure 5.6. Effect of particle size on nickel recovery (combined designs)

The great complexity of the mineralogy of nickel laterites may have also enhanced the ionic and hydrogen bond interactions. These interactions are affected by the particles of smaller sizes where greater surface area leaves each particle exposed to a greater amount of different mineral species (Makita et al, 2004). The -38µm particle size was, therefore, taken to be the critical minimum particle size in the ranges studied. However, the actual effective size range for optimum nickel recovery was yet to be determined in subsequent optimisation test works (Chapter 7).

Effect of pulp density

The pulp density effect is shown in Figure 5.7. In the range of conditions tested, the figure shows that lower recovery of nickel is obtained at higher pulp density of 15%. The reduction in the rate of bacterial leaching at higher pulp density can be attributed to the ineffective homogeneous mixing of solids and liquids leading to gas transfer limitation (Ochoa et al, 1999; Gericke et al, 2001); because the liquid becomes too thick (high viscosity) for efficient gas transfer to the cells. By contrast, the opposite is true at low pulp density, i.e., high nickel recovery at a pulp density of 5%.

On the other hand, agitation has a double purpose: to increase the rate of transfer operations, such as O_2 and CO_2 and heat transfer, and to mix the contents. The agitation speed was constant; so when the pulp density increased, the solids suspension and homogeneity for effective mass transfer was affected.

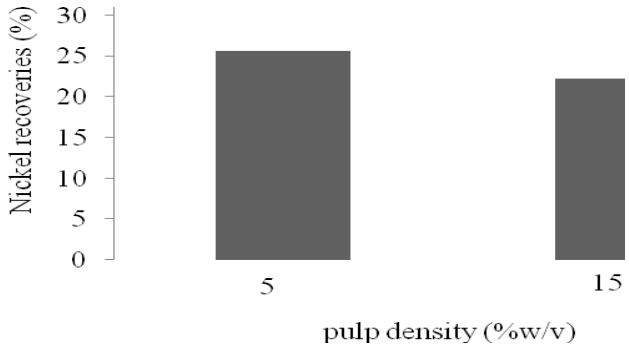


Figure 5.7. Effect of pulp density on nickel recovery (combined designs)

Effect of the type of substrate

For the pH variance figures discussed in this section reference should be made to the experimental data in Appendix D (Table D7-D8).

The effect of substrate is shown in Figure 5.8. The figure shows that higher recovery of nickel, though not very significant, is obtained with the use of sulphur as a substrate. This can be attributed to the higher production of acid with sulphur compared to pyrite as can be seen from the pH variation profiles (Figure 5.10). The higher rate of acidification (low pH values) can be considered as an indicator of the enhanced microbial activities in the leaching media (Rossi 1990; Hanford and Vargas, 2001; Schippers and Sand, 1999). Figure 5.5 already demonstrated that a low pH media optimizes nickel recovery than a high pH media. On the same basis, the postulated higher microbial activities with sulphur than pyrite substrate can be attributed to more energy gained from oxidation of sulphur compared to oxidation of pyrite (Rawlings et al., 1999; Yu et al., 2001).

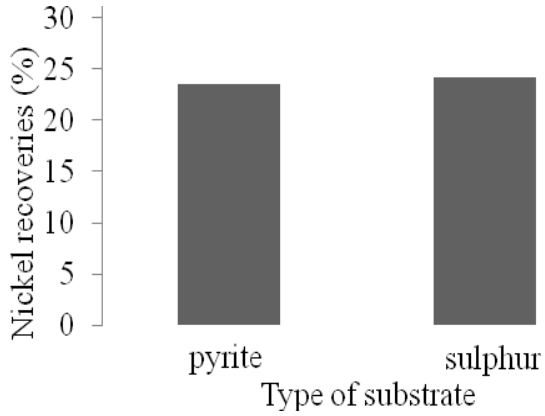


Figure 5.8. Effect of the type of substrate on nickel recovery (combined designs)

The bacterial population as determined by measuring turbidity or optical density of the bacterial suspension using UV-Visible double beam spectrophotometer also showed that there was higher bacterial concentration with sulphur substrate compared to pyrite (Figure 5.9). A detailed analysis of the effects of the type of substrate is given in Chapter 6.

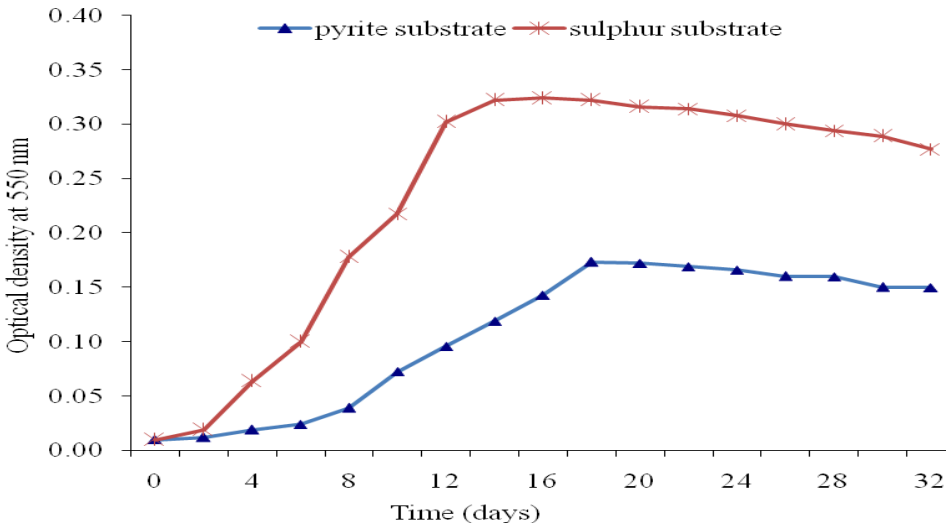


Figure 5.9. Optical density at 550 nm as a function of time at pH of 1.5

Figure 5.10 shows the degree of pH variance from the set point during bioleaching with sulphur and pyrite substrates for different runs in the basic design procedure. When sulphur was used as a substrate, irrespective of the initial pH (1.5 or 2.5), the pH decreased and stabilized at some limiting values. The limiting values were observed to be in the range of 1.9-2.0 for higher pH set points and in the range of 1.3-1.4 for lower pH set points. When pyrite was used as the substrate, the pH increased and stabilized in the pH range of 1.5 -1.6 for lower set points. The pH was, however, observed to decrease and stabilize in the pH range of 2.3-2.4 for the higher set point.

A similar pH variation trend (Figure 5.11) was observed during bioleaching in the fold-over design procedure. When sulphur was used as a substrate, the pH decreased and stabilized in the range 1.3-1.4 for the lower pH set point and stabilized in the range 1.9-2.0 for higher pH set points. The limiting values were observed to be in the range of 2.1-2.2 for higher pH set points and in the range of 1.5-1.6 for lower pH set points when pyrite was used as a substrate.

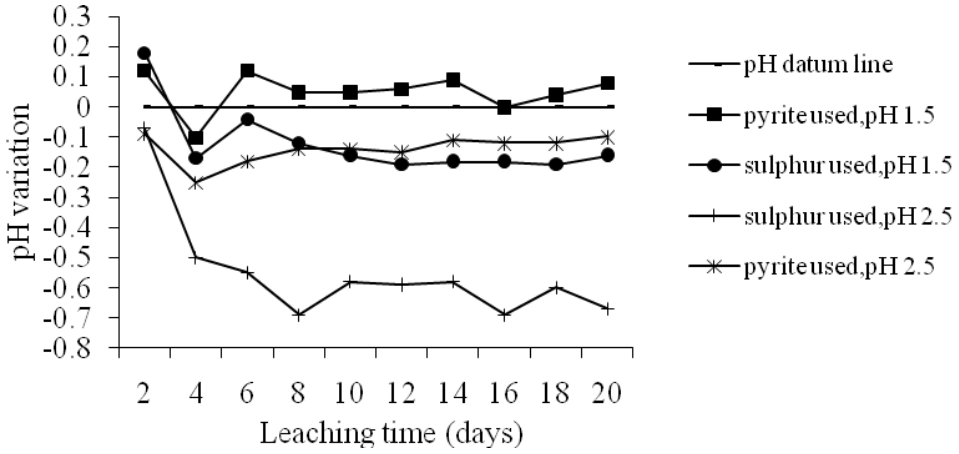


Figure 5.10. pH variation profiles (basic design)

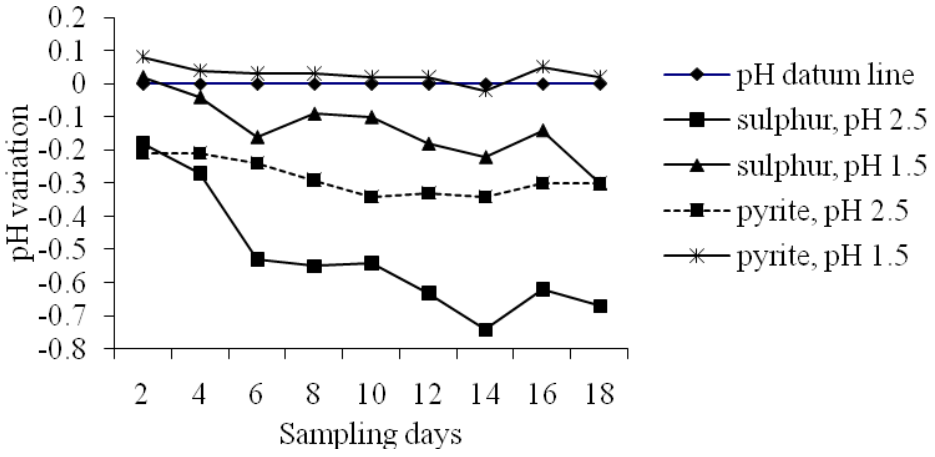


Figure 5.11. pH variation profiles (fold-over design)

In conclusion, the potential of reduced inorganic sulphur compounds (elemental sulphur and pyrite inclusive) addition and subsequent biological acid generation to maintain the low pH during the bioleaching of nickel laterite has been demonstrated for the process viability. The results have clearly demonstrated that a lower pH media created through the induction of a substrate such as sulphur or pyrite accelerates the bioleaching process, and consequently, more nickel recovery. This bioleaching process has exhibited satisfactory efficiency with greater potential for further optimization.

Effect of dosages of bacterial inoculum

The initial amount of bacterial inoculum added did not seem to have any significance (Figure 5.1). This can be explained from the fact that bacteria is not 'directly attacking' a constituent of the ore itself, unlike in the sulphide minerals where sulphur or ferrous which forms part of the minerals is being oxidised – thus having a direct impact on mineral dissolution. It seems that the effect of bacteria on the mineral

dissolution depends mostly on the relationship between the bacteria and the substrate (sulphur or pyrite) added to the media. In this study, it can be summarized that the rate of acid production by the bacteria through reduced sulphur oxidation was higher than the rate of acid consumption (nickel dissolution), irrespective of the dosages of bacterial inoculum.

Effect of factor interaction

In the ranges studied, the interaction between the variables, apart from pulp density and type of substrate, were observed to be statistically insignificant. Their effects were normally distributed with mean zero and fell along a straight line on the plot (Figure 5.1). However, there seems to be no seen logical reason for any interaction between pulp density and substrate type. The statistical significance of the interaction effect was yet to be determined in the subsequent optimisation test works (Chapter 7).

5.3.3 Leaching Profile

Nickel laterites bioleaching results for the eight experimental runs of the basic design (Table D1) are shown in Figure 5.12. In this plot a great deal of scattered data among experimental runs is observed. This shows that there is still a great deal of variability that exists among the effects of factors considered in this study. The reduction in recoveries in some cases can be attributed to the precipitation of nickel ions. A similar leaching profile (Figure 5.13) was observed during bioleaching in the fold-over design (Table D2).

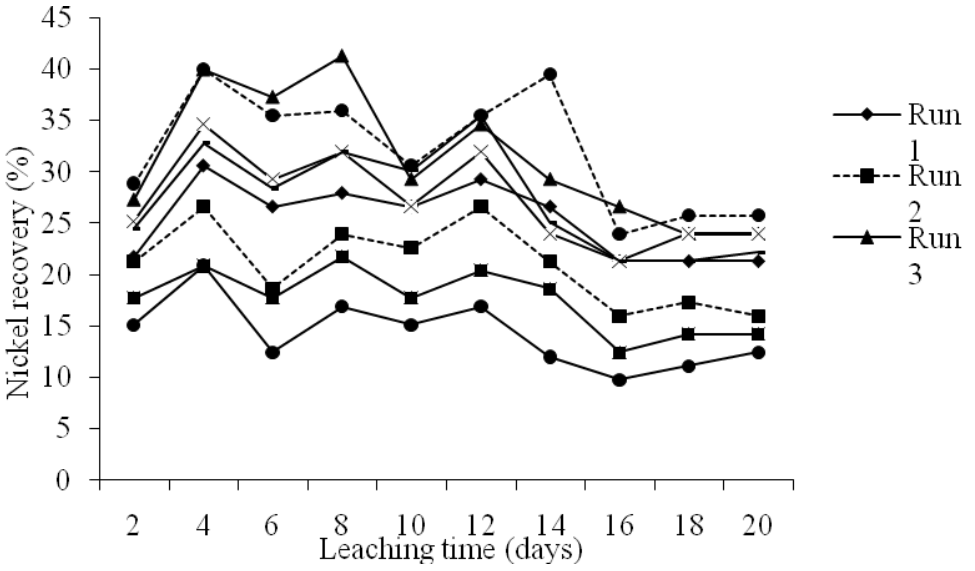


Figure 5.12. Plot of nickel recovery versus leaching time (basic design)

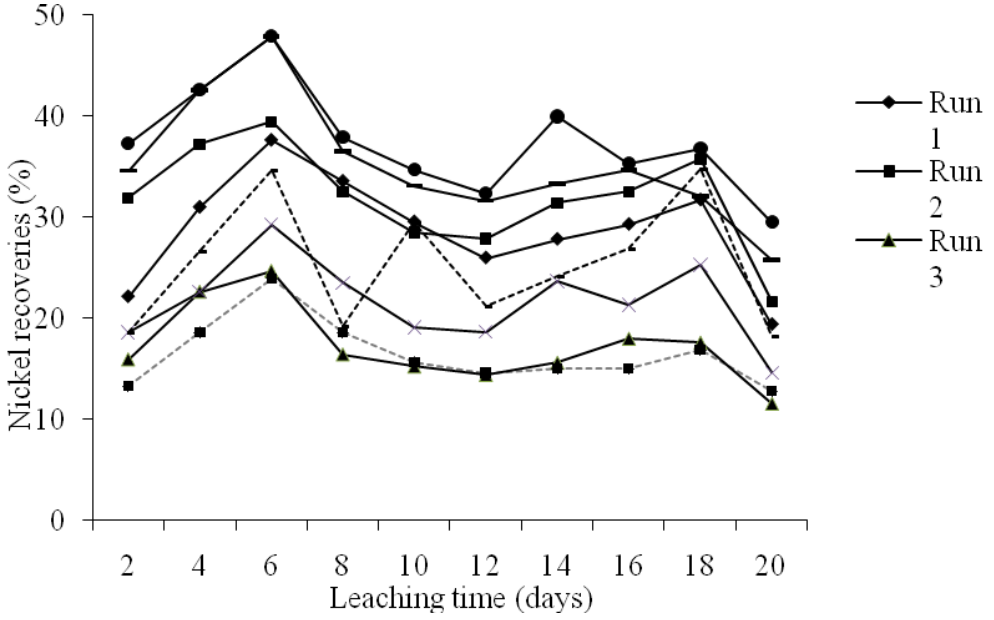


Figure 5.13. Plot of nickel recovery versus leaching time (fold-over design)

5.4 Summary and Conclusions

The purpose of the characterisation or diagnostic two-level quarter fractional design presented in this chapter was to obtain experimental data to serve as an initial approach to the final optimisation that is presented subsequently in Chapter 7; establishing which factors had significant effects on response (nickel recovery) and whether these effects were positive or negative. The factors investigated under this chapter included pulp density, particle size, pH, size of bacterial inoculum and substrate type. At this stage, factors were studied at their maximum and minimum levels. The experimental results were analysed statistically for the significance of the factors using the probability plots.

The results obtained indicated the following:-

- The statistical method and experimental design approach selected have been able to satisfactorily help in determining statistically significant and insignificant factors.
- The fold-over design tests provided clarity of results on the main effects ensuring that the main factors were not confounded with statistically insignificant two factor-level interactions.
- Inoculum size was not statistically significant while the rest of the factors were statistically significant, meaning that the initial inoculum size did not significantly influence or affect the nickel recovery process. It also meant that pulp density, particle size, pH and substrate type had significant influence on the nickel recovery process.
- Under the ranges studied, the interaction between most of the variables was found to be statistically insignificant, except that between pulp density and substrate type, which showed a marked influence on the nickel recovery process.

- The results also showed that nickel recovery was maximized at low pH and low pulp density values. Thus, low pH environments and low pulp density are desired for optimal nickel recovery.
- In the range studied, particles of less than 38μm, although having a high content of nickel, had a negative influence on the nickel recovery process in terms of the final yield. Larger particles in the range of 100-150 μm, on the other hand, gave higher recovery.
- Sulphur substrate exhibited better effects than pyrite in terms of acidification (H^+ ions production) and nickel recovery processes. The low pH obtained with the sulphur substrate indicated a production of acid which enhanced the recovery of nickel as compared to the pyrite substrate. For the test conditions considered in this study and for this kind of nickel recovery process, this finding signifies that sulphur is ultimately a better substrate than pyrite.
- Sulphur substrate gave higher optical density reading than pyrite substrate. This shows that there was a higher microbial activity in the presence of sulphur substrate than pyrite substrate.
- The large ratio of the sum of pure quadratic (SS_{PE}) and error (σ^2) indicated that there was a possibility of curvature; so, to estimate not only linear effects but, also quadratic effects and to build response surfaces for maximal nickel recovery in the region defined by the characterisation or diagnostic tests, a new experimental design during the optimisation stage in Chapter 7 was carried out.

The next chapter (Chapter 6) focuses on studying the effect of pH on substrate type (sulphur and/ or pyrite) in the bacterial leaching of nickel laterites.

CHAPTER 6

EFFECT OF INITIAL pH ON SUBSTRATE TYPE

"*Theory guides, experiment decides*".

- I. M. Kolthoff

6.1 Introduction

pH is an important parameter that can be utilized to determine the extent to which nickel laterites dissolve. It also determines the diversity of the microorganisms in a colony. The solution pH in a given bioleaching operation is determined by the balance between the acid-producing and acid-consuming reactions. Reduced inorganic sulphur compounds that are exclusively oxidised by acidophilic chemolithotrophic microorganisms for their energy supply produce sulphuric acid (Rossi, 1990). The aim of this particular work contained in this chapter was to investigate the pH requirements for the bacterial leaching of nickel laterites using a mixed culture of chemolithotrophic microorganisms in the presence of externally added elemental sulphur and pyrite as substrates.

6.2. Materials and methods

6.2.1. Ore Samples and Preparation

The nickel ore was crushed and was classified into +63-75μm size fractions using standard sieve plates. This size range was used because it represented most of the nickel laterite material in terms of mass (Table B3). The chemical composition of nickel was determined prior to chemical leaching experiments. The typical chemical composition of various oxides in the laterite ore used is given in Appendix B.

6.2.2. Microbes

The bacteria and growth media used were described previously in sections 3.3.2 and 3.3.1 of Chapter 3, respectively.

6.2.3. Experimentation

Bioleaching experiments were carried out in 250-ml Erlenmeyer flasks with 100mls of slurry (mixture of 5g nickel laterite ore and 100-mls of medium) together with an appropriate amount of sterilised energy sources (30% w/w elemental sulphur and 56 % w/w pyrite to that of nickel laterite). These quantities of energy sources were chosen so as to have the same sulphur content in both elemental sulphur and pyrite. Initially, pyrite was crushed and finely ground (Chapter 3, Section 3.2.1). The slurries were inoculated with 10% (v/v) mixed bacterial culture. Following lack of statistical significance of the inoculum size (Chapter 5, Section 5.3.1), 10% was chosen as the average of the low and high levels tested (Chapter 5, Table 5.1). The pH of the mixtures was adjusted to 1.0, 1.5, 2.0 and 2.5, respectively. These pH ranges (i.e. pH <3) were chosen because they are known to optimize the growth of acidophilic microorganisms (Norris and Johnson, 1998). Some experiments were also run at initial pH of 1.5 using fresh liquid medium with an appropriate amount of sterilised energy sources but without the inoculation of bacteria for comparison with inoculated experiments. Un-inoculated distilled water and nutrient media were run as sterile at an initial pH of 1.5.

The flasks were covered with pieces of aluminium foil to reduce evaporation and prevent contamination but allow free supply of air, and then incubated in a platform shaking incubator at 30°C and 190 rpm. The pH profiles and redox potentials of the leach solution were measured but not controlled through out the leach period using 744 pH meter Metrohm. Samples were drawn from flasks every three days to determine the concentration of metals dissolved using the Varian SpectrAA-55B atomic absorption spectrophotometer.

6.3. Results and Discussion

6.3.1. Effect of pH and Reduction Oxidation Potential on the Bioleaching of Nickel Laterites

For the results discussed in this section reference should be made to the experimental data in Appendix E (Tables E1-E4). The results discussed are an average of the runs conducted under similar experimental conditions.

The dissolution of nickel laterites was dependent on the initial pH (Figures 6.1 and 6.2). Higher recoveries were observed at lower pH; although there was a general increase in the rate of nickel dissolution with time for all pH levels.

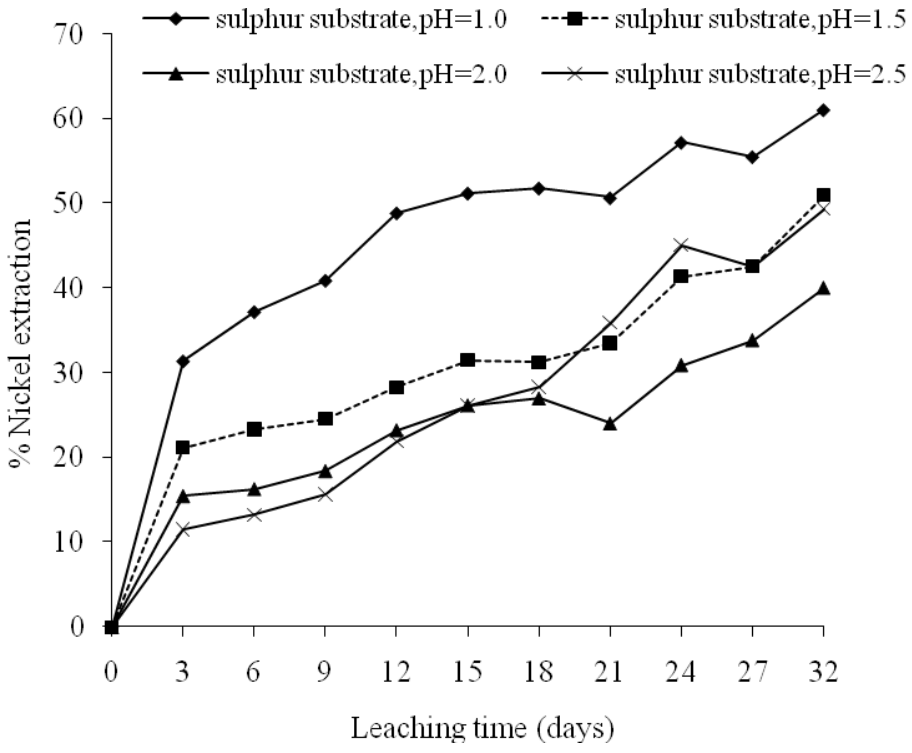


Figure 6.1. Effect of pH on the leachability of nickel laterite with sulphur substrate

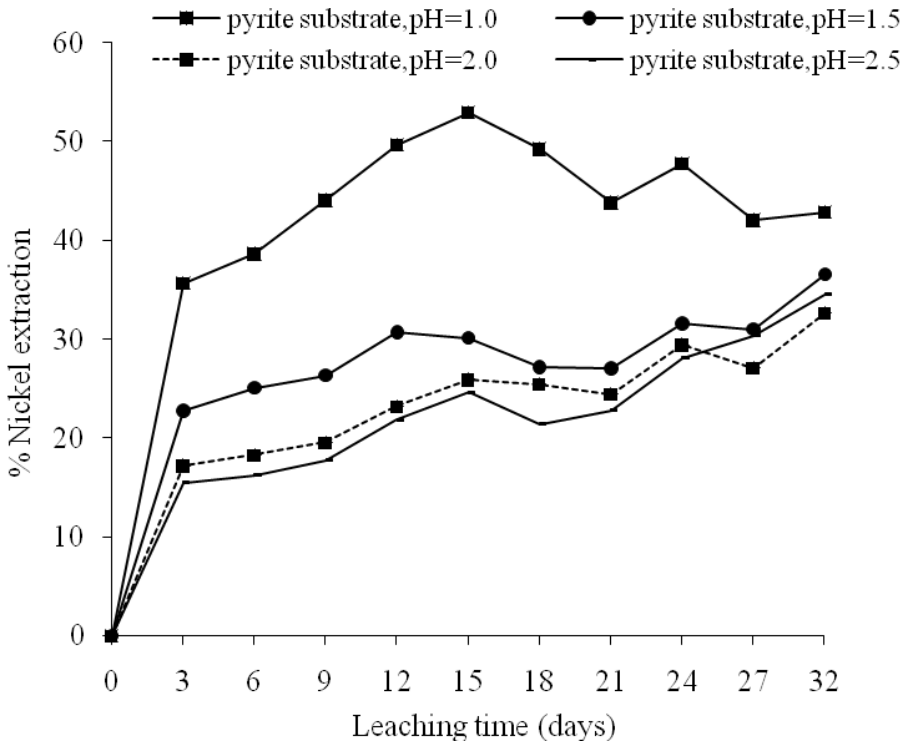


Figure 6.2. Effect of pH on the leachability of nickel laterites with pyrite substrate

The graphs also show that there was a high step change in the nickel recovery for the pH of 2.5. This was attributed to the higher rate of acidification at this pH level. Previous studies have shown that higher rates of acidification imply that there were higher microbial activities (Rossi 1990; Hanford and Vargas, 2001; Schippers and Sand, 1999). Acidification in this context means production of H^+ ions. The production of H^+ ions is depicted by the pH drop, and that pH is a measure of concentration of H^+ ions (i.e. $pH = -\log_{10}[H^+]$). Higher recoveries were observed for sulphur substrate than for pyrite substrate at all pH levels after two weeks (Figures 6.3-6.6). However, recoveries were higher for the pyrite substrate in the first two weeks.

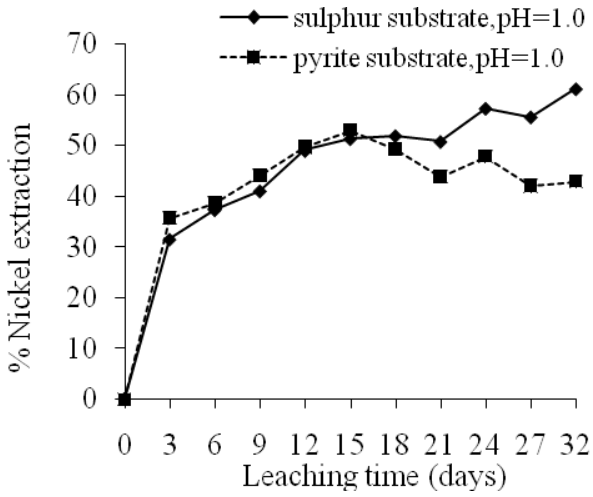


Figure 6.3. Dissolution rates of nickel laterites as a function of substrate type at initial pH of 1.0

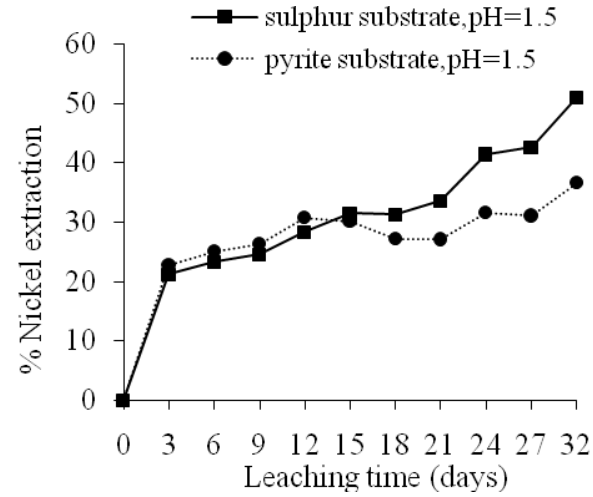


Figure 6.4. Dissolution rates of nickel laterites as a function of substrate type at initial pH of 1.5

In the initial stages, it is expected that the bacteria are not very active; so abiotic oxidation of the substrates is supposedly dominant. At acidic pH levels, elemental sulphur is inert to abiotic oxidation, although other species such as thiosulphate and tetrathionate are oxidised abiotically to sulphate (Schippers and Sand, 1999; Rohwerder et al., 2003).

Pyrite is oxidised by ferric ions via the thiosulphate route producing sulphuric acid (Schippers and Sand, 1999); thus pyrite had higher pH drops (Figure 6.9) and higher recoveries (Figures 6.3-6.6) initially. Figure 5.9 shows that bacterial concentration was higher for sulphur substrate than pyrite in the beginning. This shows that abiotic oxidation was more important than biotic oxidation in the beginning. These observations, therefore, have shown that a period of more than two weeks is an effective duration for the bacterial leaching of nickel laterites.

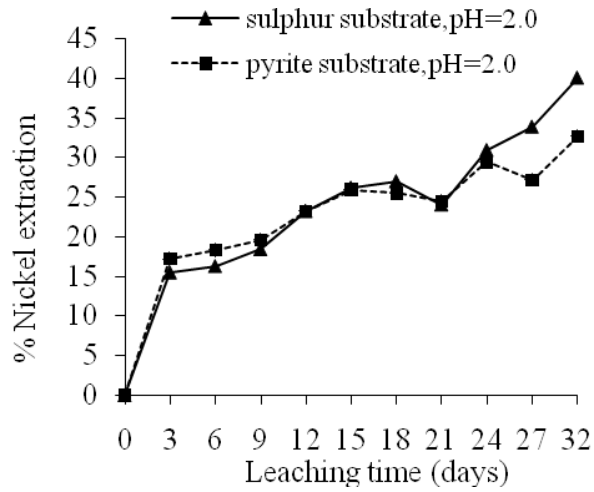


Figure 6.5. Dissolution rates of nickel laterites as a function of substrate type at initial pH of 2.0

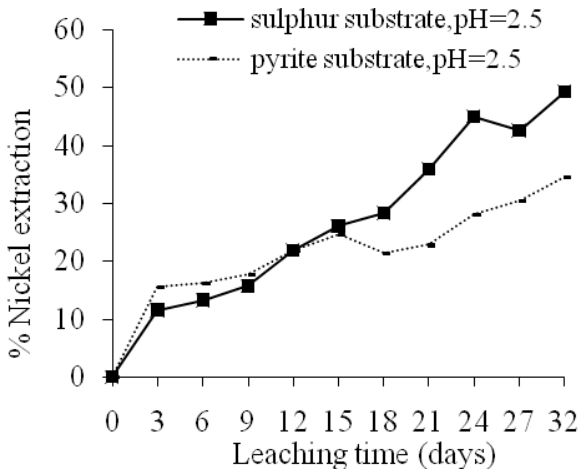


Figure 6.6. Dissolution rates of nickel laterites as a function of substrate type at initial pH of 2.5

The inoculated slurry in all cases resulted in a decrease in pH (Figure 6.7 and 6.8). The low pH is attributed to the oxidation of elemental or reduced sulphur to sulphuric acid by the leaching bacteria (Equations 2.2-2.5 of Chapter 2). The results in Figure 6.7 through 6.10 also show that the pH decreased rapidly at higher initial pH, 2.5>2.0>1.5>1.0. This can be attributed to either; (1) the bacteria were naturally inactive at the low pH or, (2) metal toxicity due to higher metal recoveries (due to initial rapid chemical leaching) at low pH. Further more, at higher pH both elemental sulphur and ferrous iron are oxidised abiotically at significant rates (Rohwerder et al., 2003). This trend in pH changes was also observed during the identification of influential factors (Chapter 5, Section 5.3.2).

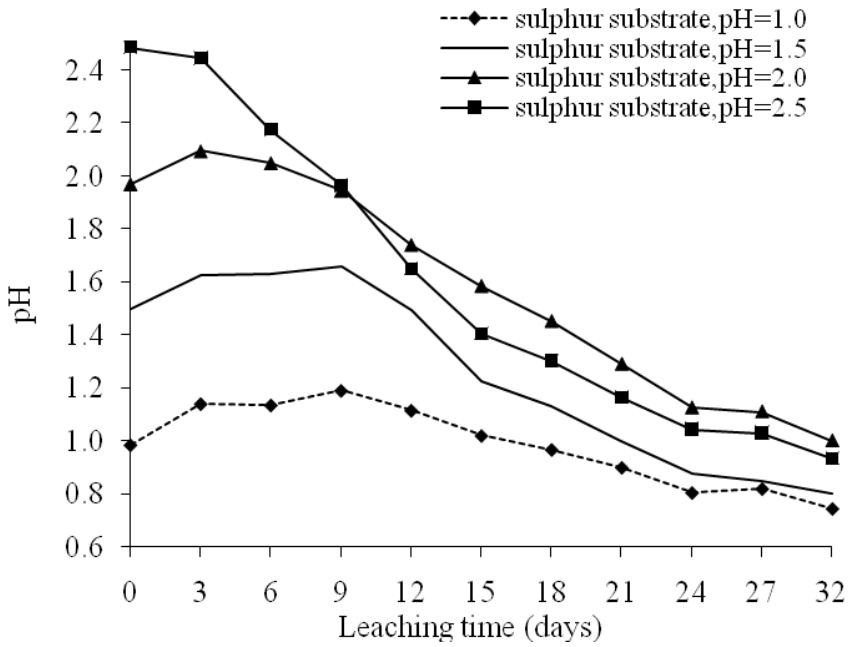


Figure 6.7. Evolution of pH with time for sulphur substrate

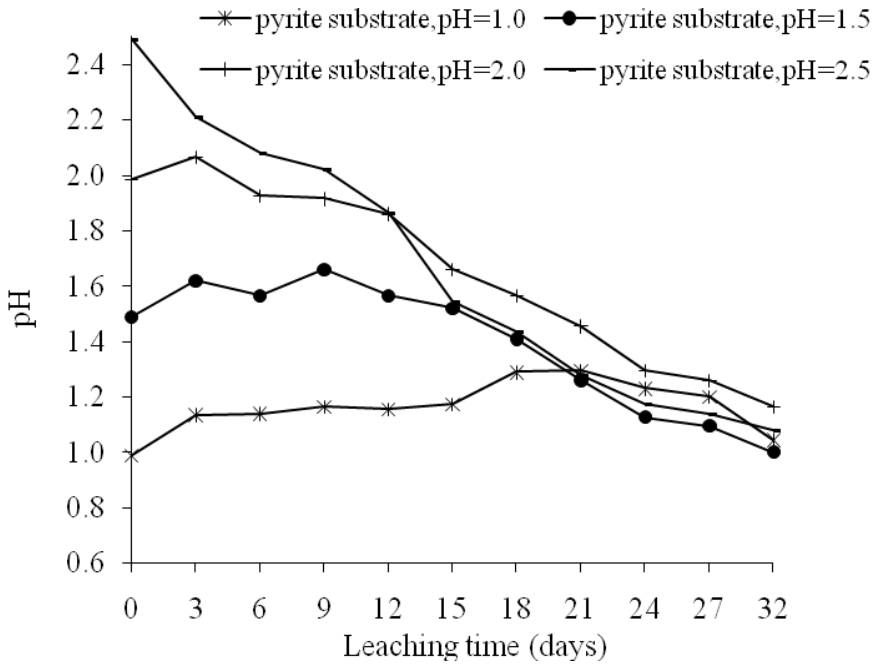


Figure 6.8. Evolution of pH with time for pyrite substrate

Apart from a pH of 2.5, an initial rise in pH in the first three to ten days was observed in all other cases (i.e. initial pH 1.0, 1.5, 2.0), implying that the bacterial activity was very low or completely absent during that time (Figure 6.7 and 6.8). The pH drop for all the pH tested (i.e. initial pH 1.0, 1.5, 2.0, 2.5) was initially higher for pyrite than sulphur (Figure 6.9).

The subsequent pH drop was higher for sulphur substrate than pyrite at the same initial pH, implying higher rate of acidification with sulphur substrate (Figure 6.10). The results of the differences in pH drops can also be seen in the recoveries, being initially higher for pyrite and subsequently higher for sulphur (Figures 6.3-6.6).

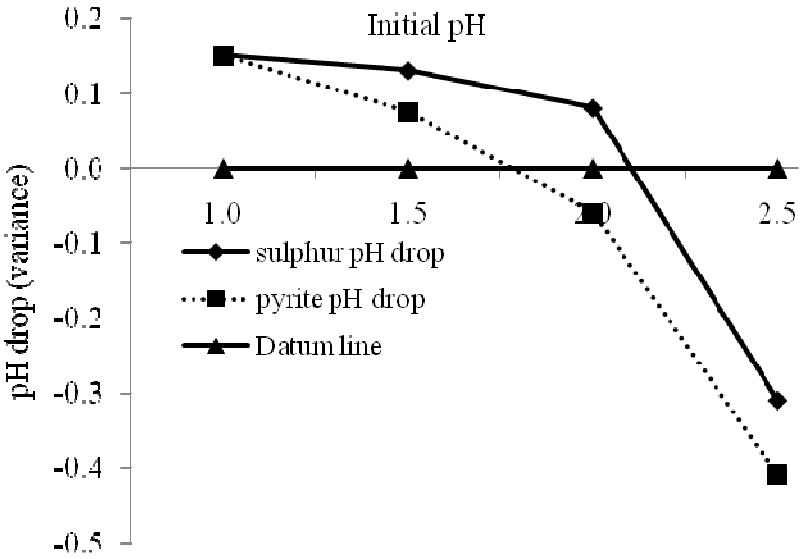


Figure 6.9. pH drop for sulphur and pyrite substrates in a week

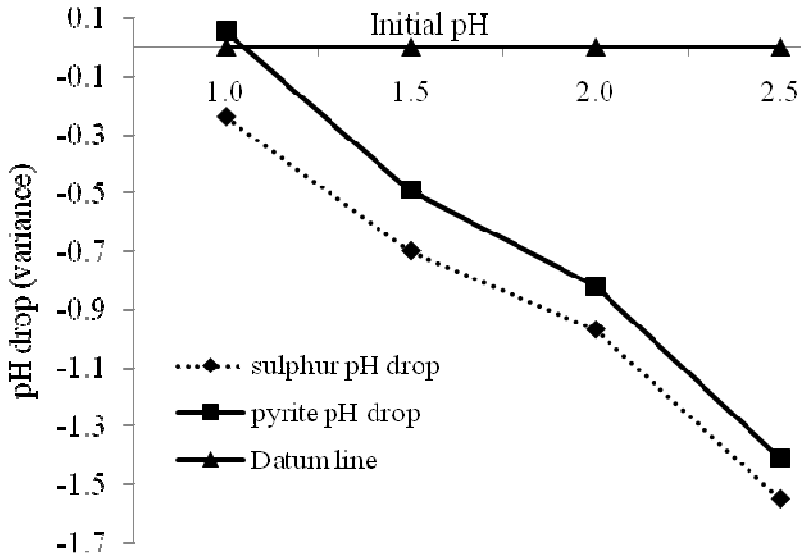


Figure 6.10. pH drop for sulphur and pyrite substrates in a month

The higher rate of acidification can be considered as an indicator of the higher microbial activities in the leaching media (Rossi 1990; Hanford and Vargas, 2001; Schippers and Sand, 1999). A higher microbial activity with sulphur was also observed previously (Chapter 5, Figure 5.9) and was explained as being due to more energy gained from oxidation of sulphur compared to the oxidation of pyrite (Rawlings et al., 1999; Yu et al., 2001).

The changes in oxidation reduction potential (ORP) during microbial leaching are shown in Figures 6.11 and 6.12. The opposite trends to that of pH were observed from these figures. The observed ORP of the solution is highly dependent on a number of parallel reactions. The figures show that ORPs were higher at lower initial pHs, implying higher ionic activities at the lower pHs. The higher ionic activities were attributed to the higher recoveries at these pHs. The figures also show that the rate of change of ORP was higher at an initial pH of 2.5.

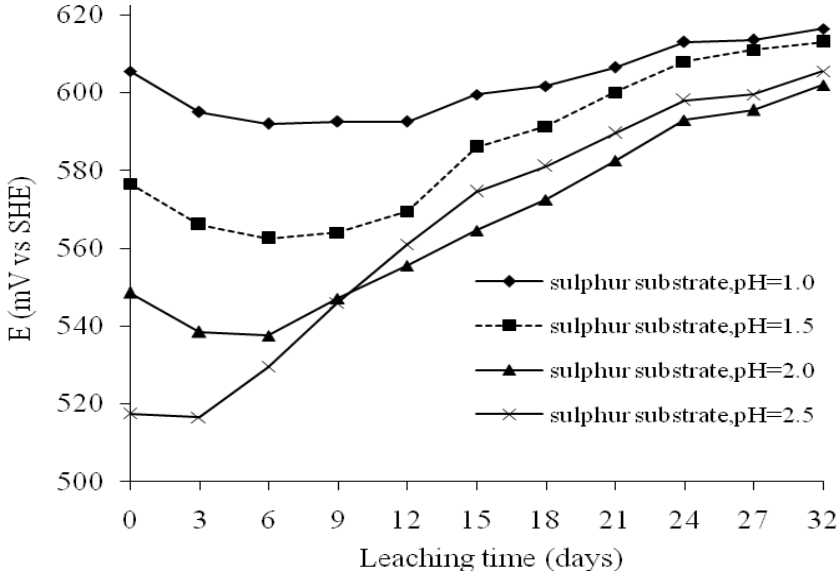


Figure 6.11. Evolution of ORP with time for sulphur substrate

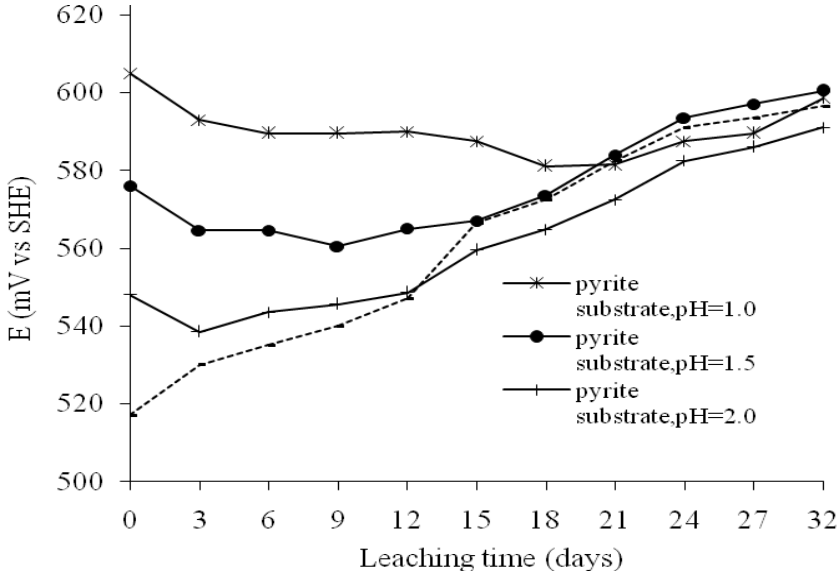


Figure 6.12. Evolution of ORP with time for pyrite substrate

6.3.2. Effect of Media Composition on the Changes in pH and Oxidation Reduction Potential

For the results discussed in this section reference should be made to the experimental data in Appendix E (Tables E3-E4). The results discussed are an average of the runs conducted under similar experimental conditions.

Figures 6.13 and 6.14 show the effects of different media composition on pH and ORP, respectively. It is observed in Figure 6.13 that for inoculated experiments, there was a slight increase of pH initially and a subsequent decrease of pH thereafter. This was most likely due to the predominance of abiotic oxidation process initially. Even though acid production took place in the long term through the subsequent bioxidation of sulphur and pyrite, the initial net leaching process was likely acid consuming and hence the initial pH rise.

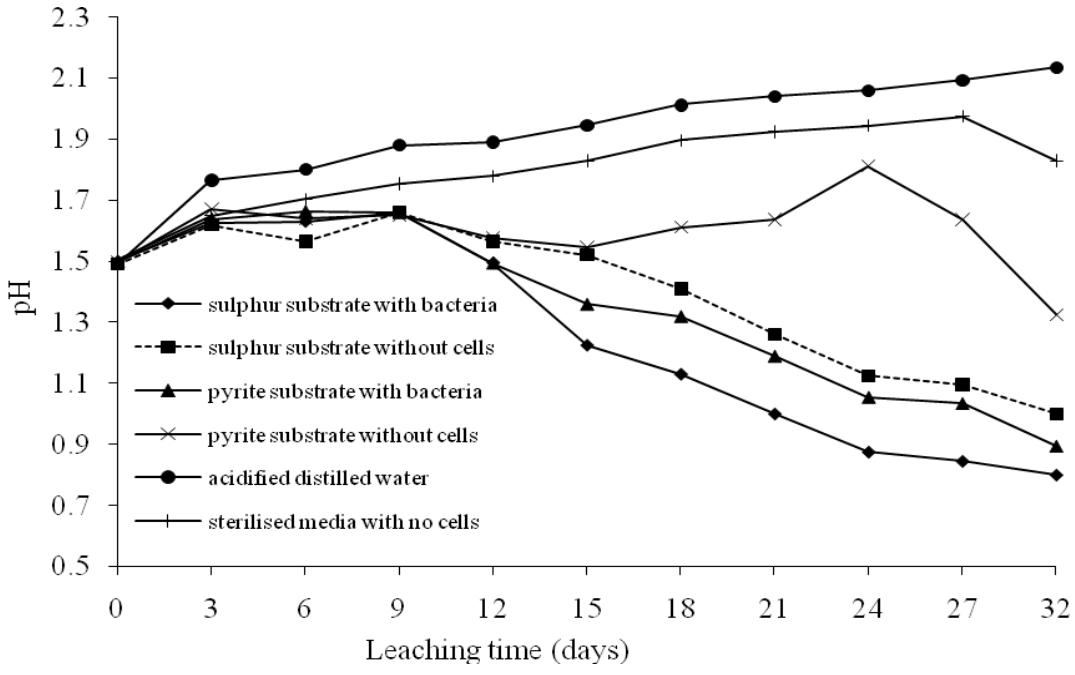


Figure 6.13. Evolution of pH with time at initial pH of 1.5 for different media compositions

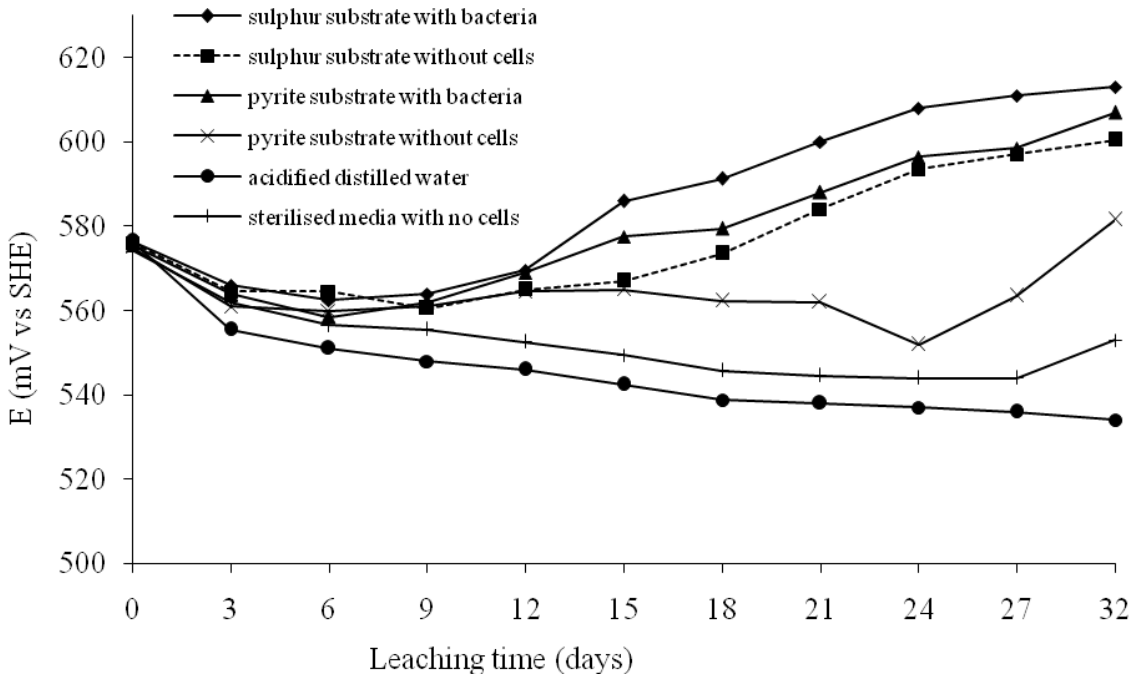


Figure 6.14. Evolution of ORP with time at initial pH of 1.5 for different media composition

In sterile controls (acidified distilled water and sterilised media with no cells), the pH decrease was not observed. An initial rise and final decrease in pH was observed in experiments where un-inoculated sulphur and pyrite media were used. However, the pH decrease for these un-inoculated media was still lower than the inoculated media. This shows the efficacy of the presence of bacteria in the production of acid leading to pH reduction. The pH drop observed with un-inoculated pyrite media can be attributed to the slow pyrite oxidation by oxygen in the presence of water forming ferrous iron and sulphate (Larsson et al., 1990) according to Equation (6.1) below. Sulphur was also assumed to be slowly oxidised by oxygen in the presence of water (Hanford and Vargas, 2001) according to Equation (6.2) below.

$$2FeS_2 + 7O_2 + 2H_2O \rightarrow 2Fe^{2+} + 4SO_4^{2-} + 4H^+ \qquad (6.1)$$

$$0.125S_8 + 1.5O_2 + H_2O \rightarrow SO_4^{2-} + 2H^+ \quad (6.2)$$

Figure 6.14 shows that higher ORPs were obtained with inoculated media than sterile media. The metal ion recoveries are high with inoculated media than sterile media, thus implying higher ionic activities in the inoculated media. The ORP, which in the framework of this study, is a measure of the activities or strength of metal ions in relation to their concentration, is thus higher in the inoculated media.

6.4. Summary and Conclusions

This chapter investigated the pH requirements for the bacterial leaching of nickel laterites using a mixed culture of chemolithotrophic microorganisms in the presence of externally added sulphur containing material (elemental sulphur and pyrite). The bacterial oxidation of sulphur and pyrite produces sulphuric acid, which dissolves nickel laterite to yield the required nickel metal.

The results presented in this chapter show that dissolution rates of nickel laterite were high in low pH and high ORP, and in the presence of bacteria. However, the study showed that microbial activities, depicted by acidification were lower at lower initial pH levels. Although un-inoculated media with energy sources appeared to induce acidification, this was less than that in active bacterial cultures. This shows that under similar conditions, an inoculated media is more effective than an un-inoculated media.

This chapter has also shown the relationships between bacterial activities, depicted by acidification, and type of substrate. The recoveries were initially higher for pyrite and subsequently higher for sulphur at all the initial pH levels studied. The test results and the high nickel recovery yield demonstrated that sulphur was more effective as a substrate than pyrite.

Having found sulphur substrate to be more effective, the next chapter focuses on optimizing the pH, pulp density and particle sizes. The study in the next chapter will be undertaken using statistically-based optimization strategy called response surface methodology.

CHAPTER SEVEN

OPTIMISATION OF INFLUENTIAL FACTORS

"*If your experiment needs statistics, then you ought to have done a better experiment*".

-Ernest Rutherford (Nobel Prize for Chemistry 1908)

7.1. Introduction

The purpose of many simulation tasks in engineering is to develop a predictive model that can be used to improve a process, and the improvement depends mainly on optimization strategies used in a specific process (Edgar and Himmelblau, 1988). Optimisation can be defined as a process of improving an existing situation, device, or system such as a metallurgical process. It consists of finding the best solution to the process within the given constraints. In fact, process optimisation is essential for gaining and maintaining a competitive edge in today's world of intense financial competition.

There are essentially two types of optimization that a metallurgical engineer needs to consider; the first which is termed topological optimization deals with the topology or the arrangement of the process equipment. The second type termed parametric optimization is concerned with the operating variables such as pH, temperature, pressure, particle sizes, and pulp density of streams for a given piece of equipment or process (Edgar and Himmelblau, 1988).

Unfortunately several popular optimisation methods usually do not work very well (Öberg and Deming, 2000). They either rely on the classical one parameter at a time approach that ignores the combined interactions between physicochemical parameters or are theoretical in nature. In this particular study, parametric optimisation was considered using a statistically-based optimisation strategy called response surface methodology (RSM) to determine the optimum conditions of pH, pulp density and particle size for bacterial leaching of nickel laterites. RSM is the most popular technique used to find the optimal conditions by using quadratic polynomial model and is applied as a consequence of a screening or diagnostic experiment (Myers and Montgomery, 2002). The central composite rotatable design (CCRD) was used to collect the data for fitting the second order response. The CCRD requires much fewer

tests than the full factorial and has been shown to be sufficient to describe the majority of steady-state responses (Obeng et al., 2005). A CCRD consists of 2^k factorial or a fractional factorial points (coded ±1), augmented by $2k$ axial or star points [(±λ,0,0,…,0), (0,±λ,0,…,0)…,(0,0,…, ±λ)] and n_c replicate points at the centre [(0,0,0,…,0)] (Oraon et al., 2006); where k is the number of factors studied, λ is distance of an axial point from the centre. To ensure a constant variance of the predicted response at all points equidistant from the design centre, the number of centre point replications, n_c, for the three factors studied was calculated using the following equation (Khuri and Cornell, 1987),

$$n_c \approx 0.8385\left(2^{k/2} + 2\right)^2 - 2^k - 2k \qquad (7.1)$$

The experimental results were analysed statistically by the analysis of variance (ANOVA) using Fisher's variance ratio test (*F-test*); standard errors of model coefficient (*t-test*), the coefficient of determination (R^2) and the absolute average deviation (*AAD*).

7.2. Materials and methods

7.2.1. Ore samples and Preparation

The ore was crushed and sized using the screen sizes given in Tables 7.2 and 7.3. The typical chemical composition of various oxides in the laterite ore used is given in Appendix B.

7.2.2. Microbes

The bacteria and growth media used were described previously in sections 3.3.2 and 3.3.1 of Chapter 3, respectively. Elemental sulphur was used as substrate for the bacteria because it gave better effects than pyrite as described in section 7.2.3.

7.2.3. Experimental Design for the Response Surface Methodology and Central Composite Design

In previous studies during the preliminary investigations into this research (Simate and Ndlovu, 2007; Simate and Ndlovu, 2008; Chapter 5 of this dissertation), it was identified that pH, particle size, pulp density and substrate type were statistically significant operating parameters, while bacterial inoculum size was not statistically significant. Follow up studies also showed that using sulphur substrate as an energy source for bacteria resulted in better nickel recoveries compared to using pyrite (Chapter 6). Response surface methodology and central composite rotatable design have been used in this study in an attempt to determine the optimal conditions of pH, pulp density and particle size for bacterial leaching of nickel laterites.

Table 7.1. Relationship between coded and actual values of the variable (Napier-Munn, 2000)

Code	Actual value of a factor
$-\lambda$	x_{min}
-1	$\frac{(x_{max} + x_{min})}{2} - \frac{(x_{max} - x_{min})}{2\lambda}$
0	$\frac{(x_{max} + x_{min})}{2}$
+1	$\frac{(x_{max} + x_{min})}{2} + \frac{(x_{max} - x_{min})}{2\lambda}$
$+\lambda$	x_{max}

x_{max} and x_{min} are the maximum and minimum values of the natural variables respectively, $\lambda = (2^{k-q})^{1/4}$ for a CCRD, k = number of factors studied, $-q$ = fraction of the number of factors (where q = 0 for full factorial design).

To simplify the calculations and for uniform comparison, factors were studied with their codified values. The five levels of each factor shown in real and coded values calculated using the relationships in Table 7.1 are shown in Table 7.2.

Sulphur substrate having been significant in the previous study was taken as a held-constant qualitative factor. The major objective of the response surface methodology was to develop the optimum conditions so as to maximize the solubilisation of nickel laterites using a mixed culture of chemolithotrophic bacteria (*Acidithiobacillus ferrooxidans, Acidithiobacillus caldus* and *Leptospirillum Ferrooxidans*). Therefore, the recovery (conversion) of nickel was taken as the desired goal (response).

Table 7.2. Experimental layout and runs for the central composite rotatable design

Standard Runs	Coded values of variables			Actual levels of variables		
	pH	Pulp density	Particle size	pH	Pulp density	Particle size
Factorial points						
1	-1	-1	-1	1.5	5	38-75µm
2	+1	-1	-1	3.0	5	38-75µm
3	-1	+1	-1	1.5	12	38-75µm
4	+1	+1	-1	3.0	12	38-75µm
5	-1	-1	+1	1.5	5	106-150µm
6	+1	-1	+1	3.0	5	106-150µm
7	-1	+1	+1	1.5	12	106-150µm
8	+1	+1	+1	3.0	12	106-150µm
Axial points						
9	- 1.682	0	0	1.0	9	75-106µm
10	+ 1.682	0	0	3.5	9	75-106µm
11	0	- 1.682	0	2.3	2	75-106µm
12	0	+ 1.682	0	2.3	15	75-106µm
13	0	0	- 1.682	2.3	9	<38µm
14	0	0	+ 1.682	2.3	9	150-212µm
Centre points						
15	0	0	0	2.3	9	75-106µm
16	0	0	0	2.3	9	75-106µm
17	0	0	0	2.3	9	75-106µm
18	0	0	0	2.3	9	75-106µm
19	0	0	0	2.3	9	75-106µm
20	0	0	0	2.3	9	75-106µm

In Table 7.2, the experimental layout and standard runs for the central composite rotatable design are outlined. Six centre point replications were deduced from Equation (7.1).

For the three variables under consideration, a second order polynomial regression model has been proposed as follows:-

$$y = \beta_0 + \sum_{i=1}^{3} \beta_i X_i + \sum_{i=1}^{3} \beta_{ii} X_i^2 + \sum_{i=1}^{3} \sum_{j=i+1}^{3} \beta_{ij} X_i X_j + \varepsilon \qquad (7.2)$$

where y is the predicted response, β_0 is the coefficient for intercept, β_i is the coefficient of linear effect, β_{ii} is the coefficient of quadratic effect, β_{ij} is the coefficient of interaction effect, ε is the term that represents other sources of variability not accounted for by the response function, and X_i and X_j are coded independent variables.

The coefficients of the regression model were estimated by fitting the experimental results in Table (7.3) using MATLAB R2006a software.

7.2.4. Experimentation

In each experiment, an appropriate amount of nickel laterite ore was added to 100mL of medium to obtain the required pulp density. The slurries were inoculated with 10% (v/v) mixed bacterial culture and the pH of the mixtures were adjusted according to the experimental design (Table 7.2). 10% w/v elemental sulphur was used as a substrate in each experiment. The flasks were covered with pieces of aluminium foil to reduce evaporation and prevent contamination but allow free supply of air. The flasks were then incubated in a platform shaking incubator at 30°C and 200 rpm. The samples were drawn from flasks every three days to determine the concentration of nickel dissolved using the Varian SpectrAA-55B atomic absorption spectrophotometer (AAS).

7.3 Results and Discussion

7.3.1. Derivation of the Fitted Model

For the results discussed in this section reference should be made to the experimental data in Appendix F (Tables F1-F2). The results discussed are an average of the runs conducted under similar experimental conditions. The detailed statistical and mathematical methods used in the analysis of data in this optimisation study are given in Appendix H. Matlab programs are also given in Appendix I.

In matrix notation (Khuri and Cornell, 1987), the proposed model form (Equation 7.2) is expressed over the *N=20* actual observations in Table 7.3, as

$$y = X\beta + \varepsilon$$

$$\begin{bmatrix} 71.7 \\ 63.4 \\ 63.1 \\ 54.4 \\ 68.3 \\ 52.4 \\ 50.5 \\ 42.9 \\ 67.7 \\ 71.7 \\ 85.1 \\ 65.5 \\ 60.6 \\ 43.3 \\ 66.8 \\ 68.3 \\ 55.4 \\ 59.5 \\ 60.4 \\ 53.9 \end{bmatrix} = \begin{bmatrix} 1 & -1 & -1 & -1 & 1 & 1 & 1 & 1 & 1 & 1 \\ 1 & 1 & -1 & -1 & 1 & 1 & 1 & -1 & -1 & 1 \\ 1 & -1 & 1 & -1 & 1 & 1 & 1 & -1 & 1 & -1 \\ 1 & 1 & 1 & -1 & 1 & 1 & 1 & 1 & -1 & -1 \\ 1 & -1 & -1 & 1 & 1 & 1 & 1 & 1 & -1 & -1 \\ 1 & 1 & -1 & 1 & 1 & 1 & 1 & -1 & 1 & -1 \\ 1 & -1 & 1 & 1 & 1 & 1 & 1 & -1 & -1 & 1 \\ 1 & 1 & 1 & 1 & 1 & 1 & 1 & 1 & 1 & 1 \\ 1 & -1.682 & 0 & 0 & 2.828 & 0 & 0 & 0 & 0 & 0 \\ 1 & 1.682 & 0 & 0 & 2.828 & 0 & 0 & 0 & 0 & 0 \\ 1 & 0 & -1.682 & 0 & 0 & 2.828 & 0 & 0 & 0 & 0 \\ 1 & 0 & 1.682 & 0 & 0 & 2.828 & 0 & 0 & 0 & 0 \\ 1 & 0 & 0 & -1.682 & 0 & 0 & 2.828 & 0 & 0 & 0 \\ 1 & 0 & 0 & 1.682 & 0 & 0 & 2.828 & 0 & 0 & 0 \\ 1 & 0 & 0 & 0 & 0 & 0 & 0 & 0 & 0 & 0 \\ 1 & 0 & 0 & 0 & 0 & 0 & 0 & 0 & 0 & 0 \\ 1 & 0 & 0 & 0 & 0 & 0 & 0 & 0 & 0 & 0 \\ 1 & 0 & 0 & 0 & 0 & 0 & 0 & 0 & 0 & 0 \\ 1 & 0 & 0 & 0 & 0 & 0 & 0 & 0 & 0 & 0 \end{bmatrix} \begin{bmatrix} \beta_0 \\ \beta_1 \\ \beta_2 \\ \beta_3 \\ \beta_{11} \\ \beta_{22} \\ \beta_{33} \\ \beta_{12} \\ \beta_{13} \\ \beta_{23} \end{bmatrix} + \begin{bmatrix} \varepsilon_1 \\ \varepsilon_2 \\ \varepsilon_3 \\ \varepsilon_4 \\ \varepsilon_5 \\ \varepsilon_6 \\ \varepsilon_7 \\ \varepsilon_8 \\ \varepsilon_9 \\ \varepsilon_{10} \\ \varepsilon_{11} \\ \varepsilon_{12} \\ \varepsilon_{13} \\ \varepsilon_{14} \\ \varepsilon_{15} \\ \varepsilon_{16} \\ \varepsilon_{17} \\ \varepsilon_{18} \\ \varepsilon_{19} \\ \varepsilon_{20} \end{bmatrix}$$

The normal equations are,

$$\underset{X^TX}{\begin{bmatrix} 20.0 & 0 & 0 & 0 & 13.7 & 13.7 & 13.7 & 0 & 0 & 0 \\ & 13.7 & 0 & 0 & 0 & 0 & 0 & 0 & 0 & 0 \\ & & 13.7 & 0 & 0 & 0 & 0 & 0 & 0 & 0 \\ & & & 13.7 & 0 & 0 & 0 & 0 & 0 & 0 \\ & & & & 24.0 & 8.0 & 8.0 & 0 & 0 & 0 \\ & & & & & 24.0 & 8.0 & 0 & 0 & 0 \\ & & & & & & 24.0 & 0 & 0 & 0 \\ & & & & & & & 8.0 & 0 & 0 \\ & & & & & & & & 8.0 & 0 \\ & & & & & & & & & 8.0 \end{bmatrix}} \underset{\beta}{\begin{bmatrix} \beta_0 \\ \beta_1 \\ \beta_2 \\ \beta_3 \\ \beta_{11} \\ \beta_{22} \\ \beta_{33} \\ \beta_{12} \\ \beta_{13} \\ \beta_{23} \end{bmatrix}} = \underset{X^TY}{\begin{bmatrix} 1224.9 \\ -33.8 \\ -77.9 \\ -67.7 \\ -861.0 \\ 892.7 \\ 760.6 \\ 7.9 \\ -6.5 \\ -9.7 \end{bmatrix}}$$

The solutions to the normal equation are:

$$\underset{\beta}{\begin{bmatrix} 61.0 \\ -2.5 \\ -5.7 \\ -4.9 \\ 1.6 \\ 3.5 \\ -4.7 \\ 1.0 \\ -0.8 \\ -1.2 \end{bmatrix}} = \underset{(X^TX)^{-1}}{\begin{bmatrix} 0.166 & 0 & 0 & 0 & -0.056 & -0.056 & -0.056 & 0 & 0 & 0 \\ & 0.073 & 0 & 0 & 0 & 0 & 0 & 0 & 0 & 0 \\ & & 0.073 & 0 & 0 & 0 & 0 & 0 & 0 & 0 \\ & & & 0.073 & 0 & 0 & 0 & 0 & 0 & 0 \\ & & & & 0.069 & 0.007 & 0.007 & 0 & 0 & 0 \\ & & & & & 0.069 & 0.007 & 0 & 0 & 0 \\ & & & & & & 0.069 & 0 & 0 & 0 \\ & & & & & & & 0.125 & 0 & 0 \\ & & & & & & & & 0.125 & 0 \\ & & & & & & & & & 0.125 \end{bmatrix}} \underset{X^TY}{\begin{bmatrix} 1224.9 \\ -33.8 \\ -77.9 \\ -67.7 \\ -861.0 \\ 892.7 \\ 760.6 \\ 7.9 \\ -6.5 \\ -9.7 \end{bmatrix}}$$

Table 7.3. Observed values for the nickel recovery

Standard Runs	Actual levels of variables			% Recoveries
	pH	Pulp density	Particle size	Observed
Factorial points				
1	1.5	5	38-75µm	71.7
2	3.0	5	38-75µm	63.4
3	1.5	12	38-75µm	63.1
4	3.0	12	38-75µm	54.4
5	1.5	5	106-150µm	68.3
6	3.0	5	106-150µm	52.4
7	1.5	12	106-150µm	50.5
8	3.0	12	106-150µm	42.9
Axial points				
9	1.0	9	75-106µm	67.7
10	3.5	9	75-106µm	71.7
11	2.3	2	75-106µm	85.1
12	2.3	15	75-106µm	65.5
13	2.3	9	<38µm	60.6
14	2.3	9	150-212µm	43.3
Centre points				
15	2.3	9	75-106µm	66.8
16	2.3	9	75-106µm	68.3
17	2.3	9	75-106µm	55.4
18	2.3	9	75-106µm	59.5
19	2.3	9	75-106µm	60.4
20	2.3	9	75-106µm	53.9

The fitted second order model is:

$$y = 61.0 - 2.5x_1 - 5.7x_2 - 4.9x_3 + 1.6x_1^2 + 3.5x_2^2 - 4.7x_3^2 + 1.0x_1x_2 - 0.8x_1x_3 - 1.2x_2x_3 \quad (7.3)$$

within the limits: $-\lambda \leq x_i \leq +\lambda$; i = 1, 2, 3; where x_i are the coded levels of process variables and $\lambda = 1.682$ is the distance of the star points from the centre of the CCRD that gives the limits of the valid region under experimentation.

7.3.2 Checking the Adequacy of the Developed Model

The adequacy of the fitted model was carried out using the Fisher's variance ratio test known as the *F-test* and the Student *t-tests*. The ANOVA for the fitted model is given in Table 7.4.

Table 7.4. ANOVA for the fitted model

Variation	Sum of squares	Degree of freedom	Mean sum of squares	*F-test*
Regression	1482.00	9	164.67	3.32
Residual	495.36	10	49.54	-
Lack of fit	325.58	5	65.12	1.92
Pure error	169.78	5	33.96	-
Total	1977.30	19	104.07	-

The lack of fit was tested using the ratio of the mean sum of squares for lack of fit and pure error given as 1.92. This is smaller than the $F_{0.05,5,5}$ value of 5.05; implying that the model does not present any evidence of lack of fit. The significance of the regression model was tested using the ratio of the mean sum of squares for regression

and residual. The value of 3.32 is greater than the table $F_{0.05,9,10}$ value of 3.02; implying that the regression is significant at a confidence level of 95%.

The effects and significance of the individual terms (both significant and insignificant) in the response surface model are shown in Table 7.5.

Table 7.5. Regression coefficients for fitted model

Term	Coefficient	est.se. (β_i)	Degree of freedom	*t-test*
β_0	61.0	2.870	10	21.240
β_{x_1}	-2.5	1.904	10	-1.899
β_{x_2}	-5.7	1.904	10	-2.994
β_{x_3}	-4.9	1.904	10	-2.599
$\beta_{x_1^2}$	1.6	1.854	10	1.847
$\beta_{x_2^2}$	3.5	1.854	10	1.914
$\beta_{x_3^2}$	-4.7	1.854	10	-2.538
$\beta_{x_1x_2}$	1.0	2.488	10	0.397
$\beta_{x_1x_3}$	-0.8	2.488	10	-0.327
$\beta_{x_2x_3}$	-1.2	2.488	10	-0.487

Testing the null hypothesis, $H_0: \beta_i = 0$, against the alternative hypothesis, $H_a: \beta_i >$ or < 0, at a confidence level of 95% gives the table $t_{0.05,10}$ value of 1.812. It can be deduced, therefore, from Table 7.5 that the constant term (β_0), all linear terms ($\beta_{x_1}, \beta_{x_2}, \beta_{x_3}$) and the quadratic terms ($\beta_{x_1^2}, \beta_{x_2^2}, \beta_{x_3^2}$) are significant at 95% confidence level. It is also shown that the interaction terms ($\beta_{x_1x_2}, \beta_{x_1x_3}, \beta_{x_2x_3}$) are

statistically insignificant. However, it must be stated here that significance in this context refers to the plausibility of the effect in the light of the data. In other words, a particular effect may be statistically insignificant but scientifically important and vice versa.

To obtain a simple and yet realistic model, it was refitted using only the variable terms that are significant at greater or equal to 95% confidence level. Results of the refits are given in Table 7.6 and 7.7.

The refitted second order model is:

$$y = 61.0 - 2.5x_1 - 5.7x_2 - 4.9x_3 + 1.6x_1^2 + 3.5x_2^2 - 4.7x_3^2 \qquad (7.4)$$

The lack of fit was tested using the ratio of the mean sum of squares for lack of fit and pure error given as 1.29. This is smaller than the table $F_{0.05,8,5}$ value of 4.82; implying that the model does not present any evidence of lack of fit. The significance of the refitted regression model was tested using the ratio of the mean sum of squares for regression and residual. The obtained value of 6.07 is greater than the table $F_{0.05,6,13}$ value of 2.92; implying that the regression is significant at a confidence level of 95%.

The coefficient of determination at 73.7% and the smaller value of absolute average deviation analysis at 7.4% show that the model is plausible, from a statistical point of view, to define the true behavior of the experimental system. This means that the nickel recovery values at any regime in the interval of the experimental design can be calculated from Equation 7.4.

The ANOVA for the refitted model is given in Table 7.6. The effects and significance of the individual terms in the refitted response surface model are shown in Table 7.7.

Table 7.6. ANOVA for the refitted model

Variation	Sum of squares	Degree of freedom	Mean sum of squares	*F-test*
Regression	1457.10	6	242.85	6.07
Residual	520.20	13	40.02	-
Lack of fit	350.43	8	43.80	1.29
Pure error	169.78	5	33.96	-
Total	1977.30	19	104.07	-

Table 7.7. Regression coefficients for refitted model

Term	Coefficient	est.se. (β_i)	Degree of freedom	*t-test*
β_0	61.0	2.580	13	23.652
β_{x_1}	-2.5	1.711	13	-2.004
β_{x_2}	-5.7	1.711	13	-3.331
β_{x_3}	-4.9	1.711	13	-2.892
$\beta_{x_1^2}$	1.6	1.666	13	1.842
$\beta_{x_2^2}$	3.5	1.666	13	2.130
$\beta_{x_3^2}$	-4.7	1.666	13	-2.824

Testing the null hypothesis, $H_0 : \beta_i = 0$, against the alternative hypothesis, , $H_a : \beta_i >$ or < 0, at a confidence level of 95% gives the table $t_{0.05,13}$ value of 1.771. It can be

deduced, therefore, from Table 7.7 that the constant term (β_0), all linear terms ($\beta_{x_1}, \beta_{x_2}, \beta_{x_3}$) and the quadratic terms ($\beta_{x_1^2}, \beta_{x_2^2}, \beta_{x_3^2}$) are significant at 95% confidence level.

Experimental results and predicted values obtained using the refitted model are given in Table 7.8. As can be seen from Figure 7.1, the predicted values are plausibly comparable to the experimental values, with the linear correlation coefficient (R^2) of 0.74. Statistically, this means that 74% of the sample variation can be explained by the independent variables.

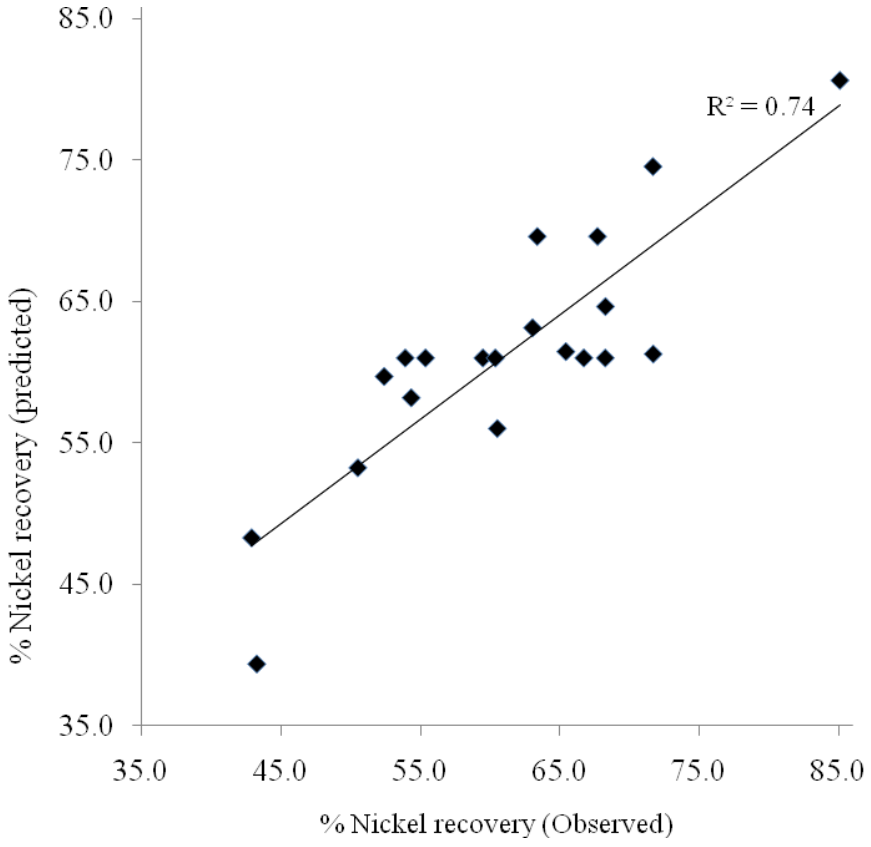


Figure 7.1. Relationship between experimental and predicted nickel recovery

Table 7.8. Observed and predicted values for the nickel recovery

Standard Runs	Actual levels of variables			% Recoveries	
	pH	Pulp density	Particle size	Observed	Predicted
Factorial points					
1	1.5	5	38-75µm	71.7	74.5
2	3.0	5	38-75µm	63.4	69.6
3	1.5	12	38-75µm	63.1	63.1
4	3.0	12	38-75µm	54.4	58.2
5	1.5	5	106-150µm	68.3	64.6
6	3.0	5	106-150µm	52.4	59.7
7	1.5	12	106-150µm	50.5	53.2
8	3.0	12	106-150µm	42.9	48.3
Axial points					
9	1.0	9	75-106µm	67.7	69.6
10	3.5	9	75-106µm	71.7	61.2
11	2.3	2	75-106µm	85.1	80.6
12	2.3	15	75-106µm	65.5	61.4
13	2.3	9	<38µm	60.6	56.0
14	2.3	9	150-212µm	43.3	39.3
Centre points					
15	2.3	9	75-106µm	66.8	61.0
16	2.3	9	75-106µm	68.3	61.0
17	2.3	9	75-106µm	55.4	61.0
18	2.3	9	75-106µm	59.5	61.0
19	2.3	9	75-106µm	60.4	61.0
20	2.3	9	75-106µm	53.9	61.0

7.3.3. Response Surfaces

Figures 7.2 through 7.4 show the three-dimensional surfaces as well as contour plots of the relationship between x_2 and x_3; x_1 and x_3; x_1 and x_2 when the values of x_1, x_2

and x_3, respectively, are held constant at the central level. This means that Equation 7.4 becomes:

$$y = 61.0 - 5.7x_2 - 4.9x_3 + 3.5x_2^2 - 4.7x_3^2 \quad \text{,when } x_1 = 0,\ x_2 \text{ and } x_3 = -1.682, -1, 0, 1, 1.682$$

$$y = 61.0 - 2.5x_1 - 4.9x_3 + 1.6x_1^2 - 4.7x_3^2 \quad \text{,when } x_2 = 0,\ x_1 \text{ and } x_3 = -1.682, -1, 0, 1, 1.682$$

$$y = 61.0 - 2.5x_1 - 5.7x_2 + 1.6x_1^2 + 3.5x_2^2 \quad \text{,when } x_3 = 0,\ x_1 \text{ and } x_2 = -1.682, -1, 0, 1, 1.682$$

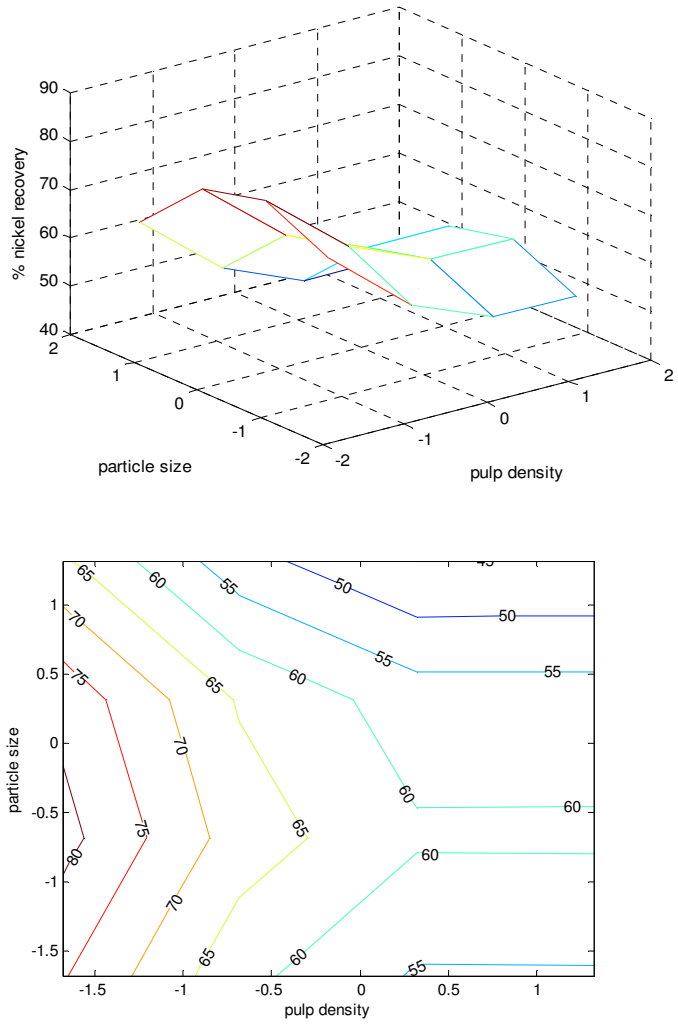


Figure 7.2. Response surface and contour plots at constant pH

Figure 7.2 shows the effect of pulp density and particle size on nickel recovery at constant pH. The figure shows that with decrease in particle size, the nickel recovery increases with a decrease in pulp density. The effect of particle size can be explained by the fact that a decrease in particle size increases the surface area of the particles that helps in increasing the specific contact area with the lixiviant. At low pulp density there is effective homogeneous mixing of solids and liquid leading to good mass transfer hence increased nickel recoveries.

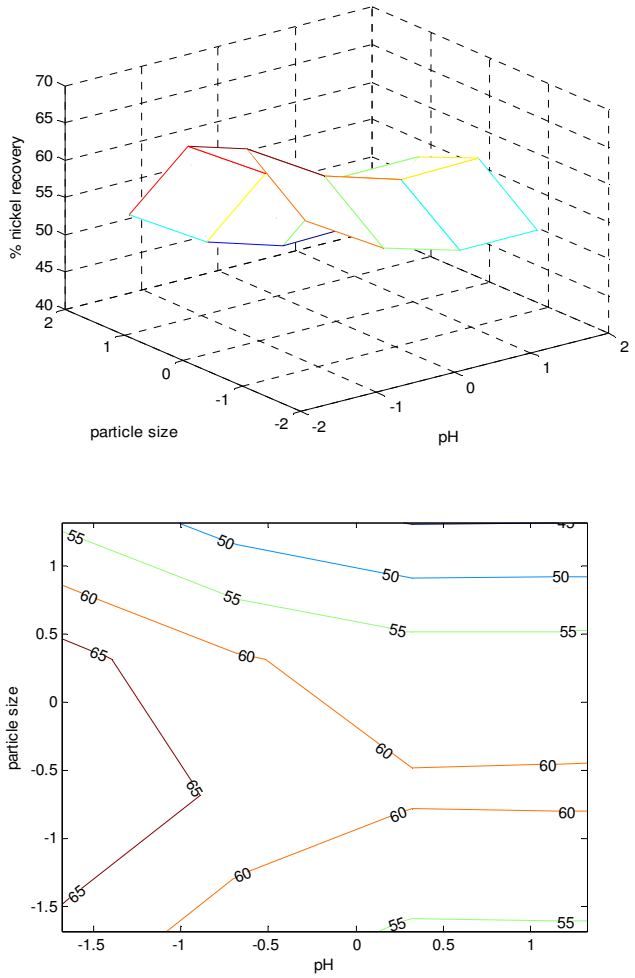


Figure 7.3. Response surface and contour plots at constant pulp size

Figure 7.3 shows the effect of pH and particle size on nickel recovery at centre level of pulp density. From Figure 7.3, it can be observed that the nickel recovery increases with reduction in both pH and particle size. At low pH, the concentration of acid (H^+ ions) is also expected to be high (pH = -log10[H^+]). It is the H^+ ions that are assumed to induce the nickel dissolution (Simate and Ndlovu, 2008). Figures 7.2 and 7.3 also show that the nickel recovery depends more on the particle size than on pulp density and pH, respectively. This is because particle size affect both the percentage of nickel in the ore and survival of the microorganisms (Simate and Ndlovu, 2008; section 5.2.2 of Chapter 5 in this dissertation). Smaller particles had higher nickel content compared to larger particles (Appendix A). In addition, particle sizes affect the physical structure of cells due to attrition (Nemati et al., 2000), and also affect the ability of the bacteria to attach to the substrates due to increased particle-to- bacteria collisions (Acevedo et al., 2004). These observations indicate that the choice of suitable particle size is paramount in the bacterial leaching of nickel laterite ore in this study.

Figure 7.4 shows the effect of pH and pulp density on nickel recovery at a centre level of particle sizes. As the figure shows, nickel recovery increases with a decrease in both pH and pulp density.

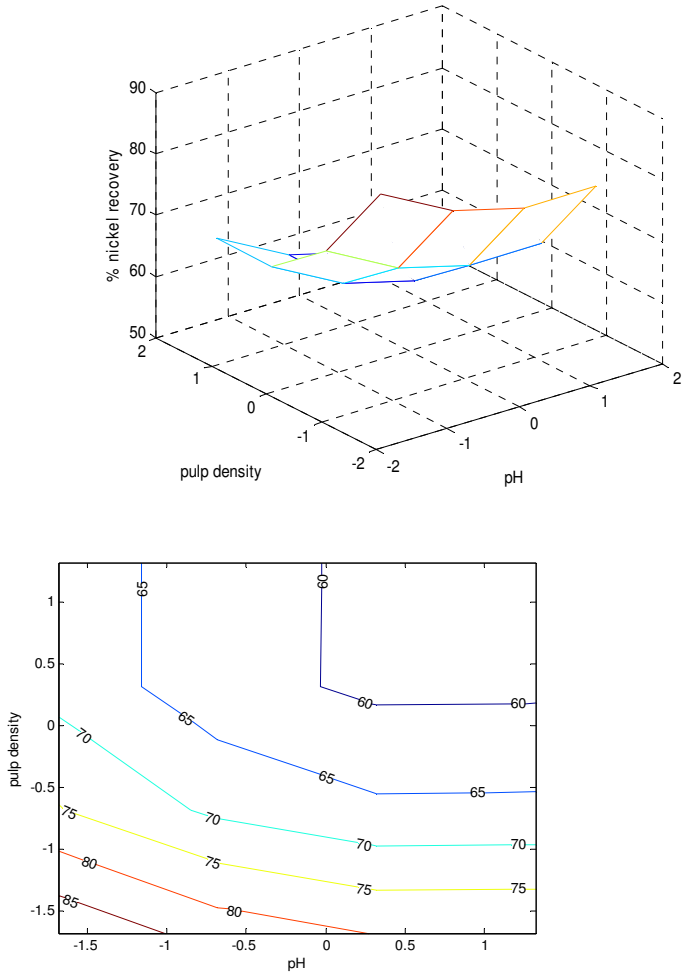


Figure 7.4. Response surface plot and contour plots at constant particle size

7.3.4. Determination of Optimum Conditions

As mentioned in Section 7.2.3, the objective of the study in this chapter was to determine the conditions that maximise the recovery of nickel. Therefore, after the fitted model was checked for adequacy of fit in the region defined by the coordinates of the design and was found to be adequate, the model was used to locate the coordinates of the stationary point (Khuri and Cornell, 1987). To obtain the

coordinates of the stationary point, the fitted second order model in *k*-variables was written in matrix notation (Khuri and Cornell, 1987; Myers and Montgomery, 2002; Montgomery, 2005). Therefore, in order to determine the conditions at the stationary point, Equation (H22) in appendix H was employed, i.e. $x_s = -\frac{\beta^{-1}b}{2}$, where in this study,

$$b = \begin{bmatrix} -2.5 \\ -5.7 \\ -4.9 \end{bmatrix} \quad \text{and} \quad \beta = \begin{bmatrix} 1.6 & 0 & 0 \\ 0 & 3.5 & 0 \\ 0 & 0 & -4.7 \end{bmatrix}$$

The conditions in coded units are $x_1 = 0.7813$, $x_2 = 0.8143$ and $x_3 = -0.5213$ giving a recovery of 57.0 %. The stationary point lies within the limits of the region of interest in this study, $-1.682 \leq x_i \leq +1.682$; $i = 1, 2, 3$; where x_i are the coded levels of process variables.

The canonical analysis was used to determine the nature of the stationary point of the objective function (Equation 7.4). In Appendix H, the formulae for determining the canonical coefficients are outlined. In the case of this study, $\beta = \begin{bmatrix} 1.6 & 0 & 0 \\ 0 & 3.5 & 0 \\ 0 & 0 & -4.7 \end{bmatrix}$, and the characteristic roots or eigenvalues of β, using MATLAB R2006a software are 3.5, 1.6 and -4.7. Therefore, the canonical equation is:

$$\hat{y} = 57.0 + 3.5W_1^2 + 1.6W_2^2 - 4.7W_3^2 \qquad (7.5)$$

where W_1, W_2, W_3 are canonical axes. Since the canonical coefficients have the mixed signs, the stationary point is a saddle point (point of inflexion) or minimax. Therefore, the stationary point cannot be used as the optimal solution. The potential

optimum conditions were determined using the constrained optimization technique called ridge analysis (Myers and Montgomery, 2002) as outlined in Appendix H.

As mentioned earlier, the objective of this study was to determine the conditions that maximise the recovery of nickel. Therefore, values of μ greater than 3.5 (the largest of the eigenvalues or characteristic roots) are substituted into Equation H32 in Appendix H. It becomes necessary, then, to solve the following matrix equation:

$$\begin{bmatrix} 1.6-\mu & 0 & 0 \\ 0 & 3.5-\mu & 0 \\ 0 & 0 & \text{-}4.7-\mu \end{bmatrix} \begin{bmatrix} x_1 \\ x_2 \\ x_3 \end{bmatrix} = \begin{bmatrix} 1.25 \\ 2.85 \\ 2.45 \end{bmatrix}$$

Thus

$$\begin{bmatrix} x_1 \\ x_2 \\ x_3 \end{bmatrix} = \begin{bmatrix} 1.6-\mu & 0 & 0 \\ 0 & 3.5-\mu & 0 \\ 0 & 0 & \text{-}4.7-\mu \end{bmatrix}^{-1} \begin{bmatrix} 1.25 \\ 2.85 \\ 2.45 \end{bmatrix}$$

and

$$\begin{bmatrix} x_1 \\ x_2 \\ x_3 \end{bmatrix} = \frac{1}{-(\mu^3 - 0.4\mu^2 - 18.37\mu + 26.32)} \begin{bmatrix} -(3.5-\mu)(4.7+\mu) & 0 & 0 \\ 0 & -(1.6-\mu)(4.7+\mu) & 0 \\ 0 & 0 & (1.6-\mu)(3.5-\mu) \end{bmatrix} \begin{bmatrix} 1.25 \\ 2.85 \\ 2.45 \end{bmatrix}$$

Therefore:

$$x_1 = \frac{1.25(3.5-\mu)(4.7+\mu)}{(\mu^3 - 0.4\mu^2 - 18.37\mu + 26.32)}$$

$$x_2 = \frac{2.85(1.6-\mu)(4.7+\mu)}{(\mu^3 - 0.4\mu^2 - 18.37\mu + 26.32)} \qquad (7.6)$$

$$x_3 = \frac{-2.45(1.6-\mu)(3.5-\mu)}{(\mu^3 - 0.4\mu^2 - 18.37\mu + 26.32)}$$

Refer to Appendix H for the detailed evaluation of the inverse of the matrix.

In this study, since there are three factorial points, it is assumed that the perimeter of the experimental design is at radius of $\sqrt{3}$ units from the design centre point. The optimal values of the studied variables in coded units at a radius of $\sqrt{3}$ units were calculated as follows: x_1 = -0.331, x_2 = -1.515 and x_3 = -0.769. The predicted response at this point using Equation 7.4 is 79.8%. The coded units were converted to actual uncoded variables by using Equation H8 in Appendix H thus giving the following variables; pH = 2.0, pulp density = 2.6%, particle size = 63 μ m.

7.3.5 Confirmatory Experiments

For the results discussed in this section reference should be made to the experimental data in Appendix F (Table F3). The results discussed are an average of the runs conducted under similar experimental conditions.

In order to test the validity of the optimised conditions given by the model, an experiment was carried out with parameters suggested by the model. The conditions used in the confirmatory experiment were as follows: - pH (2.0), pulp density (2.6% w/v), and particle sizes 53-75μm.

The nickel laterite recovery after a leaching period of 26 days was found to be 74.1% (Table 7.9), which is consistent with the model. The model can, therefore, be considered to fit the experimental data very well in these experimental conditions; with an error margin of only 7.7%. Therefore, the formulated model is acceptably valid.

Table 7.9. Nickel recoveries at optimal conditions

Parameter	pH	Pulp density	Particle size	% Nickel recovery
Model	2.0	2.6	63	79.8
Confirmation tests	2.0	2.6	53-75μm	74.1

7.5 Summary and Conclusions

The depletion of easily processed nickel sulphides and demand for the nickel metal poses a challenge of finding new effective methods of nickel recovery from low grade ores. Solving these problems successfully requires optimisation of the extraction/recovery processes. Optimisation itself can be a challenging scientific and engineering problem. In this chapter, the effect of pH, particle size and pulp density on nickel recovery from nickel laterite ore was investigated using response surface methodology and central composite rotatable design. A second order model representing the nickel recovery expressed as a function of these three variables was developed by computer simulation programming applying least squares method using MATLAB R2006a. A statistical analysis (ANOVA) was carried out to study the

effects of the individual variables as well as their combined interactive effects on nickel recovery. The results showed that the effects of the individual variables and their quadratic terms were statistically significant whilst all the interactions among the variables were statistically insignificant. To obtain a simple and yet realistic model, it was refitted using only the significant terms. The final model validation was accomplished using *F-distribution* tests, standard errors of model coefficient (Student's *t-test*), the coefficient of determination (R^2) and absolute average deviation (*AAD*); which guaranteed that convergence at the actual optimum experimental conditions was achieved.

The study has shown that low pH, finer particle sizes and low pulp density resulted in higher yields of nickel recoveries. Response surface plots drawn for spatial representation of the model showed that the nickel recovery depends more on the particle sizes than on pH and pulp density. This is because particle sizes affect both the percentage of nickel in the ore and survival of the microorganisms. Smaller particles had higher nickel content compared to larger particles. In addition, particle sizes affect the physical structure of cells due to attrition, and also affect the ability of the bacteria to attach to the substrates due to particle-to- bacteria collisions.

Under the experimental conditions considered, the set of conditions that produce the optimum nickel recovery (79.8%) were found to be a pH of 2.0, 63µm particle size, and 2.6% pulp density. To verify this, a confirmatory run was carried out under these optimum conditions. The nickel recovery found experimentally was 74.1%, clearly showing that the model fits the experimental data reasonably well, within an error margin of less than 10%.

The work contained in this chapter has, therefore, shown that the development of mathematical models for process simulation based on statistics can be useful for

predicting and understanding the effects of experimental factors. What must be noted here is that the response surface methodology does not explicate the mechanism of the processes studied, but only ascertains the effects of factors on response and interactions between the factors. This is very important, as can be seen in this study, for the optimisation of the operating conditions.

CHAPTER 8

CONCLUSIONS AND RECOMMENDATIONS

"*There are known knowns. These are things we know that we know. There are known unknowns. That is to say, there are things that we know we don't know. But there are also unknown unknowns. These are things we do not know we don't know".*

- Donald Rumsfeld (former USA Secretary of Defence on the war against terrorism)

8.1 Conclusions

8.1.1 Introduction

The ability of microorganisms to leach and mobilize metals from sulphide minerals is based on the following three mechanisms: (1) redox reactions, (2) formation of inorganic acid, and (3) excretion of complexing agents (e.g., organic acids). The main objective of this work was to extend these principles in order to investigate the possibility of using chemolithotrophic microorganisms in the bacterial leaching of nickel laterites. Nickel laterite contains metal values, but is not capable of participating in the primary bacterial oxidation because it contains neither ferrous iron nor substantial amount of reduced sulphur. A review of the literature suggested that the metal value can be recovered by allowing the primary oxidation of pyrite, or similar iron/sulphur minerals to provide sulphuric acid solutions, which solubilise the metal content.

In order to investigate this possibility, the aims of this study were defined as:

(i) To investigate the influence of sulphuric acid, citric acid, and ferric sulphate so as to provide useful insights into the process of leaching nickel laterites.

(ii) To determine the specific parameters and conditions that are suitable for the favourable bacterial leaching of nickel laterites.

(iii) To study the effects of pH and hence, the effects of substrate type (sulphur or pyrite) on pH in the bacterial leaching of nickel laterites.

(iv) To optimise the favourable parameters and conditions that will ultimately maximise the leaching process in terms of the output (nickel recovery).

8.1.2 Acidic and Ferric Leach Tests

The chemical leaching of nickel laterite ore with sulphuric acid, citric acid and ferric sulphate provided a better insight to the bioleaching process. The results presented in this study have shown that leach rates are highly dependant on the type of leaching media. Sulphuric acid was more effective (in terms of the nickel recovery) than citric acid and ferric sulphate at the same concentration. The recoveries obtained at a concentration of 0.5M and 5%w/v pulp density (at 30°C and 200 rpm) for sulphuric acid, citric acid and ferric sulphate were 71.9%, 46.6% and 20.3%, respectively. Citric acid, being a weaker acid, does not dissociate completely hence lower recoveries are obtained at the same concentration. This showed that the concentration of hydrogen ions has a significant influence in the chemical leaching process. A mixture of sulphuric acid and citric acid enhanced the nickel recovery (79.6%) indicating a synergic effect of the two acids. In the presence of ferric sulphate, dissolution was also seen to increase with sulphuric acid additions, e.g., 37.4% after addition of 0.1M sulphuric acid.

Citric acid was more effective than both sulphuric acid and ferric sulphate at the same pH of 1.0, 1.5 and 2.0, i.e., it gave better recoveries. The higher recovery with citric acid than sulphuric acid was attributed to the chelating of nickel ions by the organic acid anions at these pHs. However, a lower recovery was obtained for citric acid than sulphuric acid at a pH of 0.5, i.e., 70% and 63% for sulphuric acid and citric acid respectively. This reduction in recoveries was attributed to the protonation of citrate anions at the low pH.

8.1.3 Bacterial Leach Tests

Bacterial leach tests were carried out in standard 9K media using sulphur and pyrite substrates. The study showed that a period of more than two weeks was an effective

duration for the bacterial leaching of nickel laterite ore used. For example, at a pH of 2.0, recoveries increased from 26.1% at the end of two weeks to 40.0% at the end of 32 days for sulphur substrate. This trend was also observed for pyrite substrate (i.e., 25.9% to 32.6% for two weeks and 32 days respectively). The bioxidation of sulphur and pyrite produce sulphuric acid which ultimately leach nickel laterite ore. Comparisons of the effects of pH, particle size, pulp density, substrate type and bacterial inoculum, showed that inoculum size was not a statistically significant factor. The lack of influence by the bacterial inoculum is because bacteria was not 'directly attacking' a constituent of the ore itself, but the externally added substrates. Over a longer period sulphur exhibited better effects in terms of acidification and nickel (recovery) yield than pyrite. For example, at a pH of 1.0, duration of 32 days gave recoveries of 61.0% and 42.8% for sulphur and pyrite respectively. This is because more energy is gained during the bioxidation of sulphur compared to bioxidation of pyrite. For the test conditions considered in this study and for this kind of nickel recovery process, this finding signifies that sulphur is ultimately a better substrate than pyrite.

The results presented also showed that dissolution rates of nickel laterite are high in low pH and high oxidation reduction potential (ORP), and in the presence of bacteria. This is because at low pH the concentration of acid (H^+ ions) is expected to be high. The high ORPs signify higher ionic activities at low pH. However, the study also demonstrated that microbial activities, depicted by acidification were reduced at lower initial pH levels. There was also a reduction in recoveries at higher pulp density (15% w/v). The reduction in the rate of bacterial leaching at higher pulp density was attributed to the ineffective homogeneous mixing of solids and liquids leading to gas transfer limitation because the liquid becomes too thick (high viscosity) for efficient gas transfer to the cells. By contrast, the opposite was true at low pulp density, i.e., high nickel recovery at a pulp density of 5%.

8.1.4 Optimisation Tests

A statistically-based optimization strategy called response surface methodology was used for parametric optimization (pH, particle size and pulp density) with 10% w/v sulphur as a substrate. Sulphur was chosen since it showed better effects than pyrite. A statistical experimental design called central composite rotatable design was employed to reduce on the number of experiments, but being sufficient to describe the responses. Experimental results were analysed and an appropriate predictive empirical second order model was developed. This second order model representing the nickel recovery process is expressed as a function of the three variables tested (pH, particle size, and pulp density). The model validation was accomplished using *F-distribution* tests, standard errors of model coefficient (student's *t-test*), the coefficient of determination (R^2) and the absolute average deviation (*AAD*); which guaranteed that convergence at the actual optimum experimental conditions was achieved.

The effects of the individual variables and their quadratic terms were found to be statistically significant. The results, however, showed that all the interactions among the investigated variables were statistically insignificant. Nickel recovery was found to depend more on particle size than pH and pulp density. This is because particle size affects not only the percentage of nickel in the ore, but also the survival of the bioleaching microorganisms. Smaller particles had higher nickel content compared to larger particles. In addition, particle sizes affect the physical structure of cells due to attrition, and also affect bacteria ability to attach to the substrates due to particle-to-bacteria collisions. These observations indicate that the choice of suitable particle size is paramount in the bacterial leaching of nickel laterite ore in this study.

Within the range of conditions studied, the theoretical optimum conditions established from the statistically-based optimisation model at the projected maximum

nickel recovery of 79.8% were found to be *an initial pH of 2*.0, *63µm particle size* and *2.6% pulp density*. To verify the optimised results, a confirmatory run was carried out under optimised conditions. The nickel recovery found experimentally was 74.1%. This shows that there is a good relationship between the predicted and experimental results with a relative error of less than 10%. This study has, therefore, demonstrated that by adding sulphur containing material, nickel laterites can be leached by chemolithotrophic microorganisms through the production of sulphuric acid.

8.1.5 Kinetic Studies

In order to ascertain the reaction regime controlling the leaching of nickel laterite ore, the shrinking core model and activation energy studies were conducted. The accurate description of the dissolution phenomenon of the process is important in the scale-up from laboratory to industrial equipment. Activation energy analysis showed that the chemical reaction at the surface of the particles was the rate controlling process during the leaching for all the lixiviants used (i.e., sulphuric acid, citric acid and acidified ferric sulphate). This was in contrast to the shrinking core model which showed the diffusion through the product layer as rate controlling. This inconsistence was attributed to the samples having various sizes which resulted from poor separation during dry sieving. When the particle size distribution of a sample is not consistent, but varies, it results in varying reaction rates thus deviating from the actual reaction regime. Therefore, in order to determine the kinetics of the nickel recovery by the shrinking core model, the particle size range should be narrow in order to get homogeneous particles.

8.1.6 Potential Application in Industry

This whole study has opened up a new era to the potential application of chemolithotrophic microorganisms for the commercial processing of the difficult-to-process low grade nickel laterite ores. In regions where the nickel laterite ore body exist the sustainability of the process will depend on the supply of sulphur containing material (commercial sulphur or metal sulphide) for energy requirements of the bacteria. This is likely to form the dominant operating cost component of the bacterial leaching of nickel laterite ores using chemolithotrophic microorganisms. In addition this process is promising because sulphuric acid is produced in-situ whereas in processes such as high pressure acid leaching, sulphuric acid is produced in external facilities. With the addition of sulphur containing material the use of chemolithotrophic bacteria can be extended to the leaching of other low grade non-sulphide containing ores. Some examples where this process may be applied include silicate ores, oxidic converter furnace slags and refractory oxides.

8.2 Recommendations

With the knowledge that has been gathered from this work, the following recommendations for further studies are proposed.

Wet Screening of Nickel Laterite Ore

Studies on wet and dry screened samples have more often shown different results regarding the shrinking core model. Wet sieving is believed to be able to make the shrinking core model applicable. This particular study has shown that there are some differences in the reaction control regimes, i.e., that derived from the shrinking core model and that obtained from the use of activation energies. Further studies can compare the effects of wet and dry screening of nickel laterites on the shrinking core model and activation energies so as to ascertain the causes of such differences.

Column Leach Experiments

This study followed a procedure that simulated stirred tank reactors. However, heap leaching operations are considered to be cheaper than stirred tank reactor operations and are commercially popular especially for low grade ores. The procedures followed in a stirred tank experiment differ greatly from those used in a heap leaching system. In heap leaching there is no careful preparation of the ore and the solid-liquid contact is not perfect because there is no stirring. The oxygen and carbon dioxide transfer can be low or even non-existent, and temperature profile can vary considerably between different zones of the heap. Thus the behavior of a heap will be much complex than a simple platform shaker experiment. Further studies in the bacterial leaching process can be carried out in percolation columns to simulate heap leaching. This would offer the possibility of checking the applicability of the results obtained in stirred tank experiments during this study. Since results obtained in the laboratory can be extrapolated to the real situation this would help to show whether bacterial leaching of nickel laterites using chemolithotrophic microorganisms is possible under heap leaching conditions. The further study should also consider the stage at which sulphur (or pyrite) should be added to the heap for optimisation purposes.

Mixed Culture of Chemolithotrophic and Heterotrophic Microorganisms

This work had shown that a mixture of sulphuric acid and citric acid enhanced the dissolution of nickel laterite ore. This work can be extended to study the effects of a mixture of chemolithotrophic and heterotrophic microorganisms on the dissolution of nickel laterite ores. Chemolithotrophic microorganisms with the addition of sulphur containing materials can produce sulphuric acid and heterotrophic microorganisms can produce organic acids with the addition of organic carbon material. These microorganisms are likely to exist together under similar conditions as a bacterial consortium. Some studies have shown that organic matter such as yeast enhances the survival of some chemolithotrophic microorganisms. Heterotrophic microorganisms

can also feed on organic matter generated by chemolithotrophic microorganisms to produce organic acids.

Passivation During Leaching

During the leaching of metal sulphides such as chalcopyrite, pyrite and sphalerite solid state changes normally occur leading to the formation of a passivating layer. It has also been observed in some cases that the leaching kinetics is a mixed diffusion/chemical reaction controlled. This particular study has shown the likelihood of mixed rate control when acidified ferric sulphate was used in the leaching of nickel laterites, and that a passivating layer was formed. This study did not examine the surface of leached material to ascertain the type of the passivating layer. Further studies can examine the nature of the passivating layer and the changes that occur with temperature.

REFERENCES

"The things taught in colleges and schools are not an education, but the means of education".

-Ralph Waldo Emerson

Acevedo, F., 2000. The use of reactors in biomining processes. *Electronic Journal of Biotechnology* 3(3), 184-194.

Acevedo, F., Gentina, J.C., Valencia P., 2004. Optimisation of pulp density and particle size in the bioxidation of a pyritic gold concentrate by *Sulfolobus metallicus*. *World Journal of Microbiology and Biotechnology* 20, 865-869.

Agatzini-Leonardou, S., Zafiratos, I. G., 2004. Beneficiation of a Greek serpentinic nickeliferous ore Part II: Sulphuric acid heap and agitation leaching. *Hydrometallurgy* 74, 267-275.

Albert, A., Sergent, E.P., 1962. Ionisation constants of acids and bases. Wiley, Inc., New York.

Alibhai, K. A. K., Dudeney, A. W. L., Leak, D. J., Agatzini, S., Tzeferis, P., 1993. Bioleaching and bioprecipitation of nickel and iron from laterites. *FEMS Microbiology Reviews* 11, 87-96.

Alupoaei, C. E., García-Rubio, L. H., 2004. Growth behavior of microorganisms using UV-Vis Spectroscopy: Escherichia Coli. *Biotechnology and Bioengineering* 86(2), 163-167.

Anderson, M. J., Whitcomb, P. J., 2005. RSM Simplified: Optimizing processes using Response Surface Methods for Design of Experiments. Productivity Press, New York.

Antonijevic, M. M., Jankovic, Z., Dimitrijevic, M., 1994. Investigation of the kinetics of chalcopyrite oxidation by potassium dichromate. *Hydrometallurgy* 35, 187-201.

Barrentine, L. B., 1999. An introduction to design of experiments: A simplified approach. ASQ Quality Press, Wisconsin.

Baş, D., Boyaci, I. H., 2007. Modeling and optimization I: Usability of response surface methodology. *Journal of Food Engineering* 78, 836-845.

Boon, M., Hansford, G. S., Heijne, J. J., 1995. The role of bacterial ferrous iron oxidation in the bio-oxidation of pyrite. In: Vargas T, Jerez C.A, Wertz J.V and Toledo H (Editors), *Biohydrometallurgical Processing* 1, Santiago: University of Chile , pp. 153-181.

Bosecker, K., 1986. Leaching of lateritic nickel ores with heterotrophic microorganisms. In: Lawrence, W., Branion, R.M.R., Ebner, *H.G.* (Editors), *Fundamental and Applied Hydrometallurgy*, Elsevier, pp. 367-382.

Box, G. E. P., Wilson, K. B., 1951. On the experimental attainment of optimum conditions. *Journal of the Royal Statistical Society,* Ser. B, 13, 1-45.

Box, G. E. P., Hunter, J. S., 1957. Multi-factor experimental design for exploring response surfaces. *Annals of Mathematical Statistics* 28, 195-241.

Box, G. E. P., Hunter, W. G., Hunter, J. S., 1978. Statistics for Experimenters: An introduction to design, data analysis and model building. John Wiley and Sons, New York.

Brand, N. W., Butt, C. R. M., Elias, M., 1998. Nickel laterites: Classification and features. *AGSO Journal of Australian Geology and Geophysics* 17(4), 81-88.

Bridge, T. A. M., Johnson, D. B., 1998. Reduction of soluble iron and reductive dissolution of ferric iron-containing minerals by moderately thermophilic iron-oxidizing bacteria. *Applied and Environmental Microbiology* 64(6), 2181-2186.

Brierley, J. A., Brierley, C. L., 2001. Present and future commercial applications of biohydrometallurgy. *Hydrometallurgy* 59, 233-239.

Brochot, S., Durance, M. V., Villeneuve, J., d'Hugues, P., Mugabi, M., 2004. Modelling of the bioleaching of sulphide ores: application for the simulation of the bioleaching/gravity section of the Kasese Cobalt Company Ltd process plant. *Minerals Engineering* 17, 253-260.

Bugaytsova, Z., Lindström, E. B., 2004. Localization, purification and properties of a tetrathionate hydrolase from *Acidithiobacillus caldus*. *European Journal of Biochemistry* 271**,** 272-280.

Cancho, L., Blázquez, M. L., Bállester, A, González, F., Muñoz, J.A., 2007. Bioleaching of a chalcopyrite concentrate with moderate thermophilic microorganisms in a continuous reactor system. *Hydrometallurgy* 87**,** 272-280.

Camuti, K. S., Riel, R. G., 1996. Mineralogy of Murrin Murrin nickel laterites. In: Grimsey, E. J., Neuss, I., (Editors), Proceedings Nickel 1996, *The Australasian Institute of Mining and Metallurgy*, Melbourne, pp. 209-210.

Carley, K. M., Kamneva, N. Y., Reminga, J., 2004. Response Surface Methodology. Carnegie Mellon University, School of Computer Science, Institute for Software Research International, Technical report CMU-ISRI-04-136.

Crundwell, F. K., 1995. Progress in the mathematical modeling of leaching reactors. *Hydrometallurgy* 39, 321-335.

Cussler, E., 1997. Diffusion mass transfer in fluid systems. Cambridge University Press, New York.

Dalvi, A., D., Bacon, W. G., Osborne, R. C., 2004. The past and the future of nickel laterites. *PDAC 2004 International Convention - Trade Show and Investors Exchange*.

Daniel, C., 1959. Use of half normal plots in interpreting factorial two level experiments. *Technometrics* 1 (4), 311-341.

Dave, S. R., Natarajan, K. A., Bhat, J. V., 1981. Leaching of copper and zinc from oxidized ores by fungi. *Hydrometallurgy* 7, 235-242.

Davenport, W. G, King, M., Schlesinger, M., Biwas, A. K., 2002. Extractive Metallurgical of Copper. Elsevier Science Limited, Oxford.

Dutrizac, J. E., 1981. The dissolution of chalcopyrite in ferric sulphate and ferric chloride media. *Metallurgical Transactions B* 12B, 371-378.

Dutrizac, J. E., 1983. Factors affecting alkali jarosite precipitation. *Metallurgical and Materials Transactions B* 14(4), 531-539.

Draper, N. R., Lin, D. K. J., 1990. Small Response Surface Designs. *Technometrics* 32 (2), 187-194.

Drobner, E., Huber, H., Stetter, K. O., 1990. *Thiobacillus ferrooxidans*, a facultative hydrogen oxidiser. *Applied and Environmental Microbiology* 56(9), 2922-2923.

Edgar, T.F., Himmelblau, D. M., 1988. Optimisation of Chemical Processes. McGraw-Hill Book Company, New York.

Ehrlich, H. L., 1988. Recent advances in microbial leaching of ores. *Minerals and Metallurgical Processing* 5 (2), 57-60.

Elias, M., 2002. Nickel laterite deposits - geological overview, resources and exploitation. In: Cooke, C.R., Pontgratz, J., (Editors), Giant ore deposits: Characteristics, genesis and exploitation. *CODES Special Publication*, Centre for Ore Deposit Research, University of Tasmania, 205-220.

Eligwe, C. A., 1988. Microbial desulphurization of coal. *Fuel* 67, 451-458.

Fowler, T. A., Holmes, P. R., Crundwell, F. K., 2001. On the kinetics and mechanism of the dissolution of pyrite in the presence of *Thiobacillus ferrooxidans*. *Hydrometallurgy* 59, 257-270.

Friis, E. P., Andersen, J. E. T., Madsen, L. L.., Bonander, N., Møiler, P., Ulstrup, J., 1998. Dynamics of Pseudomonas aeruginosa azurin and its Cys3Ser mutant at single-crystal gold surfaces investigated by cyclic voltammetry and atomic force microscopy. *Electrochimica Acta* 43(9), 1114-1122.

Gbor, P. K., Jia, C. Q., 2004. Critical evaluation of coupling particle size distribution with the shrinking core model. *Chemical Engineering Science* 59, 1979-1987.

Georgiou, D., Papangelakis, V. G., 1998. Sulphuric acid pressure leaching of limonitic laterite: Chemistry and kinetics. *Hydrometallurgy* 49, 23-46.

Gericke, M., Pinches, A., 1999. Bioleaching of copper sulphide concentrate using extreme thermophilic bacteria. *Minerals Engineering* 12, 893-904.

Gericke, M., Pinches, A., van Rooyen, J.V., 2001. Bioleaching of a chalcopyrite concentrate using an extremely thermophilic culture. *International Journal of Mineral Processing* 62, 243-255.

Ghorbani, Y., Oliazadeh, M., Shahvedi, A., Roohi, R., Pirayehgar, A., 2007. Use of some isolated fungi in biological leaching of aluminium from low grade bauxite. *African Journal of Biotechnology* 6(11), 1284-1288.

Giaveno, A., Donati, E., 2001. Bioleaching of heazelwoodite by Thiobacillus spp. *Process Biochemistry* 36, 955-962.

Gleeson, S. A., Butt, C. R. M., Elias, M., 2003. Nickel laterites: Review. *Society of Economic Geologists (SEG) Newsletter*, Number 54.

Golightly, J. P., 1981. Nickeliferous laterite deposits. *Economic Geology* 75, 710-735.

Griffith, D.F., 2005. *An Introduction to Matlab. Website:* http://www.maths.dundee.ac.uk/~ftp/na-reports/MatlabNotes.pdf. Accessed April 2007.

Groudev, S. N., 1987. Use of heterotrophic microorganisms in mineral biotechnology. *Acta Biotechnology* 7(4), 299-306.

Gunaraj, V., Murugan, N., 1999. Application of response surface methodology for predicting weld bead quality in submerged arc welding of pipes. *Journal of Materials Processing Technology* 88, 266-275.

Habashi, F., 1969. Principle of Extractive Metallurgy. Gordon and Breach, New York.

Hackl, R. P., Dreisinger, D. B., Peters, E., King, J. A., 1995. Passivation of chalcopyrite during oxidative leaching in sulfate media. *HydrometaIlurgy* 39, 25-48.

Hallberg, K. B., Lindström, E. B., 1994. Characterisation of *Thiobacillus Caldu*s sp.nov., a moderately thermophilic acidophile. *Microbiology* 140, 3451-3456.

Hallberg, K. B., Dopson, M., Lindström, E. B., 1996. Reduced sulphur compound oxidation by Thiobacillus caldus. *Journal of Bacteriology* 178(1), 6-11.

Han, K. N., 2002. Fundamentals of Aqueous Metallurgy. Society for Mining, Metallurgy, & Exploration Inc, Colorado.

Hanford, G S and Vargas, T. (2001) Chemical and electrochemical basis of bioleaching processes. *Hydrometallurgy* 59, 135-145.

Hoerl, A.E., 1959. Optimum solution of many variables equations. *Chemical Engineering Progress* 55(11), 69.

Hu, W., Yao, L. G., Hua, Z. Z., 2008. Optimization of sheet metal forming processes by adaptive response surface based on intelligent sampling method. *Journal of Materials Processing Technology* 197, 77–88.

Iglesias, N., Carranza, F., 1994. Refractory gold-bearing ores, a review of treatment methods and recent advances in biotechnological techniques. *Hydrometallurgy* 34, 383-395.

Ilgar, E., Guay, R., Torma, A. E., 1993. Kinetics of lithium extraction from spodumene by *Aspergillus niger*. In: Torma, A. E., Wey, J. E., Lakshmanan, V. I (Editors), *Biohydrometallurgical Technologies, Volume 1*. TMS, Warrendale, USA, pp. 293-301.

Jackson, E., 1986. Hydrometallurgical Extraction and Reclamation. Ellis Horwood Limited, West Sussex.

Jensen, A. B., Webb, C., 1995. Ferrous sulphate oxidation using *Thiobacillus ferrooxidans*: a review. *Process Biochemistry* 30(3), 225-238.

Johnson, D. B., 2003. Importance of microbial in the development of sustainable technologies for mineral processing and wastewater treatment. *Website:* http://www.etpsmr.org/contents/pages/publicPages/nesmi/Conferences/2003-11-03Prague/Papers/Johnson.pdf. Accessed February 2007.

Karavaiko, G. I., Duvinina, G. A., Kondrat'eva, T. F., 2006. Lithotrophic microorganisms of the oxidative cycles of sulphur and iron. *Microbiology* 75(5), 512-545.

Kaplan, W., 1952. Advanced Calculus. Addison-Wesley Publishing Company, Inc., Massachusetts.

Keller, G., 2001. Applied statistics with Microsoft Excel. Duxbury, California.

Kelly, D. P., Wood, A. P., 2000. Reclassification of some species of *Thiobacillus* to the newly designated genera *Acidithiobacillus* gen. nov., *Halothiobacillus* gen nov., and *Thermithiobacillus* gen nov. *International Journal of Systematic and Elementary Microbiology* 50, 511-516.

Keyle, J. H., 1996. Pressure acid leaching of Australian nickel/cobalt laterites. *Publications of Australasian Institute of Mining and Metallurgy*, 6/96 (Nickel'96): 245-250.

Khuri, A. I., Cornell, J. A., 1987. Response Surfaces: Designs and Analyses. Marcel Dekker, Inc., New York.

Klauber, C., 2008. A critical review of the surface chemistry of acidic ferric sulphate dissolution of chalcopyrite with regards to hindered dissolution. *International Journal of Mineral Processing* 86, 1-17.

Kodali, B., Rao, M. B., Narasu, M, L., Pogaku, R., 2004. Effect of biochemical reactions in enhancement of rate of leaching. *Chemical Engineering Science* 59, 5069-503.

Krause, E., Blakey, B. C., Papangelakis, V. G., 1998. Pressure acid leaching of nickeliferous laterite ores: ALTA 1998 Nickel/Cobalt pressure leaching and hydrometallurgy forum. *ALTA Metallurgical Services*, Melbourne, Perth, Australia.

Larsson, L., Olsson, G., Holst, O., Karlsson, H. T., 1990. Pyrite oxidation by thermophilic archaebacteria. *Applied and Environmental Microbiology* 56 (3), 697-701.

Leahy, M. J., Davidson, M. R., Schwarz, M. P., 2005. A two-dimensional CFD model for heap bioleaching of chalcocite. *Australian and New Zealand Industrial and Applied Mathematics Journal* 46(E), C439-C457.

Levenspiel, O., 1972. Chemical Reaction Engineering. John Willey and Sons, New York.

Makita, M., Esperón, M., Pereyra, B., López, A., Orrantia, E., 2004. Reductions of arsenic content in a complex galena concentrate by *Acidithiobacillus ferrooxidans. BMC Biotechnology* 4, 22.

Mason, L. J., Rice, N. M., 2002. The adaptation of *Thiobacillus ferrooxidans* for the treatment of nickel-iron sulphide concentrates. *Minerals Engineering* 15, 795-808.

McBride, M.B., 1989. Reactions controlling heavy metal solubility in soils. *Advances in Soil Science* 10, 1-56.

McKenzie, D. I., Denys, L., Buchanan, A., 1987. The solubilisation of Nickel, Cobalt and Iron from Laterites by Means of Organic Chelating Acids at Low pH. *International Journal of Mineral Processing* 21, 275-292.

Mehta, K. D., Pandey, B. D., Mankhand, T. R., 2003. Studies on kinetics of biodissolution of metals from Indian ocean nodules. *Minerals Engineering* 16, 523-527.

Miles, J.N.V., Shevlin, M.E., 2001. Applying regression and correlation: A guide for students and researchers. Sage Publications, London.

Montgomery, D. C., 2005. Design and Analysis of Experiments. John Wiley and Sons, Inc., New Jersey.

Moskalyk, R. R., Alfantazi, A. M., 2002. Nickel laterite processing and electrowinning practice. *Minerals Engineering* 15, 593-605.

Myers, R. H., 1971. Response Surface Methodology. Allyn and Bacon, Inc., Boston.

Myers, R. H., Khuri, A. I., Cater, H. W., 1989. Response Surface Methodology: 1966-1988. *Technometrics* 31(2), 137-157.

Myers, R. H., Montgomery, D. C., 2002. Response Surface Methodology: Process and product optimization using designed experiments. John Wiley and Sons, Inc., New York.

Napier-Munn, T. J., 2000. The Central Composite Rotatable Design. JKMRC, The University of Queensland, Brisbane, Australia, pp 1-9.

Ndlovu, S., Monhemius, A. J., 2005. The influence of crystal orientation on the bacterial dissolution of pyrite. *Hydrometallurgy* 78, 187-197.

Ndlovu, S., 2008. Biohydrometallurgy for sustainable development in the African mineral industry. *Hydrometallurgy* 91, 20-27.

Nemati, M., Lowenadler, J., Harrison, S.T.L., 2000. Particle size effects in bioleaching of pyrite by acidophilic thermophile *Sulfolobus metallicus* (BC*). Applied Microbiology and Biotechnology* 53, 173-179.

Nestor, D., Valdivia, U., Chaves, A. P., 2001. Mechanisms of bioleaching of a refractory mineral of gold with *Thiobacillus ferrooxidans*. *International Journal of Mineral Processing* 62, 187-198.

Norris, P. R., 1983. Iron and mineral oxidation with *Leptospirillum*-like bacteria. In: Rossi, G, Torma, A. E (Editors), *Recent Progress in Biohydrometallurgy*. Iglesias, Italy: Associazione Mineria Sarda, pp. 83-96.
Norris, P. R., Johnson, D. B., 1998. Acidophilic microorganisms. In: Horikoshi, K., Grant, W. D (Editors), Extremophiles: Microbial life in extreme environments. Wiley, New York, pp. 133-154.

Obeng, D.P., Morrel, S., Napier-Munn, T.J., 2005. Application of central composite design to modeling the effect of some operating variables on the performance of the three product cyclone. *International Journal of Mineral Processing* 76, 181-192.

Öberg, T. G., Deming, S. N., 2000. Measurement and control. *Website:* http://www.tomasoberg.com. Accessed December 2007.

Ochoa, J.G., Foucher, S., Poncin, S., Morin, D., Wild, G., 1999. Bioleaching of mineral ores in a suspended solid bubble column: hydrodynamics, mass transfer and reaction aspects. *Chemical Engineering Science* 54, 3197-3205.

Olson, G. J, Brierley, J. A, Brierley, C. L, 2003. Bioleaching review part B: Progress in bioleaching: applications of microbial processes by the minerals industries. *Applied Microbiology and Biotechnology* 153, 315-324.

Oraon, B., Majumdar, G., Ghosh, B., 2006. Application of response surface method for predicting electroless nickel plating. *Materials and Design* 27, 1035-1045.

Perrin, D.D., 1982. Ionisation constants of inorganic acids and bases in aqueous solutions. Pergamon Press, Oxford.

Peters, E., 1991. The mathematical modeling of leaching systems. *Journal of Metals* 43(2), 20-26.

Plumb, J. J., Muddle, R., Franzmann, P. D., 2008. Effect of pH on rates of iron and sulphur oxidation by bioleaching organisms. *Minerals Engineering* 21, 76-82.

Pronk, J. T., Liem, K., Bos, P., Kuenen, J. G., 1991. Energy transduction by anaerobic ferric iron respiration in *Thiobacillus ferrooxidans*. *Applied and Environmental Microbiology* 57, 2063-2068.

Pronk, J. T., de Bruyn, J. C., Bos, P., Kuenen, J. G., 1992. Anaerobic growth of *Thiobacillus ferrooxidans*. *Applied and Environmental Microbiology* 58, 2227-2230.

Prosser, A. P., 1996. Review of uncertainty in the collection and interpretation of leaching data. *Hydrometallurgy* 41, 119-153.

Rawlings, D. E., Tributsch, H., Hanford, G. S., 1999. Reasons why '*Leptospirillum*'-like species rather than *Thiobacillus ferrooxidans* are the dominant iron-oxidising bacteria in many commercial processes for the bioxidation of pyrite and related ores. *Microbiology* 145, 5-13.

Rawlings, D. E., 2005. Characteristics and adaptability of iron- and sulphur-oxidising microorganisms used for the recovery of metals from minerals and their concentrates. *Microbial Cell Factories* 4, 13.

Rawlings, D. E., Johnson, D. B., 2007. The microbiology of mining: development and optimisation of mineral-oxidizing microbial consortia. *Microbiology* 153, 315-324.

Reid, J. G., 1996. Laterite ores – nickel and cobalt resources for the future. *Publications of Australasian Institute of Mining and Metallurgy*, 6/96 (Nickel'96): 11-16.

Rohwerder, T., Gehrke, T., Kinzler, K., Sand, W., 2003. Bioleaching review part A: Progress in bioleaching: fundamentals and mechanisms of bacterial metal sulphide oxidation. *Applied Microbiology and Biotechnology* 63, 239-248.

Rossi, G., 1990. Biohydrometallurgy. McGraw-Hill Book Company, New York.

Sadowski, Z., Jazdzyk, E., Karas, H., 2003. Bioleaching of copper ore flotation concentrates. *Minerals Engineering* 16, 51-53.

Sand, W., Gehrke, T., Jozsa, P-G., Schippers, A., 2001. Bio(chemistry) of bacterial leaching - direct versus indirect bioleaching. *Hydrometallurgy* 51, 115-175.

Schippers, A., Jozsa, P. G., Sand, W., 1996. Sulphur chemistry in bacterial leaching of pyrite. *Applied and Eenvironmental Microbiology* 62(9), 3424-3431.

Schippers, A., Sand, W., 1999. Bacterial leaching of metal sulphides proceeds by two indirect mechanism via thiosulphate or via polysulphides and sulphur. *Applied and Eenvironmental Microbiology* 65, 319-321.

Silverman., M. P., Lundgren, D. G., 1959. Studies on the chemoautotrophic iron bacterium *Ferrobacillus ferrooxidans* I. An improved medium and a harvesting procedure for securing high cell yields. *Journal of Bacteriology* 77, 642-647.

Simate, G. S., Ndlovu, S., 2007. Characterisation of factors in the bacterial leaching of nickel laterites using statistical design of experiments. *Advanced Materials Research* 20-21, 66-69.

Simate, G. S., Ndlovu, S., 2008. Bacterial leaching of nickel laterites using chemolithotrophic microorganisms: Identifying influential factors using statistical design of experiments. *International Journal of Mineral Processing* 88, 31-36.

Smith, G. N., 1971. An Introduction to Matrix and Finite Elements in Civil Engineering. Applied Science Publishers, London.

Smith, J.M., 1981. Chemical Engineering Kinetics. McGraw Hill, New York.

Tang, J.A., Valix, M., 2006. Leaching of low grade limonite and nontronite ore by fungi metabolic acids. *Minerals Engineering* 19, 1274-1279.

Taylor, A., 1997. Process selection, Nickel/Cobalt pressure acid leaching and hydrometallurgy forum. *ALTA Metallurgical Sservices*, Melbourne, Perth, Australia.

Temple, K. L., Colmer, A. R., 1951. The autotrophic oxidation of iron by a new bacterium: *Thiobacillus ferrooxidans*. *Journal of Bacteriology* 62(5), 605-611.

Torma, A. E., 1977. The role of *Thiobacillus ferrooxidans* in hydrometallurgical processes. In: Ghose, T. K., Fiechter, A., Blakebrough, N (Editors), *Advances in Biochemical Engineering* 6. Springer-Verlag, New York, pp. 1-37.

Tzeferis, P., Agatzini, S., Nerantzis, E.T., Dudeney, A., Leak D., Alibhai, K., 1991. Bioleaching of Greek non-sulphide nickel ores using microorganisms assisted leaching process. *Forum for Applied Biotechnology*, Gent, Belgium, September 25-27, pp. 1797-1802.

Tzeferis, P., 1992. Mechanisms important for bioleaching and metal accumulation by microorganisms. *Metalleiologika Metallourgika Chronika* 2(1), 85-107.

Tzeferis, P.G., Agatzini – Leonardou, S., 1994. Leaching of nickel and iron from Greek non-sulphide nickeliferous ores by organic acids. *Hydrometallurgy* 36, 345-360.

Tzeferis, P. G., 1994. Leaching of a low grade hematitic laterite ore using fungi and biologically produced acid metabolites. *International Journal of Mineral Processing* 42, 267-283.

Valix, M., Usai, F., Malik, R., 2001a. Fungal bioleaching of low grade laterite ores. *Minerals Engineering* 14 (2), 197-203.

Valix, M., Tang, J. Y., Cheung, W. H., 2001b. The effects of mineralogy on the biological leaching of nickel laterite ores. *Minerals Engineering* 14 (12), 1629-1635.

Varian Techtron (Pty) Ltd., 1989. Flame Absorption Spectrophotometry - Analytical Methods. Victoria, Australia.

Vasan, S. S., Modak, J. M., Natarajan, K. A., 2001. Some recent advances in the bioprocessing of bauxite. *International Journal of Mineral Processing* 62, 173-186.

Veglio, F., Trifoni, M., Pagnanell, F., Toro, L., 2001. Shrinking core model with variable activation energy: a kinetic model of manganiferous ore leaching with sulphuric acid and lactose. *Hydrometallurgy* 60(2), 167-179.

Watling, H. R., 2007. The bioleaching of nickel-copper sulphides. *Hydrometallurgy* 91, 70-80.

Willscher, S., Bosecker, K., 2003. Studies on the leaching behavior of heterotrophic microorganisms isolated from an alkaline slag dump. *Hydrometallurgy* 71, 257-264.

Yu, J-Y., McGenity, T. J., Coleman, M. L., 2001. Solution chemistry during the lag phase and exponential phase of pyrite oxidation by *Thiobacillus ferrooxidans*. *Chemical Geology* 175, 307-317.

BIBLIOGRAPHY

"The dictionary is the only place where success comes before work".

-Arthur Brisbane

Barrett, J., Hughes, M. N., Karavaiko, G. I., Spencer, P. A., 1993. Metal extraction by microbial oxidation of minerals. Ellis Horwood Limited, West Sussex, England.

Baron, D., Palmer, C. D., 1996. Solubility of jarosite at 4-35°C. *Geochimica et Cosmochimica Acta* 60(2), 185-195.

Beveridge, T. J., 1995. The periplasmic space and periplasm in Gram-positive and Gram-negative bacteria. *Features* 61(3), 125-130.

Blake, R. C., Shute, E. A., 1994. Respiratory enzymes of T*hiobacillus ferrooxidans*. Kinetic properties of an acid-stable iron:rusticyanin oxidoreductase. *Biochemistry* 33, 9220-9228.

Bohden, W., 1975. *Chemical Kinetics for Chemical Engineers*, Sterlin Swift, Manchaca.

Brierley, C. L , 1978. Bacterial leaching. *CRC Critical Review, Microbiology* 6, 207-219.

Brierley, C. L., 1982. Microbiological mining. *Scientific American* 247(2), 42-51.

Brock, T. D., Gustafson , J., 1976. Ferric iron reduction by iron and sulphur oxidising bacteria. *Applied and Environmental Microbiology* 32, 567-571.

Cabral, T., Ignatiadis, I., 2001. Mechanistic study of the pyrite-solution interface during the oxidative bacteria oxidation of pyrite (FeS_2) by using electrochemical techniques. *International Journal of Mineral Processing* 62,41-64.

Casas, J. M., Paipa, C., Godoy, I., Vargas, T., 2007. Solubility of sodium jarosite and solution speciation in the system Fe(III)-Na-H_2SO_4-H_2O at 70°C. *Journal of Geochemical Exploration* 92, 111-119.

Chen, S., Lin, J., 2001. Bioleaching of heavy metals from sediment: significance of pH. *Chemosphere* 44, 1093-1102.

Colmer, A. R., Henkle, M. E., 1947. The role of microorganisms in acid drainage. *Science* 106, 253-256.

Colmer, A. R., Temple, K. L., Henkle, M. E., 1950. The iron oxidising bacterium from the acid drainage of some bituminous coal mines. *Journal of Bacteriology* 59, 317-328.

Cooper, L., Steinberg, D., 1970. Introduction to Methods of Optimisation. W. B. Saunders Company, Philadelphia.

Corbet, C. M., Ingeldew, W. J., 1987. Is $Fe^{3+/2+}$ cycling an intermediate in sulphur oxidation by Fe^{2+}-grown *Thiobacillus ferrooxidans*. *FEM Microbilogy Letters* 41, 1-6.

Crundwell, F. K., Holmes, P. R., Fowler, T. A., 1999. The mechanism of bacteria action in the leaching of pyrite by Thiobacillus ferrooxidans-an electrochemical study. *Journal of the Electrochemical Society* 146(8), 2906-2912.

da Silva, G., Lastra, M. R., Budden, J. R., 2003. Electrochemical passivation of sphalerite during bacterial oxidation in the presence of galena. *Minerals Engineering* 16, 199-203.

Ehrlich, H. L., Brierley, C. L., 1990. In: Ehrlich, H. L., Brierley, C. L. (Editors), Microbial mineral recovery. McGraw-Hill, New York, pp. 55-73.

Ehrlich, H. L., 1997. Microbes and metals. *Applied Microbiology and Biotechnology* 48, 687-692.

Friedrich, C. G., Rother, D., Bardischewsky, F., 2001. Oxidation of reduced inorganic sulphur compounds: Emergency of a common mechanism? *Applied and Environmental Microbiology* 67(7), 2873-2882.

Huang, T. C., Lin, Y. K., Chen, C. Y., 1988. Selective separation of nickel and copper from a complexing solution by a cation-exchange membrane. *Journal of Membrane Science* 37,131-144.

Ingeldew, W. J., Cox, J. C., Hallings, O. C., 1977. A proposed mechanism for conservation during Fe^{2+} oxidation by Thiobacillus ferrooxidans: Chemiosmotic coupling to net H^+ influx. *FEM Microbilogy Letters* 2, 193-197.

Le, L., Tang, J., Ryan, D., Valix, M., 2006. Bioleaching nickel laterite ores using multi- metal tolerant *Aspergillus foetidus* organism. *Minerals Engineering* 19, 1259-1265.

Mills, A. L., Herman, J. S., Homberger, G. M., Dejesus, J. H., 1994. Effect of solution ionic strength and iron coatings on mineral grains on the sorption of bacterial cells to quartz sand. *Applied and Environmental Microbiology* 60(9), 3300-3306.

Murr, L. E., 1980. Theory and practice of copper sulphide leaching in dumps and in-situ. *Mineral Science Engineering* 12(3), 121-189.

Ohimura, N., Tsugita, K., Koizumi, J., Saiki, H., 1996. Sulphur binding protein of flagella of *Thiobacillus ferrooxidans*. *Journal of Bacteriology* 178, 5776-5780.

Seidel, H., Wennrich, R., Hoffmann, P., Loser, C., 2006. Effect of different types of elemental sulphur on bioleaching of heavy metals from contaminated sediments. *Chemosphere* 62, 1444-1453.

Sharma, P. K., 2001. Surface studies relevant to microbial adhension and bioflotation of sulphide minerals. PhD Thesis, Luleå University of Technology, Sweden.

Stamboliadis, E., Alevizos, G., Zafiratos, J., 2004. Leaching residue of nickeliferous laterites as a source of iron concentrate. *Minerals Engineering* 17, 245-252.

Sugio, T., Katagiri, T., Inagaki, K., Tano, T., 1989. Actual substrate for elemental sulphur oxidation by sulphur:ferric ion oxidoreductase purified from *Thiobacillus ferrooxidans*. *Biochimica et Biophysica Acta* 973, 250-256.

Sukla, L. B., Panchanadikar, V. V., 1993. Bioleaching of lateritic nickel ore using heterotrophic microorganism. *Hydrometallurgy* 32, 373-379.

Treybal, R. E., 1980. *Mass Transfer Operations.* McGraw-Hill Book Company, New York.

APPENDICES

"Experience does not ever err; it is only your judgement that errs in promising itself results which are not caused by your experiments".

-Leonard Da Vinci

APPENDIX A

SAMPLE CALCULATIONS

"The thing that counts is not what we know but the ability to use what we know".

-Leo L. Spears

% Nickel composition (Nickel grade)

The % nickel composition in nickel laterites was calculated as a percentage of the total mass of the nickel laterite ore. This % nickel composition in the laterite was determined using the Varian SpectrAA-55B atomic absorption spectrophotometer after digestion of ore with aqua regia (3:1 ratio of HCl and HNO_3 mixture).

Example

Mass of nickel laterite ore weighed (g) = 1.0422
Volume of aqua regia used (mls) = 50
Mass of ore per liter (gpl) = $\frac{1.0422}{50} x1000$ = 20.84 gpl

After leaching,

Volume of sample pipetted out = 2.5mls
Volume after dilution = 50mls
Concentration of nickel (ppm) as recorded by AAS (replicates) = 15.97, 16.02
Concentration of nickel metal = $\frac{50}{2.5} x \frac{(15.97+16.09)}{2} /1000$ = 0.32gpl
Therefore, this is the maximum possible concentration assuming all nickel dissolved.

$$\% \text{ nickel composition (grade)} = \frac{\text{maximum possible concentration}}{\text{mass of ore per litre}} x\ 100$$
$$= \frac{0.32}{20.84} x\ 100$$
$$= 1.5\%$$

Nickel recovery

The recovery during the leaching of nickel laterites was calculated as a percentage of nickel in the liquid phase to that in the nickel laterite ore.

Example

Run 1(Table D1)

Volume of mixture = 200 mls
Mass of ore added = $\frac{\%\text{ pulp density x volume used}}{100}$

$$= \frac{5 \times 200}{100}$$

$$= 10 \text{ g}$$

$$\text{Mass of nickel in ore} = \frac{\% \text{ Nickel composition} \times \text{mass of ore}}{100}$$

$$= \frac{1.5 \times 10}{100}$$

$$= 0.15 \text{ g}$$

The maximum possible concentration of nickel is achieved when all the mass of nickel dissolves i.e

$$\text{Maximum concentration} = \frac{\text{Mass of nickel} \times 100}{\text{volume used}}$$

$$= \frac{0.15 \times 1000}{200}$$

$$= 0.75 \text{ gpl}$$

$$= 750 \text{ ppm}$$

$$\text{Recovery} = \frac{\text{Cobalt in solution as recorded on AAS} \times 100}{\text{Maximum concentration of nickel}}$$

$$= \frac{163 \times 100}{750} = 21.7\%$$

Effect

An effect in the statistical design is done by averaging the responses that are applicable to the level of each factor. The difference between the average responses at the two levels of each factor is an indication of the significance of that factor in influencing the response measured.

Example

Run 1 (Table D1)

Therefore, factor A at level (+1) is given by averaging the results obtained by running experiments 2, 4, 6 and 8 and factor A at level (-1) by averaging the results obtained from running experiments 1, 3, 5 and 7.

Level (+1):

$$\text{Average recoveries} = \frac{\text{Sum of recoveries for experiments 2, 4, 6, 8}}{4}$$

$$= \frac{20.05+26.44+13.88+26.23}{4}$$

$$= 21.65$$

Level (-1):

$$\text{Average recoveries} = \frac{\text{Sum of recoveries for experiments 1, 3, 5, 7}}{4}$$

$$= \frac{23.97+29.61+17.19+30.28}{4}$$

$$= 25.26$$

$$\text{Difference} = 21.65 - 25.26$$

$$= -3.61$$

$$\text{Therefore, Effect} = -3.61$$

In fact the responses are multiplied by respective contrasts for each levels i.e +1 for level (+1) and -1 for level (-1) and the averages are added.

Normal probability plots

The scales for making normal probability plot of effects is such that, on the y-axis, Pi = 100 (i-1/2)/m for i = 1, 2, 3, 4, …, m, where m = the number of effects under consideration (main and or interactions), excluding the average. The plot requires that the effects are arranged in order of magnitude, before applying the y-axis scale formula, starting with the smallest and ending with the largest.

Table A1. Effects for normal probability plots

Order No. i	1	2	3	4	5
P= 100(i-1/2)/m (where m = 5)	10	30	50	70	90
Effects	-3.61	-3.12	-0.37	3.35	9.37
Identity of the effects	A	C	E	D	B

Modeling the significant effects for recovery prediction

The model or prediction equation is useful for predicting the outcome for the future validation experiments. A model is an equation that uses only the significant effects.

If an interaction effect is significant, the terms for the main effects are also included. This is due to the hierarchy rule for defining a model (Barrentine, 1999).

From the normal probability plot, it is found that the significant factors are A, B, C and D.
Therefore,

Recovery, R, $= \bar{R} + \frac{E(A)}{2}A + \frac{E(B)}{2}B + \frac{E(C)}{2}C + \frac{E(D)}{2}D$, where $\bar{R}$ represents the average of all the data for the runs (i.e average of all the recoveries) and A, B, C and D are the contrast constants (i.e +1 or -1), E(A), E(B), E(C) and E(D) are effects as indicated in part 3 of the appendix above.

The coefficients that appear in the equations are half the calculated effects because a change from x = -1 to x = +1 is a change of two units along the x-axis.

Therefore,

$$\text{Predicted recovery, R,} = 23.46 + \frac{(-3.61)}{2}A + \frac{(9.37)}{2}B + \frac{(-3.12)}{2}C + \frac{(3.35)}{2}D$$
$$= 23.46 - 1.81A + 4.68B - 1.56C + 1.68D$$

The predicted recovery is calculated by substituting an appropriate contrast constant in a particular run.

Example

Run 1 (Table D1)

In run 1, the contrast constants are A = -1, B = -1, C = -1, D = +1

Predicted recovery = 23.46 – 1.81(-1) + 4.68(-1) – 1.56(-1) + 1.68(1)
= 23.82%

Note that the negative signs in some of the variables of the prediction model equation indicate that in order to maximize bioleaching of nickel laterites, these factors must be kept in low levels. The positive signs mean the factors must be kept in high levels.

Residual

This is the difference between the actual recovery and the predicted recovery for each run.

Example

Run 1 (Table D1)

Actual recovery = 23.97, Predicted recovery = 23.82

Residual = 23.97 – 23.82
= 0.15

Fold-over design

A fold over is the exact opposite of the basic design in signs. It is achieved by replacing all plus signs with minus signs, and vice versa. The fold over design reverses the signs of the two factor interactions in the confounding pattern.

Factor A

When it is stated that the confounding is such that, A = DE, this means that the estimated effect of A is a combination of the actual values of A and DE in the relationship shown in the base design: $E(A)_{est} = E(A)_{act} + E(DE)_{act}$.

A fold over provides a confounding pattern opposite in sign such that the fold over design is $E(A)_{est} = E(A)_{act} - E(DE)_{act}$

If results of fold-over design are added to that of base design and the average calculated, the two equations show the interaction terms cancel, leaving an estimate of main effects free from confounded two factor interactions, i.e.

$$\frac{1}{2}[\text{base } E(A)_{est} + \text{foldover } E(A)_{est}] =$$

$$\frac{1}{2}\{[E(A)_{act} + E(DE)_{act}] + [E(A)_{act} - E(DE)_{act}]\} =$$

$$\frac{1}{2}\{E(A)_{act} + E(A)_{act}\} = E(A)_{act}$$

This is a characteristic and purpose of fold-over (Barrentine, 1999, Montgomery, 2005).

APPENDIX B

NICKEL LATERITE ORE COMPOSITION AND PARTICLE SIZE ANALYSIS

"The only way to learn mathematics is to do mathematics".

-Paul Halmos

Table B1

Chemical composition of nickel laterite ore sample

Mineral	% Mass
SiO_2	52.8
Fe_2O_3	21.9
Cr_2O_3	1.0
Al_2O_3	2.5
MgO	7.5
NiO	1.9
CoO	0.3
CaO	0.7
MnO	1.3
S	<0.1
P	0.1
Total	≅ 100

Table B2

Elemental composition of different nickel laterite particle sizes

Size fraction (μm)	<38	53-63	106-150
Ni (mass %)	1.7	1.5	1.4

Table B3

Particle size analysis of nickel laterite ore sample

Sieve size (μm)	Mass retained (kg)	% Mass retained
-212+150	0.12	4.8
-150+106	0.09	3.7
-106+75	0.27	10.9
-75+63	0.98	39.3
-63+53	0.55	22.1
-53+45	0.32	12.6
-45+38	0.14	5.4
-38	0.03	1.2
Total	2.50	100

APPENDIX C

ACIDIC AND FERRIC LEACHING

"If I were to prescribe one process in the training of men which is fundamental to success in any direction, it would be thoroughgoing training in the habit of accurate observation. It is a habit which every one of us should be seeking ever more to perfect".

-Eugene G. Grace

Table C1. Nickel concentration (ppm)

Conditions for chemical leaching at different concentrations: temperature 30°C, pulp density 5% w/v, Nickel content 1.5%, agitation speed ≥ 200 rpm.

Run 1

Lixiviant	**Time (days)**					
Concentration	0	2	4	6	8	10
0.5M H_2SO_4	0	352	407	458	526	604
0.5M $C_6H_8O_7$	0	236	271	293	327	347
0.5M$Fe_2(SO_4)_3$	0	113	117	124	140	165
0.1MH_2SO_4+0.5M$Fe_2(SO_4)_3$	0	151	185	186	208	322
0.5MH_2SO_4+0.5M$Fe_2(SO_4)_3$	0	266	379	342	385	331
0.5Mx(H_2SO_4+$C_6H_8O_7$)	0	485	534	534	589	670
0.5Mx(H_2SO_4+$C_6H_8O_7$+$Fe_2(SO_4)_3$)	0	407	483	474	566	635
Distilled water	0	15	4	6	6	3
1M $C_6H_8O_7$	0	283	374	412	403	445

Run 2

Lixiviant	**Time (days)**					
Concentration	0	2	4	6	8	10
0.5M H_2SO_4	0	372	510	540	501	490
0.5M $C_6H_8O_7$	0	254	345	371	372	363
0.5M$Fe_2(SO_4)_3$	0	97	122	134	149	144
0.1MH_2SO_4+0.5M$Fe_2(SO_4)_3$	0	145	209	235	273	248
0.5MH_2SO_4+0.5M$Fe_2(SO_4)_3$	0	307	413	437	456	434
0.5M (H_2SO_4+$C_6H_8O_7$)	0	494	581	588	580	542
0.5M(H_2SO_4+$C_6H_8O_7$+$Fe_2(SO_4)_3$)	0	432	504	534	564	503
Distilled water	0	5	5	3	6	4
1M $C_6H_8O_7$	0	284	377	416	403	437

Table C2. Nickel recovery (%)

Conditions for chemical leaching at different concentrations: temperature 30°C, pulp density 5% w/v, Nickel content 1.5%, agitation speed ≥ 200 rpm.

Run 1

Lixiviant	**Time (days)**					
Concentration	0	2	4	6	8	10
0.5M H_2SO_4	0	46.3	53.5	60.1	69.1	79.4
0.5M $C_6H_8O_7$	0	30.9	35.6	38.5	42.9	45.5
0.5M$Fe_2(SO_4)_3$	0	14.8	15.4	16.3	18.4	21.7
0.1MH_2SO_4+0.5M$Fe_2(SO_4)_3$	0	19.8	24.2	24.4	27.3	42.3
0.5MH_2SO_4+0.5M$Fe_2(SO_4)_3$	0	34.9	49.7	44.9	50.6	43.5
0.5M (H_2SO_4+$C_6H_8O_7$)	0	63.7	70.2	70.1	77.3	87.9
0.5M(H_2SO_4+$C_6H_8O_7$+$Fe_2(SO_4)_3$)	0	53.5	63.4	62.2	74.4	83.5
Distilled water	0	2.0	0.5	0.7	0.8	0.4
1M $C_6H_8O_7$	0	37.2	49.3	54.4	52.9	57.5

Run 2

Lixiviant	**Time (days)**					
Concentration	0	2	4	6	8	10
0.5M H_2SO_4	0	48.8	66.9	70.9	65.8	64.4
0.5M $C_6H_8O_7$	0	33.3	45.3	48.7	48.9	47.6
0.5M$Fe_2(SO_4)_3$	0	12.7	16.0	17.6	19.6	18.9
0.1MH_2SO_4+0.5M$Fe_2(SO_4)_3$	0	19.0	27.5	30.9	35.9	32.5
0.5MH_2SO_4+0.5M$Fe_2(SO_4)_3$	0	40.3	54.3	57.4	59.9	57.0
0.5M (H_2SO_4+$C_6H_8O_7$)	0	64.9	76.3	77.2	76.2	71.2
0.5M(H_2SO_4+$C_6H_8O_7$+$Fe_2(SO_4)_3$)	0	56.7	66.2	70.2	74.0	66.0
Distilled water	0	0.7	0.7	0.4	0.8	0.6
1M $C_6H_8O_7$	0	37.3	49.5	54.6	52.9	57.4

Table C3. pH changes

Conditions for chemical leaching at different concentrations: temperature 30°C, pulp density 5% w/v, Nickel content 1.5%, agitation speed ≥ 200 rpm.

Run 1

Lixiviant	**Time (days)**					
Concentration	0	2	4	6	8	10
0.5M H_2SO_4	0.34	0.42	0.48	0.55	0.66	0.72
0.5M $C_6H_8O_7$	1.40	1.80	1.83	1.84	1.88	1.98
0.5M$Fe_2(SO_4)_3$	0.87	0.95	0.96	1.00	1.09	1.15
0.1MH_2SO_4+0.5M$Fe_2(SO_4)_3$	0.70	0.75	0.77	0.83	0.93	0.95
0.5MH_2SO_4+0.5M$Fe_2(SO_4)_3$	0.28	0.34	0.36	0.41	0.49	0.55
0.5M (H_2SO_4+$C_6H_8O_7$)	0.34	0.37	0.49	0.56	0.60	0.64
0.5M(H_2SO_4+$C_6H_8O_7$+$Fe_2(SO_4)_3$)	0.20	0.24	0.24	0.32	0.37	0.40
Distilled water	5.94	7.14	8.31	8.35	8.36	8.38
1M $C_6H_8O_7$	1.28	1.61	1.63	1.73	1.67	1.71

Run 2

Lixiviant	**Time (days)**					
Concentration	0	2	4	6	8	10
0.5M H_2SO_4	0.44	0.58	0.58	0.63	0.69	0.76
0.5M $C_6H_8O_7$	1.50	2.05	1.98	2.00	2.03	2.05
0.5M$Fe_2(SO_4)_3$	0.98	1.12	1.06	1.07	1.12	1.11
0.1MH_2SO_4+0.5M$Fe_2(SO_4)_3$	0.78	0.88	0.85	0.87	0.93	0.96
0.5MH_2SO_4+0.5M$Fe_2(SO_4)_3$	0.37	0.46	0.41	0.48	0.51	0.58
0.5M (H_2SO_4+$C_6H_8O_7$)	0.38	0.46	0.54	0.58	0.61	0.62
0.5M(H_2SO_4+$C_6H_8O_7$+$Fe_2(SO_4)_3$)	0.26	0.35	0.32	0.35	0.39	0.41
Distilled water	5.82	7.11	8.25	8.28	8.38	8.39
1M $C_6H_8O_7$	1.29	1.65	1.61	1.75	1.70	1.70

Table C4. Nickel concentration (ppm)

Conditions for chemical leaching at different initial pHs: pulp density 5% w/v, Nickel content 1.5%, agitation speed ≥ 200 rpm.

Initial pH: 0.5

Time	Run 1			Run2		
(days)	H_2SO_4	$C_6H_8O_7$	$Fe_2(SO_4)_3$	H_2SO_4	$C_6H_8O_7$	$Fe_2(SO_4)_3$
0	0	0	0	0	0	0
2	390	413	186	385	415	179
4	443	446	237	431	456	231
6	488	468	246	490	473	245
8	543	481	277	527	492	279

Initial pH: 1.0

Time	Run 1			Run2		
(days)	H_2SO_4	$C_6H_8O_7$	$Fe_2(SO_4)_3$	H_2SO_4	$C_6H_8O_7$	$Fe_2(SO_4)_3$
0	0	0	0	0	0	0
2	197	256	84	133	268	77
4	262	351	96	180	401	81
6	327	383	91	212	468	130
8	361	470	141	242	499	157

Initial pH: 1.5

Time	Run 1			Run2		
(days)	H_2SO_4	$C_6H_8O_7$	$Fe_2(SO_4)_3$	H_2SO_4	$C_6H_8O_7$	$Fe_2(SO_4)_3$
0	0	0	0	0	0	0
2	120	295	37	122	286	34
4	166	373	40	165	370	41
6	198	413	61	205	409	57
8	212	451	73	212	453	69

Initial pH: 2.0

Time	Run 1			Run2		
(days)	H_2SO_4	$C_6H_8O_7$	$Fe_2(SO_4)_3$	H_2SO_4	$C_6H_8O_7$	$Fe_2(SO_4)_3$
0	0	0	0	0	0	0
2	153	301	39	146	299	44
4	174	361	50	174	366	52
6	204	426	63	213	430	71
8	219	462	63	233	475	73

Table C5. Nickel recovery (%)

Conditions for chemical leaching at different initial pHs: pulp density 5% w/v, Nickel content 1.5%, agitation speed ≥ 200 rpm.

Initial pH: 0.5

Time	Run 1			Run2		
(days)	H_2SO_4	$C_6H_8O_7$	$Fe_2(SO_4)_3$	H_2SO_4	$C_6H_8O_7$	$Fe_2(SO_4)_3$
0	0	0	0	0	0	0
2	50.7	53.7	24.1	50.0	54.0	23.2
4	57.6	58.0	30.7	56.0	59.2	30.1
6	63.4	60.9	31.9	63.7	61.5	31.9
8	70.6	62.5	36.0	68.5	64.0	36.3

Initial pH: 1.0

Time	Run 1			Run2		
(days)	H_2SO_4	$C_6H_8O_7$	$Fe_2(SO_4)_3$	H_2SO_4	$C_6H_8O_7$	$Fe_2(SO_4)_3$
0	0	0	0	0	0	0
2	25.9	33.6	11.0	17.6	35.3	10.1
4	34.4	46.2	12.7	23.7	52.8	10.7
6	43.0	50.3	12.0	27.9	61.5	17.0
8	47.5	61.9	18.6	31.8	65.6	20.6

Initial pH: 1.5

Time	Run 1			Run2		
(days)	H_2SO_4	$C_6H_8O_7$	$Fe_2(SO_4)_3$	H_2SO_4	$C_6H_8O_7$	$Fe_2(SO_4)_3$
0	0	0	0	0	0	0
2	20.1	39.6	5.1	19.1	39.3	5.7
4	22.9	47.5	6.5	22.8	48.2	6.9
6	26.8	56.0	8.2	28.0	56.5	9.3
8	28.8	60.7	8.2	30.6	62.5	9.6

Initial pH: 2.0

Time	Run 1			Run2		
(days)	H_2SO_4	$C_6H_8O_7$	$Fe_2(SO_4)_3$	H_2SO_4	$C_6H_8O_7$	$Fe_2(SO_4)_3$
0	0	0	0	0	0	0
2	15.7	38.8	4.8	16.0	37.6	4.5
4	21.8	49.1	5.3	21.7	48.6	5.3
6	26.1	54.3	8.0	27.0	53.8	7.4
8	27.9	59.3	9.5	27.9	59.5	9.1

Table C6. pH changes

Conditions for chemical leaching at different initial pHs: pulp density 5% w/v, Nickel content 1.5%, agitation speed ≥ 200 rpm.

Initial pH: 0.5

Time	Run 1			Run2		
(days)	H_2SO_4	$Fe_2(SO_4)_3$	$C_6H_8O_7$	H_2SO_4	$Fe_2(SO_4)_3$	$C_6H_8O_7$
0	0.50	0.50	0.50	0.50	0.50	0.50
2	0.64	0.64	0.82	0.68	0.65	0.82
4	0.67	0.62	0.87	0.70	0.64	0.86
6	0.71	0.61	0.88	0.67	0.63	0.89
8	0.72	0.65	0.94	0.73	0.65	0.92

Initial pH: 1.0

Time	Run 1			Run2		
(days)	H_2SO_4	$Fe_2(SO_4)_3$	$C_6H_8O_7$	H_2SO_4	$Fe_2(SO_4)_3$	$C_6H_8O_7$
0	1.00	1.00	1.00	1.00	1.00	1.00
2	1.15	1.04	1.30	1.07	0.96	1.08
4	1.13	0.97	1.30	1.16	1.02	1.13
6	1.23	1.04	1.35	1.17	1.01	1.14
8	1.21	1.01	1.34	1.20	1.00	1.10
10	1.25	1.02	1.32	1.21	0.98	1.07
12	1.27	0.98	1.37	1.25	1.06	0.91

Initial pH: 1.5

Time	Run 1			Run2		
(days)	H_2SO_4	$Fe_2(SO_4)_3$	$C_6H_8O_7$	H_2SO_4	$Fe_2(SO_4)_3$	$C_6H_8O_7$
0	1.50	1.50	1.50	1.50	1.50	1.50
2	1.79	1.78	1.73	1.78	1.77	1.73
4	1.86	1.78	176	1.85	1.77	1.75
6	1.81	1.86	1.82	1.77	1.84	1.81
8	1.85	1.79	1.86	1.77	1.74	1.83

Initial pH: 2.0

Time	Run 1			Run2		
(days)	H_2SO_4	$Fe_2(SO_4)_3$	$C_6H_8O_7$	H_2SO_4	$Fe_2(SO_4)_3$	$C_6H_8O_7$
0	2.00	2.00	2.00	2.00	2.00	2.00
2	2.36	2.10	2.11	2.32	2.10	2.11
4	2.40	2.03	2.14	2.37	2.02	2.13
6	2.43	1.96	2.17	2.40	1.95	2.17
8	2.63	1.83	2.20	2.62	1.81	2.17

Table C7. Nickel concentration (ppm)

Conditions for chemical leaching at different temperatures: concentration of lixiviants 0.5M, pulp density 5% w/v, Nickel content 1.5%, agitation speed ≥ 200 rpm.

Temperature: 30°C

Time	Run 1			Run2		
(days)	H_2SO_4	$C_6H_8O_7$	[a]$Fe_2(SO_4)_3$	H_2SO_4	$C_6H_8O_7$	[a]$Fe_2(SO_4)_3$
0	0	0	0	0	0	0
2	255	185	206	249	182	215
4	346	249	291	336	241	276
6	400	283	357	400	288	361
8	477	329	418	468	322	405
10	504	365	434	521	361	424
12	560	401	460	590	411	460

[a] 0.5M $Fe_2(SO_4)_3$ acidified with 0.5M H_2SO_4

Temperature: 40°C

Time	Run 1			Run2		
(days)	H_2SO_4	$C_6H_8O_7$	[a]$Fe_2(SO_4)_3$	H_2SO_4	$C_6H_8O_7$	[a]$Fe_2(SO_4)_3$
0	0	0	0	0	0	0
2	423	257	350	399	257	342
4	527	317	436	505	328	421
6	623	426	527	572	369	554
8	675	431	612	644	414	592

[a] 0.5M $Fe_2(SO_4)_3$ acidified with 0.5M H_2SO_4

Temperature: 45°C

Time	Run 1			Run2		
(days)	H_2SO_4	$C_6H_8O_7$	[a]$Fe_2(SO_4)_3$	H_2SO_4	$C_6H_8O_7$	[a]$Fe_2(SO_4)_3$
0	0	0	0	0	0	0
2	469	298	361	449	294	378
4	561	364	455	562	361	478
6	651	449	594	683	446	664
8	692	498	698	741	490	747

[a] 0.5M $Fe_2(SO_4)_3$ acidified with 0.5M H_2SO_4

Table C8: Nickel recoveries (%)

Conditions for chemical leaching at different temperatures: concentration of lixiviants 0.5M, pulp density 5% w/v, Nickel content 1.5%, agitation speed ≥ 200 rpm.

Temperature: 30°C

Time	Run 1			Run2		
(days)	H_2SO_4	$C_6H_8O_7$	[a]$Fe_2(SO_4)_3$	H_2SO_4	$C_6H_8O_7$	[a]$Fe_2(SO_4)_3$
0	0	0	0	0	0	0
2	33.6	23.4	27.1	32.8	23.9	28.2
4	45.6	37.2	38.4	44.3	31.7	36.4
6	52.7	37.2	47.0	52.7	37.9	47.5
8	62.8	43.3	55.1	61.7	42.4	53.3

[a] 0.5M $Fe_2(SO_4)_3$ acidified with 0.5M H_2SO_4

Temperature: 40°C

Time	Run 1			Run2		
(days)	H_2SO_4	$C_6H_8O_7$	[a]$Fe_2(SO_4)_3$	H_2SO_4	$C_6H_8O_7$	[a]$Fe_2(SO_4)_3$
0	0	0	0	0	0	0
2	55.7	33.8	46.1	52.5	33.8	44.9
4	69.4	41.7	57.4	66.5	43.1	55.4
6	82.0	56.1	69.4	75.3	48.6	72.8
8	88.8	56.7	80.6	84.8	54.5	77.9

[a] 0.5M $Fe_2(SO_4)_3$ acidified with 0.5M H_2SO_4

Temperature: 45°C

Time	Run 1			Run2		
(days)	H_2SO_4	$C_6H_8O_7$	[a]$Fe_2(SO_4)_3$	H_2SO_4	$C_6H_8O_7$	[a]$Fe_2(SO_4)_3$
0	0	0	0	0	0	0
2	61.7	39.2	47.5	59.1	38.6	49.7
4	73.8	47.9	60.0	74.0	47.4	62.9
6	85.7	59.1	78.2	89.9	58.7	87.3
8	91.1	65.6	91.9	97.5	64.5	98.3

[a] 0.5M $Fe_2(SO_4)_3$ acidified with 0.5M H_2SO_4

Table C9. pH changes

Conditions for chemical leaching at different temperatures: concentration of lixiviants 0.5M, pulp density 5% w/v, Nickel content 1.5%, agitation speed ≥ 200 rpm.

Temperature: 30°C

Time	Run 1			Run2		
(days)	H_2SO_4	[a]$Fe_2(SO_4)_3$	$C_6H_8O_7$	H_2SO_4	[a]$Fe_2(SO_4)_3$	$C_6H_8O_7$
0	0.50	0.39	1.59	0.49	0.38	1.61
2	0.53	0.45	1.91	0.51	0.37	1.95
4	0.49	0.32	1.92	0.47	0.32	1.96
6	0.55	0.45	1.98	0.54	0.42	2.01
8	0.59	0.43	1.94	0.58	0.41	2.01

[a] 0.5M $Fe_2(SO_4)_3$ acidified with 0.5M H_2SO_4

Temperature: 40°C

Time	Run 1			Run2		
(days)	H_2SO_4	[a]$Fe_2(SO_4)_3$	$C_6H_8O_7$	H_2SO_4	[a]$Fe_2(SO_4)_3$	$C_6H_8O_7$
0	0.41	0.33	1.53	0.41	0.34	1.52
2	0.56	0.45	2.08	0.56	0.43	2.05
4	0.63	0.52	2.09	0.62	0.48	2.09
6	0.68	0.50	2.15	0.67	0.49	0.95
8	0.69	0.50	2.18	0.68	0.49	2.04

[a] 0.5M $Fe_2(SO_4)_3$ acidified with 0.5M H_2SO_4

Temperature: 45°C

Time	Run 1			Run2		
(days)	H_2SO_4	[a]$Fe_2(SO_4)_3$	$C_6H_8O_7$	H_2SO_4	[a]$Fe_2(SO_4)_3$	$C_6H_8O_7$
0	0.40	0.33	1.55	0.40	0.31	1.58
2	0.61	0.40	2.04	0.57	0.37	2.05
4	0.68	0.46	2.13	0.65	0.41	2.14
6	0.77	0.49	2.19	0.71	0.44	2.19
8	0.75	0.53	2.19	0.72	0.44	2.20

[a] 0.5M $Fe_2(SO_4)_3$ acidified with 0.5M H_2SO_4

APPENDIX D

IDENTIFICATION OF INFLUENTIAL FACTORS

"Think before you think".

-Stanislaw J. Lec

Table D1. Nickel recovery (%) for basic design

Bacterial leaching conditions: Nickel content 1.5%, mixed culture inoculum, pure 9K nutrient media, temperature 30°C, agitation speed 190 rpm.

	1	2	3	4	5	6	7	8	Runs
	-1	+1	-1	+1	-1	+1	-1	+1	A
Time	-1	-1	+1	+1	-1	-1	+1	+1	B
(days)	-1	-1	-1	-1	+1	+1	+1	+1	C
	+1	+1	-1	-1	-1	-1	+1	+1	D
	-1	+1	+1	-1	+1	-1	-1	+1	E
0	0	0	0	0	0	0	0	0	
2	21.7	21.3	27.3	25.2	17.7	15.1	28.8	24.5	
4	30.6	26.6	39.9	34.6	20.8	20.8	39.9	32.8	
6	26.6	18.6	37.2	29.3	17.7	12.4	35.5	28.4	
8	27.9	23.9	41.2	31.9	21.7	16.8	35.9	31.9	
10	26.6	22.6	29.3	26.6	17.7	15.1	30.6	30.1	
12	29.3	26.6	34.6	31.9	20.4	16.8	35.5	35.5	
14	26.6	21.3	29.3	23.9	18.6	12.0	39.5	25.0	
16	21.3	16.0	26.6	21.3	12.4	9.8	23.9	21.3	
18	21.3	17.3	23.9	23.9	14.2	11.1	25.7	21.3	
20	21.3	16.0	23.9	23.9	14.2	12.4	25.7	22.2	
22	21.3	18.6	26.6	23.9	16.0	12.4	26.6	24.6	
24	18.6	18.6	23.9	26.6	16.8	15.1	24.4	23.9	
26	18.6	13.3	21.3	20.6	15.1	10.6	21.7	19.5	
Average	24.0	20.1	29.6	26.4	17.2	13.9	30.3	26.2	

The actual factor levels, coded as values of -1 and +1 in the table were as follows: for pH (A):1.5 (-1) and 2.5 (+1); particle size (B): -38μm (-1) and -150+100μm (+1); pulp density (C):5% w/v(-1) and 15% w/v(+1); substrate type (D): sulphur (-1) and pyrite (+1); inoculum size (E):5% v/v (-1) and 15% v/v (+1).

Table D2. Nickel recovery (%) for fold-over design

Bacterial leaching conditions: Nickel content 1.5%, mixed culture inoculum, pure 9K nutrient media, temperature 30°C, agitation speed 190 rpm.

	+1	-1	+1	-1	+1	-1	+1	-1	A
Time	+1	+1	-1	-1	+1	+1	-1	-1	B
(days)	+1	+1	+1	+1	-1	-1	-1	-1	C
	-1	-1	+1	+1	+1	+1	-1	-1	D
	+1	-1	-1	+1	-1	+1	+1	-1	E
0	0	0	0	0	0	0	0	0	
2	22.2	31.9	16.0	18.6	34.6	37.2	13.3	18.6	
4	31.0	37.2	22.6	22.6	42.6	42.6	18.6	26.6	
6	37.7	39.4	24.6	29.3	47.9	47.9	23.9	34.6	
8	33.6	32.6	16.4	23.5	36.5	37.9	18.6	19.2	
10	29.6	28.5	15.2	19.1	33.1	34.7	15.7	29.4	
12	26.0	27.9	14.4	18.6	31.6	32.4	14.6	21.2	
14	27.9	31.5	15.6	23.7	33.3	39.9	15.0	24.2	
16	29.3	32.6	18.0	21.3	34.6	35.3	15.0	26.8	
18	31.8	35.5	17.6	25.3	32.1	36.8	16.9	34.7	
20	19.4	21.7	11.6	14.6	25.7	29.5	12.8	18.2	
22	18.6	23.1	10.4	14.5	22.7	27.9	11.0	19.5	
24	19.1	23.1	10.7	15.0	24.0	27.1	11.0	18.2	
26	15.0	18.0	8.8	12.8	20.4	24.9	9.0	14.2	
Average	26.2	29.5	15.5	19.9	32.2	34.9	15.0	23.5	

The actual factor levels, coded as values of -1 and +1 in the table were as follows: for pH (A):1.5 (-1) and 2.5 (+1); particle size (B): -38µm (-1) and -150+100µm (+1); pulp density (C):5% w/v(-1) and 15% w/v(+1); substrate type (D): sulphur (-1) and pyrite (+1); inoculum size (E):5% v/v (-1) and 15% v/v (+1).

Table D3. Nickel concentration (ppm) for basic design

Bacterial leaching conditions: Nickel content 1.5%, mixed culture inoculum, pure 9K nutrient media, temperature 30°C, agitation speed 190 rpm.

	-1	+1	-1	+1	-1	+1	-1	+1	A
Time	-1	-1	+1	+1	-1	-1	+1	+1	B
(days)	-1	-1	-1	-1	+1	+1	+1	+1	C
	+1	+1	-1	-1	-1	-1	+1	+1	D
	-1	+1	+1	-1	+1	-1	-1	+1	E
0	0	0	0	0	0	0	0	0	
2	163	160	205	167	400	340	650	552	
4	230	200	300	260	470	470	900	740	
6	200	140	280	220	400	280	800	640	
8	210	180	310	240	490	380	810	720	
10	200	170	220	200	400	340	690	680	
12	220	200	260	240	460	380	800	800	
14	200	160	220	180	420	270	890	790	
16	160	120	200	160	280	220	540	480	
18	160	130	180	180	320	250	580	480	
20	160	120	180	180	320	280	580	500	
22	160	140	200	180	360	280	600	556	
24	140	140	180	200	380	340	550	540	
26	140	100	160	140	340	240	490	440	

The actual factor levels, coded as values of -1 and +1 in the table were as follows: for pH (A):1.5 (-1) and 2.5 (+1); particle size (B): -38μm (-1) and -150+100μm (+1); pulp density (C):5% w/v(-1) and 15% w/v(+1); substrate type (D): sulphur (-1) and pyrite (+1); inoculum size (E):5% v/v (-1) and 15% v/v (+1).

Table D4. Nickel concentration (ppm) for fold-over design

Bacterial leaching conditions: Nickel content 1.5%, mixed culture inoculum, pure 9K nutrient media, temperature 30°C, agitation speed 190 rpm.

Time	+1	-1	+1	-1	+1	-1	+1	-1	A
(days)	+1	+1	-1	-1	+1	+1	-1	-1	B
	+1	+1	+1	+1	-1	-1	-1	-1	C
	-1	-1	+1	+1	+1	+1	-1	-1	D
	+1	-1	-1	+1	-1	+1	+1	-1	E
0	0	0	0	0	0	0	0	0	
2	500	720	360	420	260	280	100	140	
4	700	840	510	510	320	320	140	200	
6	850	980	556	660	360	360	180	260	
8	758	938	371	530	274	285	140	144	
10	667	644	344	432	249	261	118	221	
12	587	629	326	421	238	243	110	159	
14	628	710	352	534	250	300	113	182	
16	662	758	406	481	260	265	113	201	
18	716	933	397	570	241	277	127	261	
20	438	490	261	330	194	222	96	137	
22	420	522	236	326	171	210	83	147	
24	431	521	241	338	180	204	83	137	
26	338	405	199	288	154	188	68	107	

The actual factor levels, coded as values of -1 and +1 in the table were as follows: for pH (A):1.5 (-1) and 2.5 (+1); particle size (B): -38µm (-1) and -150+100µm (+1); pulp density (C):5% w/v(-1) and 15% w/v(+1); substrate type (D): sulphur (-1) and pyrite (+1); inoculum size (E):5% v/v (-1) and 15% v/v (+1).

Table D5. Nickel concentration (ppm) for centre points design

Bacterial leaching conditions: Nickel content 1.5%, mixed culture inoculum, pure 9K nutrient media, temperature 30°C, agitation speed 190 rpm.

Time	0	0	0	0	A
(days)	0	0	0	0	B
	0	0	0	0	C
	0	0	0	0	D
	0	0	0	0	E
0	0	0	0	0	
2	270	320	340	320	
4	400	420	460	440	
6	320	320	600	540	
8	390	380	513	431	
10	340	320	374	350	
12	420	380	325	269	
14	320	320	410	336	
16	240	240	421	378	
18	260	260	618	427	
20	260	260	247	246	
22	280	280	223	234	
24	260	300	223	225	
26	240	240	191	183	
Average	20.5	20.7	25.3	22.4	

The actual factor levels, coded as values of -1 and +1 in the table were as follows: for pH (A):2.0 (0); particle size (B): 75-63µm (0); pulp density (C):10% w/v(0); substrate type (D): sulphur (0); inoculum size (E):10% v/v (0)

Table D6. Nickel recovery (%) for centre points design

Bacterial leaching conditions: Nickel content 1.5%, mixed culture inoculum, pure 9K nutrient media, temperature 30°C, agitation speed 190 rpm.

Time	0	0	0	0	A
(days)	0	0	0	0	B
	0	0	0	0	C
	0	0	0	0	D
	0	0	0	0	E
0	0	0	0	0	
2	18.0	21.3	22.6	21.3	
4	26.6	27.7	30.6	29.3	
6	21.3	21.3	39.9	35.9	
8	25.9	25.3	34.1	28.7	
10	22.6	21.3	24.9	23.3	
12	27.9	25.3	21.6	17.9	
14	21.3	21.3	27.3	22.3	
16	16.0	16.0	28.0	25.1	
18	17.3	17.3	41.1	28.4	
20	17.3	17.3	16.4	16.4	
22	18.6	18.6	14.8	15.5	
24	17.3	19.9	14.6	15.0	
26	16.0	16.0	12.7	12.2	
Average	20.5	20.7	25.3	22.4	

The actual factor levels, coded as values of -1 and +1 in the table were as follows: for pH (A):2.0 (0); particle size (B): 75-63µm (0); pulp density (C):10% w/v(0); substrate type (D): sulphur (0); inoculum size (E):10% v/v (0)

Table D7. pH changes for basic design

Bacterial leaching conditions: Nickel content 1.5%, mixed culture inoculum, pure 9K nutrient media, temperature 30°C, agitation speed 190 rpm.

Time	+1	-1	+1	-1	+1	-1	+1	-1	A
(days)	+1	+1	-1	-1	+1	+1	-1	-1	B
	+1	+1	+1	+1	-1	-1	-1	-1	C
	-1	-1	+1	+1	+1	+1	-1	-1	D
	+1	-1	-1	+1	-1	+1	+1	-1	E
0	1.5	2.5	1.5	2.5	1.5	2.5	1.5	2.5	
2	1.62	2.45	1.61	2.46	1.68	2.45	1.62	2.43	
4	1.61	2.41	1.60	2.46	1.67	2.44	1.62	2.41	
6	1.40	2.27	1.34	2.11	1.33	2.00	1.40	2.27	
8	1.63	2.38	1.50	2.15	1.46	1.96	1.62	2.31	
10	1.56	2.38	1.42	1.98	1.38	1.80	1.55	2.38	
12	1.51	2.36	1.38	2.05	1.32	1.92	1.50	2.35	
14	1.55	2.38	1.38	1.97	1.31	1.90	1.54	2.36	
16	1.58	2.38	1.39	1.94	1.31	1.93	1.57	2.38	
18	1.50	2.38	1.31	1.85	1.31	1.81	1.51	2.37	
20	1.54	2.39	1.31	1.90	1.30	1.90	1.54	2.38	
22	1.57	2.39	1.36	1.89	1.33	1.83	1.57	2.40	
24									
26									

The actual factor levels, coded as values of -1 and +1 in the table were as follows: for pH (A):1.5 (-1) and 2.5 (+1); particle size (B): -38μm (-1) and -150+100μm (+1); pulp density (C):5% w/v(-1) and 15% w/v(+1); substrate type (D): sulphur (-1) and pyrite (+1); inoculum size (E):5% v/v (-1) and 15% v/v (+1).

Table D8. pH changes for fold-over design

Bacterial leaching conditions: Nickel content 1.5%, mixed culture inoculum, pure 9K nutrient media, temperature 30°C, agitation speed 190 rpm.

Time (days)	+1	-1	+1	-1	+1	-1	+1	-1	A
	+1	+1	-1	-1	+1	+1	-1	-1	B
	+1	+1	+1	+1	-1	-1	-1	-1	C
	-1	-1	+1	+1	+1	+1	-1	-1	D
	+1	-1	-1	+1	-1	+1	+1	-1	E
0	2.5	1.5	2.5	1.5	2.5	1.5	2.5	1.5	
2	2.40	1.80	2.29	1.69	2.29	1.61	2.40	1.69	
4	2.32	1.52	2.29	1.58	2.26	1.55	2.18	1.47	
6	2.23	1.45	2.28	1.54	2.25	1.51	1.84	1.35	
8	1.98	1.34	2.25	1.52	2.22	1.51	1.71	1.24	
10	1.96	1.40	2.20	1.53	2.21	1.52	1.85	1.37	
12	1.96	1.40	2.16	1.52	2.18	1.50	1.95	1.40	
14	1.87	1.32	2.17	1.51	2.18	1.49	1.95	1.33	
16	1.77	1.27	2.16	1.47	2.13	1.46	1.91	1.20	
18	1.88	1.36	2.20	1.54	2.16	1.54	1.94	1.26	
20	1.84	1.19	2.20	1.51	2.19	1.49	1.79	1.22	
22	1.96	1.32	2.22	1.50	2.22	1.51	1.90	1.32	
24	2.01	1.35	2.23	1.49	2.19	1.50	1.91	1.31	
26	1.99	1.36	2.26	1.57	2.03	1.54	1.98	1.35	

The actual factor levels, coded as values of -1 and +1 in the table were as follows: for pH (A):1.5 (-1) and 2.5 (+1); particle size (B): -38μm (-1) and -150+100μm (+1); pulp density (C):5% w/v(-1) and 15% w/v(+1); substrate type (D): sulphur (-1) and pyrite (+1); inoculum size (E):5% v/v (-1) and 15% v/v (+1).

Table D9. pH changes for centre points design

Bacterial leaching conditions: Nickel content 1.5%, mixed culture inoculum, pure 9K nutrient media, temperature 30°C, agitation speed 190 rpm.

Time (days)	0	0	0	0	A
	0	0	0	0	B
	0	0	0	0	C
	0	0	0	0	D
	0	0	0	0	E
0	2.0	2.0	2.0	2.0	
2	2.10	2.10	2.10	2.05	
4	2.09	2.10	1.87	1.79	
6	1.84	1.74	1.60	1.66	
8	1.83	1.86	1.46	1.52	
10	1.72	1.73	1.57	1.61	
12	1.73	1.73	1.66	1.64	
14	1.70	1.70	1.63	1.60	
16	1.75	1.69	1.55	1.55	
18	1.73	1.63	1.60	1.63	
20	1.71	1.63	1.58	1.59	
22	1.74	1.68	1.68	1.66	
24			1.70	1.70	
26			1.73	1.70	
Average					

The actual factor levels, coded as values of -1 and +1 in the table were as follows: for pH (A):2.0 (0); particle size (B): 75-63µm (0); pulp density (C):10% w/v(0); substrate type (D): sulphur (0); inoculum size (E):10% v/v (0)

APPENDIX E

EFFECTS OF INITIAL pH ON SUBSTRATE TYPE

"Sixty minutes of thinking of any kind is bound to lead to confusion and unhappiness".

-James Thurber

Table E1. Nickel recovery

Bacterial leaching conditions: Nickel content 1.5%, 10% v/v mixed culture inoculum, pure 9K nutrient media, temperature 30°C, agitation speed 190 rpm.

Run 1

Time (days)	A				B				C	D	E	F	[a]Media Composition
	1.0	1.5	2.0	2.5	1.0	1.5	2.0	2.5	1.5	1.5	1.5	1.5	Initial pH
0	0	0	0	0	0	0	0	0	0	0	0	0	
3	35.5	21.2	15.7	12.4	38.1	23.8	17.8	16.7	23.8	24.2	20.1	20.1	
6	37.6	23.1	16.9	15.0	40.6	25.7	19.1	17.3	24.4	26.0	22.6	22.6	
9	42.8	25.6	20.8	19.1	46.8	28.3	22.2	19.5	28.8	32.3	28.3	28.3	
12	49.8	27.4	23.9	24.6	49.6	31.8	25.1	21.9	34.4	36.2	34.7	34.7	
15	51.9	31.7	31.5	35.4	53.9	29.6	29.5	25.0	34.1	32.9	33.3	33.3	
18	57.8	33.5	34.8	39.6	53.6	27.3	30.9	21.9	35.6	29.6	32.7	32.7	
21	60.1	40.3	30.5	54.5	49.9	30.6	31.2	28.2	40.2	30.9	32.8	32.8	
24	64.7	45.9	38.1	63.7	52.0	35.2	36.4	32.7	46.1	34.4	32.9	32.9	
27	61.2	46.7	40.9	59.0	44.4	35.4	32.4	34.7	44.1	22.4	30.3	30.3	
32	67.8	56.0	46.8	64.3	44.9	42.9	38.0	38.9	55.9	29.4	30.2	30.2	

[a]The media composition is as follows: (A):sulphur substrate with bacteria; (B): pyrite substrate with bacteria; (C):sulphur substrate with no bacteria; (D):pyrite substrate with no bacteria; (E):distilled water only; (F):9K media with no substrate or bacteria.

Run 2

Time (days)	A				B				C	D	E	F	[a]Media Composition
	1.0	1.5	2.0	2.5	1.0	1.5	2.0	2.5	1.5	1.5	1.5	1.5	Initial pH
0	0	0	0	0	0	0	0	0	0	0	0	0	
3	27.2	21.1	15.2	10.7	33.1	21.8	16.5	14.1	23.0	27.7	20.4	22.0	
6	36.8	23.5	15.6	11.5	36.7	24.5	17.4	15.1	25.0	25.4	22.0	23.5	
9	39.0	23.6	16.0	12.2	41.3	24.4	16.9	16.0	25.6	26.4	20.3	21.8	
12	47.9	29.2	22.5	19.1	49.7	29.6	21.2	21.8	30.3	31.7	23.6	25.7	
15	50.5	31.2	20.8	16.8	51.9	30.7	22.3	24.2	36.8	33.9	25.6	28.6	
18	45.8	29.0	19.1	17.0	44.8	27.1	19.9	20.8	32.5	28.0	23.4	24.1	
21	41.1	26.8	17.5	17.3	37.6	23.5	17.6	17.3	28.1	22.0	21.1	19.5	
24	49.7	36.9	23.7	26.4	43.6	28.0	22.3	23.5	35.9	26.8	25.2	23.6	
27	49.8	38.5	26.7	26.1	39.7	26.7	21.8	26.1	35.1	24.6	22.7	21.1	
32	54.3	45.8	33.1	34.3	40.8	30.2	27.2	30.1	39.6	26.0	24.4	21.5	

[a]The media composition is as follows: (A):sulphur substrate with bacteria; (B): pyrite substrate with bacteria; (C):sulphur substrate with no bacteria; (D):pyrite substrate with no bacteria; (E):distilled water only; (F):9K media with no substrate or bacteria.

Table E2. Nickel concentrations (ppm)

Bacterial leaching conditions: Nickel content 1.5%, 10% v/v mixed culture inoculum, pure 9K nutrient media, temperature 30°C, agitation speed 190 rpm.

Run 1

Time (days)	A				B				C	D	E	F	[a]Media Composition
	1.0	1.5	2.0	2.5	1.0	1.5	2.0	2.5	1.5	1.5	1.5	1.5	Initial pH
0	0	0	0	0	0	0	0	0	0	0	0	0	
3	271	162	120	95	291	182	136	128	182	185	153	153	
6	287	177	129	115	310	197	146	132	186	199	173	173	
9	327	195	158	146	357	216	169	149	220	246	216	216	
12	380	209	183	188	379	243	192	167	263	276	265	265	
15	396	242	241	270	411	226	225	191	261	251	254	254	
18	441	256	265	302	410	209	236	168	272	226	250	250	
21	459	308	233	416	381	234	238	215	307	236	250	250	
24	494	350	290	486	397	269	278	250	352	262	251	251	
27	467	356	312	451	339	271	247	265	337	171	231	231	
32	518	428	357	491	343	328	290	297	426	225	230	230	

[a]The media composition is as follows: (A):sulphur substrate with bacteria; (B): pyrite substrate with bacteria; (C):sulphur substrate without bacteria; (D):pyrite substrate without bacteria; (E):distilled water only; (F):9K media with neither substrate nor bacteria.

Run 2

Time (days)	A				B				C	D	E	F	[a]Media Composition
	1.0	1.5	2.0	2.5	1.0	1.5	2.0	2.5	1.5	1.5	1.5	1.5	Initial pH
0	0	0	0	0	0	0	0	0	0	0	0	0	
3	208	161	116	81	253	166	126	108	176	174	167	168	
6	281	179	119	88	280	187	133	115	191	194	181	179	
9	298	180	122	94	315	186	129	122	195	202	167	167	
12	366	223	171	146	379	226	162	166	231	242	194	196	
15	385	238	159	128	396	235	170	185	281	259	216	219	
18	350	221	146	130	342	207	152	158	248	214	185	184	
21	314	204	134	132	287	180	135	132	215	168	147	149	
24	379	281	181	202	333	214	171	179	274	204	180	180	
27	380	293	204	199	303	204	167	199	268	187	163	161	
32	414	350	253	262	311	231	208	230	302	198	164	164	

[a]The media composition is as follows: (A):sulphur substrate with bacteria; (B): pyrite substrate with bacteria; (C):sulphur substrate without bacteria; (D):pyrite substrate without bacteria; (E):distilled water only; (F):9K media with neither substrate nor bacteria.

Table E3. pH changes

Bacterial leaching conditions: Nickel content 1.5%, 10% v/v mixed culture inoculum, pure 9K nutrient media, temperature 30°C, agitation speed 190 rpm.

Run 1

Time (days)	A				B				C	D	E	F	[a]Media Composition
	1.0	1.5	2.0	2.5	1.0	1.5	2.0	2.5	1.5	1.5	1.5	1.5	Initial pH
0	1.0	1.5	2.0	2.5	1.0	1.5	2.0	2.5	1.5	1.5	1.5	1.5	
3	1.16	1.65	2.14	2.35	1.17	1.68	2.14	2.15	1.66	1.71	1.72	1.68	
6	1.16	1.63	2.03	1.97	1.17	1.70	1.88	2.00	1.56	1.68	1.74	1.71	
9	1.20	1.58	1.86	1.68	1.20	1.64	1.89	1.91	1.73	1.66	1.80	1.76	
12	1.06	1.30	1.56	1.25	1.16	1.34	1.81	1.61	1.52	1.54	1.80	1.78	
15	0.89	1.03	1.21	0.97	1.16	1.19	1.39	1.26	1.26	1.45	1.84	1.82	
18	0.86	1.00	1.16	0.94	1.30	1.22	1.32	1.22	1.18	1.54	1.94	1.91	
21	0.80	0.90	1.05	0.84	1.22	1.07	1.22	1.08	1.02	1.55	1.96	1.92	
24	0.70	0.79	0.93	0.76	1.12	0.91	1.14	0.98	0.92	1.64	1.97	1.94	
27	0.82	0.84	0.99	0.85	1.16	0.95	1.19	1.03	0.98	1.49	2.07	2.07	
32	0.69	0.76	0.89	0.75	0.96	0.78	1.09	0.93	0.85	1.28	2.07	1.84	

[a]The media composition is as follows: (A):sulphur substrate with bacteria; (B): pyrite substrate with bacteria; (C):sulphur substrate without bacteria; (D):pyrite substrate without bacteria; (E):distilled water only; (F):9K media with neither substrate nor bacteria.

Run 2

Time (days)	A				B				C	D	E	F	[a]Media Composition
	1.0	1.5	2.0	2.5	1.0	1.5	2.0	2.5	1.5	1.5	1.5	1.5	Initial pH
0	1.0	1.5	2.0	2.5	1.0	1.5	2.0	2.5	1.5	1.5	1.5	1.5	
3	1.12	1.60	2.05	2.54	1.10	1.60	1.99	2.27	1.58	1.63	1.81	1.62	
6	1.11	1.63	2.07	2.38	1.11	1.63	1.97	2.16	1.57	1.60	1.86	1.70	
9	1.18	1.74	2.03	2.25	1.13	1.68	1.94	2.13	1.59	1.64	1.96	1.75	
12	1.17	1.69	1.92	2.05	1.15	1.65	1.91	2.12	1.61	1.61	1.98	1.78	
15	1.15	1.42	1.96	1.84	1.19	1.53	1.93	1.83	1.78	1.64	2.05	1.84	
18	1.08	1.26	1.75	1.67	1.28	1.42	1.81	1.66	1.64	1.68	2.09	1.89	
21	1.00	1.10	1.53	1.49	1.37	1.31	1.69	1.48	1.50	1.72	2.12	1.93	
24	0.91	0.96	1.32	1.33	1.34	1.20	1.45	1.37	1.33	1.98	2.15	1.95	
27	0.82	0.85	1.23	1.21	1.24	1.12	1.33	1.25	1.21	1.78	2.12	1.88	
32	0.80	0.84	1.11	1.12	1.13	1.01	1.24	1.23	1.15	1.37	2.20	1.82	

[a]The media composition is as follows: (A):sulphur substrate with bacteria; (B): pyrite substrate with bacteria; (C):sulphur substrate without bacteria; (D):pyrite substrate without bacteria; (E):distilled water only; (F):9K media with neither substrate nor bacteria.

Table E4. Redox potential changes (mV vs SHE)

Bacterial leaching conditions: Nickel content 1.5%, 10% v/v mixed culture inoculum, pure 9K nutrient media, temperature 30°C, agitation speed 190 rpm.

Run 1

Time (days)	A				B				C	D	E	F	[a]Media Composition
	1.0	1.5	2.0	2.5	1.0	1.5	2.0	2.5	1.5	1.5	1.5	1.5	Initial pH
0	607	577	548	518	607	577	547	518	577	576	578	576	
3	600	571	542	529	598	569	541	540	569	565	565	567	
6	591	563	539	542	588	557	547	540	565	558	555	557	
9	594	571	554	563	589	565	548	547	557	561	554	557	
12	594	579	565	582	587	576	550	561	566	565	550	551	
15	605	599	585	598	586	586	573	580	580	568	547	548	
18	606	597	588	600	578	583	576	582	584	564	541	543	
21	612	605	595	606	584	593	584	592	596	565	541	543	
24	617	612	603	612	592	604	590	600	604	561	542	544	
27	616	614	605	611	593	605	592	601	607	574	539	540	
32	619	615	608	615	602	613	595	604	608	583	537	551	

[a]The media composition is as follows: (A):sulphur substrate with bacteria; (B): pyrite substrate with bacteria; (C):sulphur substrate without bacteria; (D):pyrite substrate without bacteria; (E):distilled water only; (F):9K media with neither substrate nor bacteria.

Run 2

Time (days)	A				B				C	D	E	F	[a]Media Composition
	1.0	1.5	2.0	2.5	1.0	1.5	2.0	2.5	1.5	1.5	1.5	1.5	Initial pH
0	604	576	549	517	603	574	549	516	575	574	575	573	
3	590	561	535	504	588	559	536	520	560	557	546	557	
6	593	562	546	517	591	560	540	530	564	562	547	556	
9	591	557	540	529	590	559	543	533	564	561	542	554	
12	591	560	546	540	593	562	547	533	564	564	542	554	
15	594	576	544	551	589	569	546	553	554	562	538	551	
18	598	586	557	562	584	576	554	563	563	561	537	549	
21	601	595	570	573	579	583	561	573	572	559	535	546	
24	609	604	583	584	583	589	575	582	583	543	532	544	
27	611	608	586	588	586	592	580	586	587	553	533	548	
32	614	611	596	596	595	601	587	589	593	580	531	555	

[a]The media composition is as follows: (A):sulphur substrate with bacteria; (B): pyrite substrate with bacteria; (C):sulphur substrate without bacteria; (D):pyrite substrate without bacteria; (E):distilled water only; (F):9K media with neither substrate nor bacteria.

APPENDIX F

OPTIMISATION OF INFLUENTIAL FACTORS

"The million, million, million ... to one chance happens once in a million, million ... times no matter how surprised we may be that it results".

-R. A. Fisher

Table F1. Nickel concentrations (ppm)

Bacterial leaching conditions: Nickel content 1.5%, 10% v/v mixed culture inoculum, pure 9K nutrient media with sulphur substrate, temperature 30°C and agitation speed ≥200 rpm. The actual factor levels, coded as values of -λ, -1,0,+1,+λ were as follows: for pH (X_1): 1.0 (-λ), 1.5 (-1), 2.3 (0), 3.0 (+1), 3.5 (+λ); pulp density, % w/v (X_2): 2 (-λ), 5 (-1), 9 (0), 12 (+1), 15 (+λ); particle size, μm (X_1):<38 (-λ), 38-75 (-1), 75-106 (0), 106-150 (+1), 150-212 (+λ), λ=1.682

Run	Factors			Time (days)						
	X_1	X_2	X_3	0	3	6	11	16	21	26
1	-1	-1	-1	0	145	160	214	319	427	551
2	+1	-1	-1	0	92	132	184	268	376	487
3	-1	+1	-1	0	302	334	449	677	894	1149
4	+1	+1	-1	0	221	252	377	569	797	990
5	-1	-1	+1	0	195	218	254	315	412	525
6	+1	-1	+1	0	137	181	232	248	306	403
7	-1	+1	+1	0	417	453	564	610	782	921
8	+1	+1	+1	0	234	315	465	540	606	782
9	- λ	0	0	0	380	444	553	666	801	928
10	+ λ	0	0	0	156	227	310	491	722	983
11	0	- λ	0	0	55	72	106	162	226	270
12	0	+ λ	0	0	321	382	470	709	1069	1488
13	0	0	- λ	0	153	181	329	491	700	829
14	0	0	+ λ	0	194	229	277	318	423	593
15	0	0	0	0	207	250	330	511	717	915
16	0	0	0	0	205	233	344	506	699	936
17	0	0	0	0	207	234	327	471	600	759
18	0	0	0	0	210	235	308	474	639	816
19	0	0	0	0	202	231	345	512	671	827
20	0	0	0	0	199	229	302	411	562	739

Table F2. Nickel recoveries (%)

Bacterial leaching conditions: Nickel content 1.5%, 10% v/v mixed culture inoculum, pure 9K nutrient media with sulphur substrate, temperature 30°C and agitation speed ≥200 rpm. The actual factor levels, coded as values of -λ, -1,0,+1,+λ were as follows: for pH (X_1): 1.0 (-λ), 1.5 (-1), 2.3 (0), 3.0 (+1), 3.5 (+λ); pulp density, % w/v (X_2): 2 (-λ), 5 (-1), 9 (0), 12 (+1), 15 (+λ); particle size, μm (X_1):<38 (-λ), 38-75 (-1), 75-106 (0), 106-150 (+1), 150-212 (+λ), λ=1.682

Run	Factors			Time (days)						
	X_1	X_2	X_3	0	3	6	11	16	21	26
1	-1	-1	-1	0	18.9	20.8	27.8	41.6	55.6	71.7
2	+1	-1	-1	0	12.0	17.2	23.9	34.9	48.9	63.4
3	-1	+1	-1	0	16.6	18.4	24.7	37.2	49.1	63.1
4	+1	+1	-1	0	12.2	13.8	20.7	31.2	43.8	54.4
5	-1	-1	+1	0	25.4	28.4	33.1	40.9	53.6	68.3
6	+1	-1	+1	0	17.8	23.6	30.2	32.2	39.8	52.4
7	-1	+1	+1	0	22.9	24.9	31.0	33.5	42.9	50.5
8	+1	+1	+1	0	12.9	17.3	25.5	29.6	33.3	42.9
9	- λ	0	0	0	27.7	32.4	40.4	48.6	58.4	67.7
10	+ λ	0	0	0	11.4	16.6	22.6	35.8	52.7	71.7
11	0	- λ	0	0	17.5	22.8	33.3	51.0	71.2	85.1
12	0	+ λ	0	0	14.1	16.8	20.7	31.2	47.0	65.5
13	0	0	- λ	0	11.2	13.2	24.0	35.9	51.1	60.6
14	0	0	+ λ	0	14.1	16.7	20.2	23.2	30.9	43.3
15	0	0	0	0	15.1	18.3	24.1	37.3	52.4	66.8
16	0	0	0	0	15.0	17.0	25.1	36.9	51.1	68.3
17	0	0	0	0	15.1	17.1	23.9	34.4	43.8	55.4
18	0	0	0	0	15.4	17.1	22.5	34.6	46.7	59.5
19	0	0	0	0	14.8	16.9	25.2	37.4	49.0	60.4
20	0	0	0	0	14.6	16.7	22.0	30.0	41.0	53.9

Table F3. Confirmatory tests

Bacterial leaching conditions: Nickel content 1.5%, 10% v/v mixed culture inoculum, pure 9K nutrient media with sulphur substrate, temperature 30°C and agitation speed ≥200 rpm. The actual factor levels were as follows: pH = 2.0; pulp density = 2.6; particle size, μm = 53-75

Nickel concentrations (ppm)

Run	Time (days)						
	0	3	6	11	16	21	26
1	0	56	72	106	162	246	295
2	0	56	71	106	161	243	289
3	0	55	70	105	160	245	291
4	0	54	70	104	159	260	310

Nickel recoveries (%)

Run	Time (days)						
	0	3	6	11	16	21	26
1	0	14.1	18.4	26.6	41.9	62.4	74.9
2	0	14.0	18.3	26.8	40.9	61.5	73.2
3	0	13.8	18.0	26.4	40.3	61.0	72.6
4	0	13.5	17.7	25.8	39.5	63.5	75.7

APPENDIX G

STATISTICAL ANALYSIS

"A human being is the best computer available to place in a space ... It is also the only one that can be mass produced with unskilled labour".

-Werner von Braun

Determination of the accuracy of Varian SpectrAA-55B atomic absorption spectrophotometer analysis

The accuracy of the Varian SpectrAA-55B atomic absorption spectrophotometer for estimating nickel concentration was tested by comparing the mean of the ten samples with the known concentration of 2.000 ppm.

Table G1. Determination of the accuracy of the AAS

Sample number	Measured concentration of nickel (ppm)
1	2.091
2	2.007
4	2.016
5	1.995
6	2.012
7	2.005
8	1.948
9	1.973
10	2.002

$t_{calculated}$ is computed from equation G1 and compared with t_{table}. If $t_{calculated}$ is greater than t_{table} at the 99% confidence level, then the two results are considered to be different.

$$t_{calculated} = \frac{|\overline{x} - \text{known value}|}{s}\sqrt{n} \qquad \textbf{(G1)}$$

Known concentration	2.000
Mean, $\overline{x}$	2.001
Standard deviation, *s*	0.014
Number of observations, *n*	10
Degree of freedom, *n-1*	9

$$t_{calculated} = \frac{|2.001 - 2.000|}{0.013638}\sqrt{10} = 0.232$$

For α=0.001, the $t_{table} = 4.781$.

The $t_{calculated}$ is smaller than the t_{table}, therefore, the mean is a good estimate of the Ni concentration. At 99% confidence level, therefore, the Varian SpectrAA-55B atomic absorption spectrophotometer can be used to measure the nickel concentration of the samples with minimum error.

Determination of the accuracy of 744 Metrohm model pH meter analysis

The accuracy of the 744 Metrohm model pH meter for estimating pH was tested by comparing the mean of the ten standards having the same known pH of 4.00.

Table G2. Determination of the accuracy of the pH meter

Sample number	Measured pH
1	4.01
2	4.01
4	4.00
5	3.99
6	4.01
7	4.00
8	3.99
9	3.99
10	4.00

$t_{calculated}$ is computed from equation G1 and compared with t_{table}. If $t_{calculated}$ is greater than t_{table} at the 99% confidence level, then the two results are considered to be different.

$$t_{calculated} = \frac{|\overline{x} - \text{known value}|}{s}\sqrt{n} \qquad \textbf{(G1)}$$

Known pH	4.00	
Mean, $\overline{x}$		4.00
Standard deviation, *s*		0.009
Number of observations, *n*		10
Degree of freedom, *n-1*		9

$$t_{calculated} = \frac{|4.00 - 4.00|}{0.008660}\sqrt{10} = 0.00$$

For α=0.001, the $t_{table} = 4.781$.

The $t_{calculated}$ is smaller than the t_{table}, therefore, the mean is a good estimate of the pH. At 99% confidence level, therefore, the 744 Metrohm model pH meter can be used to measure the pH of the samples with minimum error.

APPENDIX H

STATISTICAL AND MATHEMATICAL METHODS

"One cannot escape the feeling that these mathematical formulae have an independent existence and an intelligence of their own, that they are wiser than we are, wiser even than their discoverers, that we get more out of them than we originally put into them".

-Henrich Hertz

Response Surface Methodology (RSM)

RSM is a mathematical and statistical technique which is useful for the modeling and analysis of problems in which a response of interest is influenced by several significant variables and the objective is to optimise this response (Myers and Montgomery, 2002; Montgomery, 2005; Baş and Boyaci, 2007). RSM attempts to analyse the effect of the independent variables, alone or in combination, on a specific dependent variable (response). Furthermore, RSM also generates a mathematical model (Myers and Montgomery, 2002). The graphical representation of the model has led to the coined term Response Surface Methodology (Myers and Montgomery, 2002). The independent variables are presumed to be measurable and continuous, and can be controlled with negligible error, where as the response is postulated to be a random variable (Oraon et al., 2006).

In general, the relationship between the response and the independent variables is

$$\eta = f(x_1, x_2, \ldots, x_k) + \varepsilon, \qquad \text{(H1)}$$

where, η is the response; f is the unknown function of the true response function (or response surface); $x_1, x_2, \ldots, x_k$ represent experimental variables, also called natural variables because they are expressed in the natural units of measurement, such as degrees Celsius, pounds per square inch, etc (Carley et al., 2004); k is the number of independent variables; ε is the term that represents other sources of variability not accounted for by f. Usually ε includes effects such as measurement error on the response, background noise, the effects of other variables, and so on. ε is treated as a statistical error, often assumed to have normal distribution with mean zero and common variance (Carley et al., 2004; Baş and Boyaci, 2007).

For most of the response surfaces, the functions for the approximations are polynomials because of simplicity, though the functions are not limited to the polynomials (Hu et al., 2008). For the case of quadratic polynomials (second order models), the response surface can be represented as follows (Hu et al., 2008):

$$y = \beta_0 + \sum_{i=1}^{k} \beta_i X_i + \sum_{i=1}^{k} \beta_{ii} X_i^2 + \sum_{i=1}^{k} \sum_{j=i+1}^{k} \beta_{ij} X_i X_j + \varepsilon \qquad \text{(H2)}$$

where y is the predicted response, β_0 is the coefficient for intercept, β_i is the coefficient of linear effect, β_{ii} is the coefficient of quadratic effect, β_{ij} is the coefficient of interaction effect, k is the number of variables, and X_i and X_j are coded independent variables.

The quadratic model has a constant term, k-first order terms, k-quadratic terms, and $k(k-1)/2$ interaction terms and thus, has a total of $p = (k+1)(k+2)/2$ terms (Draper and Lin, 1990).

In the case where the total number of experiments is N, the response surface can be expressed as follows using the matrix notation (Khuri and Cornell, 1987):

$$y = X\beta + \varepsilon$$

$$\begin{bmatrix} y_1 \\ y_2 \\ . \\ . \\ . \\ y_n \end{bmatrix} = \begin{bmatrix} 1 & x_{11} & x_{12} & . & . & . & x_{1k} \\ 1 & x_{21} & x_{22} & . & . & . & x_{2k} \\ . & . & . & . & . & . & . \\ . & . & . & . & . & . & . \\ . & . & . & . & . & . & . \\ 1 & x_{n1} & x_{n2} & . & . & . & x_{nk} \end{bmatrix} \begin{bmatrix} \beta_0 \\ \beta_1 \\ . \\ . \\ . \\ \beta_k \end{bmatrix} + \begin{bmatrix} \varepsilon_1 \\ \varepsilon_2 \\ . \\ . \\ . \\ \varepsilon_n \end{bmatrix} \qquad \text{(H3)}$$

y X β ε

where y is an N x 1 vector of the observations; X is an N x (k+1) matrix of the levels of the independent variables; β is a (k+1) x 1 vector of the estimates of the regression coefficients; ε is an N x 1 vector of random errors.

The equations given above are solved using the method of least squares which is a multiple regression technique. The difference between the observed and the fitted values for the ith observation $\varepsilon_i = y_{i,\exp} - y_{i,cal}$ is called the residual and is an estimate of the corresponding ε_i, where ε_i is the residual, $y_{i,\exp}$ is the observed values, $y_{i,cal}$ is the predicted values.

The criterion for choosing the regression coefficient estimates (β_i) is that they should minimize the sum of the squares of the residuals, which is often called the sum of squares of the errors denoted as SS_E. Thus (Baş and Boyaci, 2007),

$$SS_E = \sum_{i=1}^{N} \varepsilon_i^2 = \sum_{i=1}^{N} (y_{i,\exp} - y_{i,cal})^2 \qquad \text{(H4)}$$

The residuals may be written as $\varepsilon = y - X\beta$ (refer to Equation H3). Therefore, the least squares estimates of the elements of β in Equation H3 are given as (Baş and Boyaci, 2007):

$$\beta = (X^T X)^{-1} X^T y \qquad \text{(H5)}$$

where X^T is the transpose of X ; $(X^T X)^{-1}$ is the inverse of $(X^T X)$.

After the regression coefficients have been obtained, the estimated response can then be easily calculated by substitution into the second order model Equation (H2).

Central Composite Rotatable Design (CCRD)

The experimental design techniques commonly used for the process analysis and modeling of response surfaces for second order designs are the full factorial, partial factorial and central composite rotatable designs (Obeng et al., 2005). If the design is rotatable as in the case of the CCRD, the variance of the predicted response, y, remains constant at all points, which are equidistant from the design centre and is not a function of direction (Khuri and Cornell, 1987; Montgomery, 2005). The CCRD is an effective second order design which was pioneered in 1951 by Box and Wilson and later improved upon in 1957 by Box and Hunter. It is useful than the full factorial designs, since it requires much fewer tests, but is shown to be sufficient to describe the responses (Obeng et al., 2005).

The CCRD involves the use of three portions, (i) 2^k factorial (or a $2^{(k-q)}$ fractional factorial with resolution V) portion with its origin at the centre (conventionally called a cube with ±1 being the factorial levels) allowing estimates of first order effects or first order + two factor interactions; (ii) $2k$ axial or star points fixed axially at a distance λ from the origin representing a one factor-at-a-time portion designed to generate the pure quadratic terms, $\beta_{ii} x_i^2$, in Equation (H2) (Myers et al., 1989); (iii) and n_c replicate points at the centre to provide information about the existence of the curvature in the system and stabilizes, the variance of the predicted response (Myers and Montgomery, 2002; Montgomery, 2005; Draper and Lin, 1990), and provide an independent estimate of experimental error (Myers and Montgomery, 2002; Montgomery, 2005; Obeng et al., 2005). Thus, there is a total of 2^k (or $2^{(k-q)}$) + $2k + n_c$ points in the design; where k is the number of factors to be studied.

The axial points are chosen so that they allow rotatability (Box and Hunter, 1957) which ensures that the variance of the model prediction is constant at all points equidistant from the design centre. A value of $\lambda = (2^{k-q})^{1/4}$ guarantees rotatability despite the number of centre points (Myers et al., 1989; Myers and Montgomery, 2002); where 2^{k-q} specifies a two level design on k factors and the $-q$ represents the fraction of the number of factors (where $q = 0$ for full factorial design).

The number of centre point replications, n_c, can also be chosen to cause a CCRD to have the variance of the predicted response, y, remaining constant at all points which

are equidistant from the design centre, such that for three factors (Khuri and Cornell, 1987),

$$n_c \approx 0.8385\left(2^{k/2} + 2\right)^2 - 2^k - 2k \quad \text{(H6)}$$

The number of centre points should never be less than 5; in fact replication of centre points must be two times the number of factors ($2k$), but capping the number at ten (Anderson and Whitcomb, 2005).

The units of the independent variables differ from one another. Since parameters have different units and/or ranges in the experimental domain, the regression analysis should only be performed once the parameters have been normalized. Once the desired ranges of values of the variables are defined, they are then coded. Coding ensures that all the variables affect the response more evenly, and so, the units of the parameters are irrelevant (Montgomery, 2002). In general, the factorial points are designed such that the nth column consists of 2^{n-1} minus signs followed by 2^{n-1} plus signs (Box et al, 1978). The n_c centre points are defined as (0, 0, 0, … 0). The axial or star points with their levels are designed as follows (Myers and Montgomery, 2002):

X_1	X_2	…	X_k	
$-\lambda$	0	…	0	
$+\lambda$	0	…	0	
0	$-\lambda$	…	0	(H7)
0	$+\lambda$	…	0	
.	.	…	.	
0	0	…	$-\lambda$	
0	0	…	$+\lambda$	

Relationships between coded and actual values of the variables in a CCRD are calculated as given in Table 7.1 (i.e in Chapter 7) in accordance with Napier-Munn (2000). A convenient formula derived through interpolation for converting the coded variable, x_i, is given as, follows:

$$X_i = X_{iH} - \frac{(X_{iH} - X_{iL})(x_{iH} - x_i)}{(x_{iH} - x_{iL})} \quad , i = 1, 2, 3 \quad \text{(H8)}$$

where X_{iL} and X_{iH} are the actual low and high levels of X_i, respectively, x_{iL} and x_{iH} are the coded low and high levels of X_i, respectively, and x_i is the coded variable that is being converted.

Model validation

Following the program of experimentation and after the regression coefficients have been obtained, the adequacies of the models are checked using the analysis of variance (ANOVA) technique (Khuri and Cornell, 1987). ANOVA is a statistical method that can be used to quantify the significant differences between factors and levels. It compares the magnitude of the estimated effects of factors with the magnitude of experimental error (Keller, 2001). If the magnitude of a factor effect is large when compared with the experimental error, it is decided that the changes in the selected response can not occur by chance and, therefore, those changes in the response can be considered to be the effects of the factors. The factors causing a variation in the response are called significant. The results of the analysis are displayed in a tabular format.

Total Sum of Squares
The total variation in a set of data is called the *Total Sum of Squares*. It is computed by summing the squares of the deviations of the observed $y_{i,\exp}$'s about their average value, $\overline{y} = (y_1 + y_2 + ... + y_N)/N$ (Khuri and Cornel, 1987),

$$SS_T = \sum_{i=1}^{N} \left(y_{i,\exp} - \overline{y} \right)^2 \qquad \text{(H9)}$$

The quantity SS_T is associated with $N-1$ degrees of freedom.

The square term is used as a means of factoring out whether the sample is below or above the mean. If the square is not taken, variations below the mean may cancel variation above the mean to make it seem as if there is no variation (Keller, 2001).

The total sum of squares can be partitioned into two parts; the sum of squares due to regression (sum of squares explained by the fitted model) and the sum of squares unaccounted for by the fitted model.

Sum of Squares of Regression
The formula for calculating the sum of squares due to regression (SS_R) is

$$SS_R = \sum_{i=1}^{N}\left(y_{i,cal} - \overline{y}\right)^2 \quad \text{(H10)}$$

The deviation $y_{i,cal} - \overline{y}$ is the difference between the value predicted by the model for the i^{th} observation and the overall average of the observed, $y_{i,exp}$'s. If the model contains *p*-parameters, then the degree of freedom associated with SS_R is *p-1*.

Sum of Squares of Errors
Khuri and Cornell (1987) give the sum of squares unaccounted for by the fitted model or sum of squares of residuals or errors (SS_E) as

$$SS_E = \sum_{i=1}^{N}(y_{i,exp} - y_{i,cal})^2 \quad \text{(H11)}$$

The deviation $y_{i,exp} - y_{i,cal}$ is the difference between the observed value and value predicted by the model for the i^{th} observation. The number of degrees of freedom of SS_E is *N-p*.

Determination of SST, SS_R, and SS_E using matrices
Using matrix notation and letting O be a *1 x N* vector of ones, the quickest methods for calculating SS_T, SS_R, and SS_E are given as (Khuri and Cornell, 1987),

$$\begin{aligned} SS_T &= y^T y - \frac{(Oy)^2}{N} \\ SS_R &= \beta^T X^T y - \frac{(Oy)^2}{N} \\ SS_E &= y^T y - \beta^T X^T y \end{aligned} \quad \text{(H12)}$$

where y is an N *x 1* vector of the observations; X is an N x (k+1) matrix of the levels of the independent variables; β is a *(k+1) x 1* vector of the estimates of the regression coefficients; y^T, X^T and β^T refers to the transpose of y, X and β, respectively.

Test of lack of fit of the fitted model
A procedure for checking the adequacy of the fitted model is called testing lack of fit of the fitted model (Khuri and Cornell, 1987). The fitted model is inadequate or is lacking in fit when it does not contain sufficient number of terms due to the omission of factors (other than those in the proposed model) that affect the response, and/or,

omission of higher-order terms involving the factors in the proposed model. The inability of the fitted model (Equation H2) to adequately account for the variation in the observed response values is reflected in the portion of the total variation that is called residual variation or the variation unaccounted for by the fitted model (Khuri and Cornell, 1987; Myers and Montgomery, 2002; Montgomery, 2005).

Isolating the portion of the residual variation that is directly attributed to underfitting the true surface with the fitted model is necessary in order to test for adequacy of the fitted model. The residual sum of squares, SS_E, can be partitioned into two sources of variation; (1) the variation among the replicates at the design points where replicates have been collected, and (2) variations arising from lack of fit of the fitted model. The sum of squares due to replicate observations is called the sum of squares due to pure error (SS_{PE}). In other words, it is the sum of squares of differences between all the individual experimental values and the average of the experimental values at the same level. Once SS_{PE} is calculated, it is then subtracted from the SS_E to produce the sum of squares due to lack of fit (SS_{LOF}).

SS_{PE} can also be calculated from the replicated centre points of the experiments (Myers and Montgomery, 2002; Montgomery, 2005) as given below:

$$SS_{PE} = \sum_{centre-points} (Y_{c,i} - \bar{Y}_c)^2 \qquad \text{(H13)}$$

where $Y_{c,i}$ are the observations of the centre points, $\bar{Y}_C$ is the average of the observations of the n_c runs at the centre.

The number of degrees of freedom associated with SS_{PE} in this case is n_c-*1*. By subtraction, the sum of squares due to lack of fit is then calculated as:

$$SS_{LOF} = SS_E - SS_{PE} \qquad \text{(H14)}$$

The test of the null hypothesis of adequacy of fit (or lack of fit is zero) involves calculating the value of the Fisher's variance ratio test (*F-test*):

$$F = \frac{SS_{LOF}/(N - p - n_c + 1)}{SS_{PE}/(n_c - 1)} \qquad \text{(H15)}$$

where n_C is the number of replicates of centre points, p is the number of terms in the fitted model, N is the number of observations. $N - p - n_c + 1$ is the degree of freedom for SS_{LOF}.

The calculated value is then compared with the standard table value of *F* ratio for the desired level of confidence; α. Lack of fit exists at α level of significance if the calculated value of *F* exceeds the standard table value, $F_{\alpha,N-p-n_c+1,n_c-1}$ (Khuri and Cornell, 1987). If not, the model can be accepted at the desired confidence level as providing an adequate representation of the data.

Test for significance of regression

The test for significance of regression is a test to determine whether a linear relationship exists between the response variable, *y,* and the regression coefficients, β_i (Montgomery, 2005). The usual test of the significance of the fitted regression equation is a test of the null hypothesis, H_0: all values of β_i (excluding β_0) are zero. The alternative hypothesis is, H_a: at least one value of β_i (excluding β_0) is not zero. Assuming normality of the errors, the test of H_0 involves first calculating the value of the F-statistic,

$$F = \frac{\text{Mean Square Regresssion}}{\text{Mean Square Residual}} = \frac{SS_R/(p-1)}{SS_E/(N-p)} \quad \text{(H16)}$$

If the null hypothesis is true, then the *F-statistic* Equation (H16) follows an F-distribution with *p-1* and *N-p* degrees of freedom under the ν_1 (numerator) and ν_2 (denominator) *F-distribution*, respectively, where *p* is the number of terms in the fitted model, *N* is the number of observations. The second step of the test of H_0 is to compare the calculated values of *F* to the standard table value, $F_{\alpha,p-1,N-p}$, for the desired level of confidence, α, with *p-1* and *N-p* degrees of freedom for upper and lower, respectively. If the calculated value of *F* exceeds the standard table value, $F_{\alpha,p-1,N-p}$, then the null hypothesis is rejected at α level of significance and it is therefore inferred that the variation accounted for by the model (through the values of β_i, i ≠ 0) is significantly greater than the unexplained variation. In other words, the regression is significant if the calculated *F-value* is greater than the value obtained from standard table. A confidence level is typically set at $\alpha = 0.05$. This signifies that the criterion is (1-α) or 95% accurate.

It must be noted, however, that this *F-test* is only valid for models for which there is no evidence of lack of fit.

Coefficient of determination and Absolute Average Deviation
An accompanying statistic to the *F-test* of Equation (H16) is the coefficient of determination:

$$R^2 = \frac{SS_R}{SS_T} \qquad \text{(H17)}$$

The value of R^2 is a measure of the proportion of the total variation of the values of $y_{i,exp}$ about the mean $\bar{y}$ explained by the fitted model (Khuri and Cornel, 1987). Although this coefficient is a measure of how close the model fits the data, it can not be used to judge model lack of fit because it does not take into account the number of degrees of freedom for model determination. In fact, a large value of R^2 does not necessarily mean that the regression model is a good one since addition of a variable to the model will always increase R^2 regardless of whether the additional variable is statistically significant or not. Thus, it is possible for models that have large values of R^2 to yield poor predictions of new observations or estimates of the new response (Montgomery, 2005).

These types of errors can be eliminated by using the absolute average deviation (AAD) analysis, which is a direct method for describing the deviations (Baş and Boyaci, 2007). The AAD is calculated by the following equation:

$$AAD = \left\{ \left[\sum_{i=1}^{N} (| y_{i,exp} - y_{i,cal} | / y_{i,exp}) \right] / N \right\} x\ 100 \qquad \text{(H18)}$$

where $y_{i,exp}$ and $y_{i,cal}$ are the experimental and calculated responses, respectively, and N is the number of experimental runs.

Evaluation of R^2 and *AAD* together is a better way of checking the adequacy of the model. R^2 must be close to 1.0 and *AAD* between the predicted and the observed data must be as small as possible. The acceptable values of R^2 and *AAD* values mean that the model equation defines the true behaviour of the system and it can be used for interpolation in the experimental domain, but, care must be taken about extrapolating beyond the region containing the original observations (Baş and Boyaci, 2007).

Test of hypothesis concerning individual parameters in the model
This test looks at the specific effects of the factors used in an experiment. The test of hypothesis concerning individual parameters in the model is performed by comparing the parameter estimates in the fitted model to their respective estimated standard errors (Khuri and Cornell, 1987). The test of the null hypothesis, $H_0 : \beta_i = 0$, is

performed by calculating the value of the test statistic and comparing the value of *t* in Equation (H19) against a standard table value, t_α, from the t-tables:

$$t = \frac{\beta_i}{\text{est.s.e}\,(\beta_i)} \qquad \text{(H19)}$$

where β_i is the least squares estimate of coefficients, est.s.e. (β_i) is the estimated standard errors of coefficient β_i.

The estimated standard errors are the positive square roots of the products of the diagonal elements of $(X^T X)^{-1}$ and the mean sum of squares for residuals (errors), MS_E (Khuri and Cornell, 1987).

The choice of table value, t_α, depends on the alternative hypothesis, H_a, the level of significance, α, and the degree of freedom for *t* in Equation (H19). If the alternative hypothesis is, $H_a : \beta_i \neq 0$, the test is called two-sided test, and the value of t_α is taken from the column corresponding to $t_{\alpha/2}$ in the standard table.

If, on the other hand, the alternative hypothesis is $H_a : \beta_i > 0$ or $H_a : \beta_i < 0$, the test is a one sided, and the value of t_α is taken from the column for t_α in the table. The degree of freedom for *t* in Equation (H19) is the degree of freedom of SS_E used in Equation (H11).

If the absolute value of *t*, $|t|$, in Equation (H19) exceeds the standard table value, $t_{\alpha,N-p}$, then the null hypothesis, H_0, is rejected in favour of the alternative, H_a, (Khuri and Cornell, 1987; Montgomery, 2005); meaning the model coefficient is statistically significant.

Determining the Coordinates of the Stationary Point

After the fitted model is checked for adequacy of fit in the region defined by the coordinates of the design and is found to be adequate, the model is then used to locate the coordinates of the stationary point (Khuri and Cornell, 1987). To obtain the coordinates of the stationary point, the fitted second order model in k-variables is written in matrix notation (Khuri and Cornell, 1987; Myers and Montgomery, 2002; Montgomery, 2005) as:

$$\hat{y}(x) = \beta_0 + x'b + x'\beta x \qquad \text{(H20)}$$

where

$$x = \begin{bmatrix} x_1 \\ x_2 \\ . \\ . \\ . \\ x_k \end{bmatrix} \qquad b = \begin{bmatrix} \beta_1 \\ \beta_2 \\ . \\ . \\ . \\ \beta_k \end{bmatrix} \quad \text{and} \quad \beta = \begin{bmatrix} \beta_{11} & \frac{\beta_{12}}{2} & \cdots & \frac{\beta_{1k}}{2} \\ & \beta_{22} & \cdots & \frac{\beta_{2k}}{2} \\ & & . & . \\ & & . & . \\ & & . & . \\ \text{(symmetric)} & & & \frac{\beta_{k-1,k}}{2} \\ & & & \beta_{kk} \end{bmatrix}$$

The elements of the k x 1 vector b are the estimated coefficients of the first order terms of Equation (H20), and the elements of the k x k symmetric matrix β are the estimated coefficients of the second order terms in Equation (H20). The partial derivatives of $\hat{y}(x)$ with respect to x_1, x_2, … and x_k are

$$\left.\begin{aligned} \frac{\partial \hat{y}(x)}{\partial x_1} &= \beta_1 + 2\beta_{11}x_1 + \sum_{i=2}^{k} \beta_{1i}x_i \\ \frac{\partial \hat{y}(x)}{\partial x_2} &= \beta_2 + 2\beta_{22}x_2 + \sum_{i\neq 2}^{k} \beta_{2i}x_i \\ &. \\ &. \\ &. \\ \frac{\partial \hat{y}(x)}{\partial x_k} &= \beta_k + 2\beta_{kk}x_k + \sum_{i=2}^{k-1} \beta_{ki}x_i \end{aligned}\right\} = b + 2Bx \qquad \text{(H21)}$$

Setting each of the k derivatives equal to zero and solving for the values of x_i, the coordinates of the stationary point are the values of the elements of the k x 1 vector x_s given by:

$$x_s = -\frac{\beta^{-1}b}{2} \qquad \text{(H22)}$$

where β^{-1} is the inverse of the matrix β in equation H20.

The predicted response at the stationary point is given as

$$\begin{aligned} \hat{y}_s &= \beta_0 + x_s'b + x_s'\beta x_s \\ &= \beta_0 + \frac{1}{2}x_s'b \end{aligned} \qquad \text{(H23)}$$

Nature of the Stationary Point (Canonical analysis)

The nature of the response surface system or stationary point (maximum, minimum, or saddle point) depends on the signs and magnitudes of the coefficients in the model of Equation (H2) (Myers and Montgomery, 2002). The second order coefficients (interaction and pure quadratic terms) play a vital role. The nature of the stationary point is determined from the signs of the eigenvalues of the matrix β (Myers and Montgomery, 2002). The eigenvalues, γ_i, represent the coefficients of the W_i^2 terms in the canonical equation:

$$\hat{y} = \hat{y}_s + \sum_{i=1}^{k} \gamma_i W_i^2 \qquad \text{(H24)}$$

where $\hat{y}$ is the predicted response, $\hat{y}_s$ is the estimate of the response at the stationary point, $\hat{y}_s$, W_i are the principal axes of the response system.

Derivation of the Canonical Equation.
The first step in developing the canonical equation for a k-variable system is to translate the origin of the system from the centre of the design to the stationary point, that is, to move ($x_1, x_2, \ldots, x_k$) = (0,0,…, 0) to x_s (Khuri and Cornell, 1987). This is done by defining the intermediate variables ($z_1, z_2, \ldots, z_k$)′ = ($x_1 - x_{1s}, x_2 - x_{2s}, \ldots, x_k - x_{ks}$)′ or $z = x - x_s$. Then, the second order response equation (H20) is expressed in terms of the values of z_i as

$$\begin{aligned} \hat{y}(z) &= \beta_0 + (\mathrm{z}+x_s)'b + (\mathrm{z}+x_s)'\beta(\mathrm{z}+x_s) \\ &= \left[\beta_0 + x_s'b + x_s'\beta x_s\right] + \mathrm{z}'b + \mathrm{z}'\beta\mathrm{z} + 2x_s'\beta\mathrm{z}, \\ &= \hat{y}_s + z'\mathrm{B}\,z \end{aligned} \qquad \text{(H25)}$$

where $2x_s'\beta z = -z'b$ from equation (H22).

Equation (H25) shows that in the intermediate variables, the predicted response is a linear function of the estimate of the response at the stationary point, $\hat{y}_s$, plus a quadratic form in the values of z_i. The axes of the values of z_i are aligned with the corresponding axes of x_i.

Now, to obtain the canonical form of the predicted response, let a set of variables $W_1, W_2, \ldots, W_k$ defined such that $(W_1, W_2, \ldots, W_k)'$ is given by

$$W = M' z \qquad \text{(H26)}$$

where M is a k x k orthogonal matrix whose columns are the normalized eigenvectors associated with eigenvalues of matrix β.

The matrix M has the effect of diagonalising β, that is, $M'\beta M = \text{diag}(\gamma_1, \gamma_2, \ldots, \gamma_k)$, where $\gamma_1, \gamma_2, \ldots, \gamma_k$ are the corresponding eigenvalues of β. The axes associated with $W_1, W_2, \ldots, W_k$ are the principal axes of the response system. The transformation in Equation (H26) is a rotation of the z_i axes to form the W_i axes.

To express Equation (H25) in the W_i variables, the quadratic form $z' \beta z$ is written as:

$$\begin{aligned} z' \beta z &= W'M'\beta MW \\ &= \gamma_1 W_1^2 + \gamma_2 W_2^2 + \ldots + \gamma_k W_k^2 \end{aligned} \qquad \text{(H27)}$$

The eigenvalues γ_i represent the coefficients of the W_i^2 terms in the canonical equation:

$$\hat{y} = \hat{y}_s + \sum_{i=1}^{k} \gamma_i W_i^2 \qquad \text{(H28)}$$

In the MATLAB R2006a software, the code for calculating the eigenvalues of β is, eig(β) (Griffiths, 2005).

The signs of the eigenvalues (γ_i) determine the nature of the stationary point (x_s). If $\gamma_1, \gamma_2, \ldots, \gamma_k$ are all negative, the stationary point is a point of maximum response.

If $\gamma_1, \gamma_2, \ldots, \gamma_k$ are all positive, the stationary point is a point of minimum response. If $\gamma_1, \gamma_2, \ldots, \gamma_k$ are mixed in signs, the stationary point is a saddle point of the fitted surface.

Sometimes it is also necessary to use constrained optimization (Ridge analysis) to arrive at the potential operating conditions when the stationary point is a saddle point or point of maximum or minimum response that resides well outside the experimental region, or where several response variables must be considered (Myers and Montgomery, 2002).

Ridge Analysis

This section briefly sets forth the strategy of the ridge analysis, the term that was first used by Hoerl in 1959. When the location of a stationary point is a saddle or is outside the experimental region, a search for the optimal value $\hat{y}$ is possible by the method of ridge analysis (Myers, 1971; Khuri and Cornell, 1987; Myers and Montgomery, 2002). In general, this method is used to finding the absolute maximum or minimum of $\hat{y}$ on concentric spheres of varying radii, R_i (i=1,2, …) which are centred at $(x_1, x_2, \ldots, x_k) = (0, 0, \ldots, 0)$ and are contained within the experimental region (Khuri and Cornell, 1987).

Given the fitted second order response surface model of Equation (H20) over the region of the k - coded variables $(x_1, x_2, \ldots, x_k)$ as,

$$\hat{y} = \beta_0 + x'b + x'\beta x$$

If the coordinates of the variables that maximize $\hat{y}$ are restricted to the point lying on the boundary of a sphere of radius R, then the constraint becomes,

$$\sum_{i=1}^{k} x_i^2 = R^2 \qquad \text{(H29)}$$

To maximize $\hat{y}$ in Equation (H20) subject to the constraint of Equation (H29), the function below is considered in accordance with the theorem by Kaplan (1952),

$$F = \hat{y} - \mu(x'x - R^2) \qquad \text{(H30)}$$

or $$F = \beta_0 + x'b + x'\beta x - \mu(x'x - R^2)$$

where μ is the Lagrangian multiplier and $x' = (x_1, x_2, \ldots, x_k)$.

Differentiating Equation (H30) with respect to x_i, gives

$$\frac{\partial F}{\partial x} = b + 2\beta x - 2\mu x \qquad \text{(H31)}$$

Equating Equation (H31) to zero, and solving for x gives,

$$(\beta - \mu I_k)x = -\frac{b}{2} \qquad \text{(H32)}$$

or $$x = -(\beta - \mu I_k)^{-1}\left(\frac{b}{2}\right)$$

where I is the identity matrix.

Predetermined values of μ can be inserted into Equation (H32), then solve for x_1, x_2, …, x_k, compute R from Equation (H29), and $\hat{y}$ from Equation (H20). However, it must be noted that the nature of the stationary point depends on the value of μ chosen (Myers, 1971; Khuri and Cornell, 1987).

The choice of the value of μ for generating a particular type of stationary point

To help in the development of the properties of the stationary points, a well known mathematical theorem (Kaplan, 1952) is given here by considering the stationary points of a function $f(x_1, x_2, ..., x_k)$ of k - variables, subject to the n constraints.

$$h_j(x_1, x_2, ..., x_k) = 0 \qquad (j = 1, 2, ..., n) \qquad \text{(H33)}$$

The function, F, is first formed as follows,

$$F = f(x_1, x_2, ..., x_k) - \sum_{j=1}^{n} \mu_j h_j(x_1, x_2, ..., x_k) \qquad \text{(H34)}$$

where the μ_j are Lagrange multipliers.

Differentiating Equation (H34) partially with respect to x_i and setting the results equal to zero produces the k equations as,

$$\frac{\partial F}{\partial x_i} = \frac{\partial f(x_1, x_2, ..., x_k)}{\partial x_i} - \sum_{j=1}^{n} \mu_j \frac{\partial h_j(x_1, x_2, ..., x_k)}{\partial x_i} = 0 \qquad (i = 1, 2, \ldots, k) \qquad \text{(H35)}$$

Equations (H33) and (H35) represent $n+k$ equations in a like number of unknowns. These equations can be solved for the values of x_1, x_2, …, x_k and $\mu_1, \mu_2, \ldots, \mu_n$. However, the values of $\mu_1, \mu_2, \ldots, \mu_n$ are not of interest except to use them for calculating the values of x_1, x_2, …, x_k. Therefore, these equations can be solved for the x_i by first eliminating the values of μ_j rather than calculate values for μ_j. If $x' = a' = (a_1, a_2, \ldots, a_k)$ is the solution of equations (H33) and (H35) after the elimination of μ_j, then the properties of the symmetric matrix

$$M(x) = \begin{bmatrix} \partial^2 F/\partial x_1^2 & \partial^2 F/\partial x_1 \partial x_2 & \ldots & \partial^2 F/\partial x_1 \partial x_k \\ & \partial^2 F/\partial x_2^2 & \ldots & \partial^2 F/\partial x_2 \partial x_k \\ & & \ldots & \ldots \\ & & & \partial^2 F/\partial x_k^2 \end{bmatrix} = 2(\beta - \mu I_k) \quad \text{(H36)}$$

evaluated at $x_1 = a_1, x_2 = a_2, \ldots, x_k =$, determine the nature of the stationary point $a_1, a_2, \ldots, a_k$. In particular,

1. If $M(a)$ is positive definite, that is, if $d' M(a) d > 0$, for all d where d is any none zero k x 1 real vector, then the solution is a local minimum for $f(x_1, x_2, ..., x_k)$.
2. If $M(a)$ is negative definite, that is, if $d' M(a) d < 0$, for all $d \neq 0$, then the solution is a local minimum for $f(x_1, x_2, ..., x_k)$.
3. If $M(a)$ is indefinite, further investigations of the mean response near the point $x_i = a_i$ is required to determine what sort of stationary point has been obtained.

Several results regarding the value of μ and the corresponding values of x_1, x_2, …, x_k, of R and $\hat{y}$ are stated below (Myers, 1971) and some of the proofs to the theorems are outlined in Myers (1971).

Result 1. If one considers two solutions of equation (H32), $x_1' = (a_1, a_2, \ldots, a_k)$ for $\mu = \mu_1$ and $x_2' = (c_1, c_2, \ldots, c_k)$ for $\mu = \mu_2$ resulting in estimates $\hat{y}_1$ and $\hat{y}_2$ on the spheres of radii R_1 and R_2, respectively. Then if $R_1 = R_2$ and $\mu_1 > \mu_2$, then $\hat{y}_1 > \hat{y}_2$. The results essentially says for two stationary points that are the same distance from the design centre, the response estimate will be larger for that stationary point corresponding to the larger value of μ.

Result 2. If $R_1 = R_2$, and $M(x_1)$ is positive definite but $M(x_2)$ is indefinite, then $\hat{y}_1 < \hat{y}_2$.

Result 3. If μ_1 is the chosen value of μ in equation (H32) with x_1 being the resulting solution, and R_1 the corresponding radius, then if $\mu_1 > \gamma_i$ (all i), where γ_i is the i^{th} eigenvalues of β, then x_1 is a point at which $\hat{y}$ attains a local maximum on R_1. On the other hand, when $\mu_1 < \gamma_i$ (all i), then x_1 is a point at which $\hat{y}$ attains a local minimum on R_1.

It must be noted also that the radii of the solution to equation (H32) should fall in the interval $0, R_b$, where R_b is the radius approximately representing the boundary of the experimental region (Myers and Montgomery, 2002).

Evaluation of the inverse matrix, A^{-1}

Essentially in finding the inverse of a matrix, the evaluation $AA^{-1} = I$ must be solved where I is the unit matrix. In order to examine the procedure two other forms of matrix must be looked at.

Cofactor matrix, A^c

This matrix is formed by replacing every element of the original matrix by its corresponding cofactor. The cofactor of a particular term in a determinant is simply the respective minor given a positive or negative sign. The rule for obtaining the sign is such that, if the sum of the column and the row of the element considered is even the sign of the cofactor is positive and, if the sum of the column and the row of the element considered is odd the sign of the cofactor is negative. A minor is the determinant obtained by ignoring the row and column in which an element appears.

Adjoint matrix, A^a

The adjoint matrix is the transpose of the cofactor matrix.

The inverse of a matrix is equal to its adjoint matrix divided by its determinant (Smith, 1971),

$$A^{-1} = \frac{A^a}{|A|} \qquad \text{(H37)}$$

where $|A|$ is the determinant of matrix A.

Definitions

1. A diagonal matrix is a square matrix whose off diagonal elements, m_{ij}, $i \neq j$, are zero.
2. An identity matrix I is a diagonal matrix with ones on the diagonal.

APPENDIX I

MATLAB PROGRAMS

"A mathematician is a machine for turning coffee into theorems".

-Paul Erdös

Program for determining the regression coefficients in a fitted model

```
X=[1 -1 -1 -1 1 1 1 1 1 1;
   1 1 -1 -1 1 1 1 -1 -1 1;
   1 -1 1 -1 1 1 1 -1 1 -1;
   1 1 1 -1 1 1 1 1 -1 -1;
   1 -1 -1 1 1 1 1 1 -1 -1;
   1 1 -1 1 1 1 1 -1 1 -1;
   1 -1 1 1 1 1 1 -1 -1 1;
   1 1 1 1 1 1 1 1 1 1;
   1 -2^(3/4) 0 0 2^(3/2) 0 0 0 0 0;
   1 2^(3/4) 0 0 2^(3/2) 0 0 0 0 0;
   1 0 -2^(3/4) 0 0 2^(3/2) 0 0 0 0;
   1 0 2^(3/4) 0 0 2^(3/2) 0 0 0 0;
   1 0 0 -2^(3/4) 0 0 2^(3/2) 0 0 0;
   1 0 0 2^(3/4) 0 0 2^(3/2) 0 0 0;
   1 0 0 0 0 0 0 0 0 0;
   1 0 0 0 0 0 0 0 0 0;
   1 0 0 0 0 0 0 0 0 0;
   1 0 0 0 0 0 0 0 0 0;
   1 0 0 0 0 0 0 0 0 0;
   1 0 0 0 0 0 0 0 0 0];
O=[1 1 1 1 1 1 1 1 1 1 1 1 1 1 1 1 1 1 1 1];
I=eye(10);
Y=[71.7;63.4;63.1;54.4;68.3;52.4;50.5;42.9;67.7;71.7;85.1;65.5;60.6;43.3;66.8;68.3;
55.4;59.5;60.4;53.9];
N=20;p=10;n=6;
T=X'*X
U=X'*Y
V=inv(X'*X)
B=(X'*X)\(X'*Y)
SST=(Y'*Y)-(((O*Y).^2)./N)
SSR=(B'*X'*Y)-(((O*Y).^2)./N)
SSE=(Y'*Y)-(B'*X'*Y)
```

Program for determining the regression coefficients in a refitted model

```
X=[1 -1 -1 -1 1 1 1;
   1 1 -1 -1 1 1 1;
   1 -1 1 -1 1 1 1;
   1 1 1 -1 1 1 1;
   1 -1 -1 1 1 1 1;
   1 1 -1 1 1 1 1;
   1 -1 1 1 1 1 1;
   1 1 1 1 1 1 1;
   1 -2^(3/4) 0 0 2^(3/2) 0 0;
   1 2^(3/4) 0 0 2^(3/2) 0 0;
   1 0 -2^(3/4) 0 0 2^(3/2) 0;
   1 0 2^(3/4) 0 0 2^(3/2) 0;
   1 0 0 -2^(3/4) 0 0 2^(3/2);
   1 0 0 2^(3/4) 0 0 2^(3/2);
   1 0 0 0 0 0 0;
   1 0 0 0 0 0 0;
   1 0 0 0 0 0 0;
   1 0 0 0 0 0 0;
   1 0 0 0 0 0 0;
   1 0 0 0 0 0 0];
O=[1 1 1 1 1 1 1 1 1 1 1 1 1 1 1 1 1 1 1 1];
I=eye(7);
Y=[71.7;63.4;63.1;54.4;68.3;52.4;50.5;42.9;67.9;71.7;85.1;65.5;60.6;43.3;666.8;68.3
;55.4;59.5;60.4;53.9];
N=20;p=10;n=6;
T=X'*X
U=X'*Y
V=inv(X'*X)
B=(X'*X)\(X'*Y)
SST=(Y'*Y)-(((O*Y).^2)./N)
SSR=(B'*X'*Y)-(((O*Y).^2)./N)
SSE=(Y'*Y)-(B'*X'*Y)
```

Program for plotting response surfaces and contours

Response surface and contour at constant pulp density

```
RESPONSE SURFACE
[x,y]=meshgrid(-1.682:1:1.682,-1.682:1:1.682);
z=61.0-2.5*x-4.9*y+1.6*(x.^2)-4.7*(y.^2);
mesh(x,y,z)
xlabel('pH'),ylabel('particle size')

CONTOUR PLOT
[x,y]=meshgrid(-1.682:1:1.682,-1.682:1:1.682);
z=61.0-2.5*x-4.9*y+1.6*(x.^2)-4.7*(y.^2);
contour(x,y,z)
xlabel('pH'),ylabel('particle size')
```

Response surface and contour at constant particle size

```
RESPONSE SURFACE
[x,y]=meshgrid(-1.682:1:1.682,-1.682:1:1.682);
z=61.0-2.5*x-5.7*y+1.6*(x.^2)+3.5*(y.^2);
mesh(x,y,z)
xlabel('pH'),ylabel('pulp density')

CONTOUR PLOT
[x,y]=meshgrid(-1.682:1:1.682,-1.682:1:1.682);
z=61.0-2.5*x-5.7*y+1.6*(x.^2)+3.5*(y.^2);
contour(x,y,z)
xlabel('pH'),ylabel('pulp density')
```

Response surface and contour at constant pH

```
RESPONSE SURFACE
[x,y]=meshgrid(-1.682:1:1.682,-1.682:1:1.682);
z=61.0-5.7*x-4.9*y+3.5*(x.^2)-4.7*(y.^2);
mesh(x,y,z)
xlabel('pulp density'),ylabel('particle size')

CONTOUR PLOT
[x,y]=meshgrid(-1.682:1:1.682,-1.682:1:1.682);
z=61.0-5.7*x-4.9*y+3.5*(x.^2)-4.7*(y.^2);
contour(x,y,z)
xlabel('pulp density'),ylabel('particle size')
```

Program for determining the stationery point and optimum recovery

```
b=[-2.5;-5.7;-4.9];
B=[1.6 0/2 0/2
   0/2 3.5 0/2
   0/2 0/2 -4.7];
S=-0.5*inv(B)*b;
a=61.0;
y=a+S'*b
```